Microbiomes of Disease and Resistance: Deciphering the Role of a Plant Immune Receptor in Bacterial Community Assembly

By

Adam Bigott

A dissertation submitted in partial fulfillment of the
requirements for the degree of

Doctor of Philosophy
(Plant Pathology)

At the
UNIVERSITY OF WISCONSIN-MADISON
2023

Date of final oral examination: 6/20/2023

The dissertation is approved by the following members of the Final Oral Committee:

Caitilyn Allen, Professor, Plant Pathology
Richard Lankau, Associate Professor, Plant Pathology
Andrew Bent, Professor, Plant Pathology
Jean-Michel Ané, Professor, Bacteriology
Paul Koch, Associate Professor, Plant Pathology

Acknowledgements

First, I would like to acknowledge my advisors, Caitilyn Allen and Rick Lankau, and past advisor, Jeri Barak, for their guidance and support throughout my Ph.D. journey. I would also like to thank the many great scientists I have worked alongside in these three labs. It has been a privilege to call them my labmates.

Next, I would like to thank the professors I was fortunate enough to work alongside in the classroom: Andrew Bent, Doug Rouse, and my advisor, Caitilyn Allen. Additionally, I'm grateful for our department's Teaching Specialists Armila Aeilts and Jack Mouradian for the amazing work they do to make our classroom experiences run so smoothly. The motivation I gained in the classroom was essential to my success in the program.

I'd also like to thank the members of the wider UW Plant Pathology community: faculty, staff, and graduate students. From LSU to UW, my plant pathology family continues to grow larger and larger. Of course, I would be remiss if I did not thank the members for my cohort: Mike Riga, Dianiris Luciano, Mariama Carter, Dandan Shao, Helena Jaramillo Mesa, Vicky Lason, Shannon Piper, Nate Westrick, and our various honorary members. I hope to see you at the Library.

Last, I'd like to thank my family. Mom, Dad, Katharine, words cannot express what your love means to me. It has been a long route going from a Pokémon obsessed kid to the plant pathologist I am today and I'm so grateful to have had you by my side the whole way. I love you.

Thesis Abstract

Plants associate with a complex microbial community that has diverse but poorly understood roles in plant health. At the same time, plants possess an innate immune system consisting of two overlapping pathways: Effector Triggered Immunity (ETI) and Pattern Triggered Immunity (PTI). While ETI involves the recognition of specific pathogen effectors by NLR receptors in a gene-for-gene fashion, PTI is initiated when broadly distributed Microbe Associated Molecular Patterns (MAMPs) bind to host Pattern Recognition Receptors (PRRs). In cropping systems where no natural source of pathogen resistance is available, the transgenic insertion of a PTI receptor confers novel, broad spectrum disease resistance. Despite the demonstrated efficacy of transgenic ETI-based (Bs2) and PTI-based (EFR) resistance, we do not know how the incorporation of additional genes involved in the initiation of plant immunity affects the broader, non-pathogenic bacterial communities that associate with these plants. For instance, does the incorporation of an additional PRR and the resulting capacity to perceive an additional MAMP trigger increased basal defenses and thus alter the composition of plant associated microbial communities? Do microbial communities associated with plants expressing ETI- or PTI-based resistance differ from those of non-transgenic but otherwise similar plants? In order to answer these questions, we conducted two multi-year field studies to assess the communities associated with tomato lines carrying the PTI-activating PRR EFR and/or the ETI-activating NLR Bs2.

TABLE OF CONTENTS

Acknowledgments……..……...i

Abstract……...ii

Table of Contents…….iii

List of Figures…….……..……v

List of Tables……..…….vii

CHAPTER 1: AN INTRODUCTION TO MICROBIOMES OF DISEASE AND RESISTANCE: DECIPHERING THE ROLE OF A PLANT IMMUNE RECEPTOR IN BACTERIAL COMMUNTIY ASSEMBLY……..1

Introduction……..…..2

Literature Cited……14

CHAPTER 2: NARROW, BUT NOT BROAD, SPECTRUM RESISTANCE AND DISEASE RESHAPE PHYLLOSPHERE BACTERIAL COMMUNITIES……...18

Abstract……19

Introduction……..…….…..20

Materials and Methods……..……...25

Results……..…31

Discussion……...36

Literature Cited……..61

CHAPTER 3: PTI-BASED TRANSGENIC RESISTANCE HAS LITTLE EFFECT ON TOMATO MICROBIOMES IN THE FIELD……..……...66

Abstract…….....……..…67

Introduction……..……68

Methods……...71

Results…….……77

Discussion…….……..81

Literature Cited……..……..……...104

CHAPTER 4: CONCLUSIONS TO MICROBIOMES OF DISEASE AND RESISTANCE: DECIPHERING THE ROLE OF A PLANT IMMUNE RECEPTOR IN BACTERIAL COMMUNTIY ASSEMBLY……107

Conclusion……...…….……107

Literature Cited……...……..……112

LIST OF FIGURES

CHAPTER 1

Figure 1. How does resistance change plant-associated microbial communites?.....13

CHAPTER 2

Figure 1. Little to no bacterial leaf spot was found on *Bs2* expressing plants and more disease occurred during the spring crop……...43

Figure 2. Richness is greater in plants expressing *Bs2*.……..……..44

Figure 3. Shannon Diversity is greater in plants expressing Bs2……..45

Figure 4. *Bs2* expression and season affect phyllosphere community structure……....46

Figure 5. Xanthomonas, Pseudomonas ASVs correlate with ordination of phyllosphere community……..……47

Figure 6. *Bs2* expression influenced individual taxa relative abundance…..……..48

Figure 7. The twelve most abundant genera represented 85% of the overall phyllosphere bacterial community..……..……..49

Figure S1. Rarefaction curves of the number of genera identified per sample at increasing sampling depths up to 10,000 reads.……..50

Figure S2: Maximum likelihood phylogeny of *Salmonella enterica* sequences and three ASVs identified as belonging to the genus *Salmonella*……..……51

CHAPTER 3

Figure 1. Root-associated communities are dominated by Proteobacteria, Actinobacteria. ……...87

Figure 2. Xylem-associated communities are dominated by Proteobacteria, Bacteriodetes.……88

Figure 3. Transgenic expression of *EFR* affects richness, Shannon Index of the tomato root-associated bacterial community, but supplemental *R. solanacearum* inoculation increased Shannon diversity..……..89

Figure 4. Transgenic expression of *EFR* increased xylem sap richness in supplementally inoculated plants, supplemental *R. solanacearum* inoculation decreased Shannon diversity in xylem-associated bacterial communities..…….90

Figure 5. The composition of root- associated communities in 2018 was similar in transgenic *EFR* and isogenic FL8000 tomato plants……91

Figure 6. The composition of xylem associated communities in 2018 was similar in transgenic *EFR* and isogenic FL8000 tomato plants…….....……92

Figure S1. …… Rarefaction curves of the number of genera per sample at increasing sampling depths in root and xylem communities..……..……..……93

Figure S2. The composition of root- associated communities in 2017 was similar in transgenic *EFR* and isogenic FL8000 tomato plants……..…….……94

LIST OF TABLES

CHAPTER 2

Table 1. Little to no bacterial leaf spot was found on *Bs2* expressing plants and more disease occurred during the spring crop ……..….52

Table S1. ANOVA results for bacterial spot disease severity ratings……..…..53

Table S2. P-values for alpha diversity analyses ……..……54

Table S3. perMANOVA results of phyllosphere bacterial community composition excluding Xanthomonas …….....55

Table S4. Monthly rainfall (mm) measured at 2 m height at the Gulf Coast Research Center in Balm, FL. …….....56

Table S5. Mediation of effects of *BS2* gene versus bacterial spot disease severity on bacterial community composition …….....57

Table S6. Accessions of full-length 16S rRNA genes from Greengenes used to construct a maximum likelihood phylogeny……..…….58

Table S7. Percentage of specific sequences from the bacterial community identified as *Salmonella enterica*. ……..……..59

CHAPTER 3

Table 1. ANOVA results of richness in whole root and xylem sap communities ……...95

Table 2. ANOVA results of Shannon-Weaver indices in whole root and xylem sap communities ……..……..…...96

Table 3. perMANOVAs results of whole root and xylem sap bacterial community composition……..……...97

Table 4. ANOVA results of richness in whole root and xylem sap communities with *R. solanacearum* removed from the dataset.……..…...98

Table 5. ANOVA results of Shannon-Weaver indices in whole root and xylem sap communities with *R. solanacearum* removed from the dataset……..……...99

Table 6. perMANOVAs results of whole root and xylem sap bacterial community composition with *R. solanacearum* removed from the dataset ……....100

Table S1. List of whole root samples used in 16S metabarcoding experiments, their sequencing depth, rarefaction levels, and *R. solanacearum* relative abundance, and year sampled ……..……....101

Table S2. List of whole root samples used in 16S metabarcoding experiments, their sequencing depth, rarefaction levels, and *R. solanacearum* relative abundance, and year sampled ……102

Table S3. ANOVA results *of R. solanacearum* relative abundance in whole root and xylem sap communities ……..…...103

Chapter 1: **An Introduction to Microbiomes of Disease and Resistance: Deciphering the Role of a Plant Immune Receptor in Bacterial Community Assembly**

Author Contributions: This chapter was written by Bigott, A.F. with editing assistance from Allen, C. and Lankau, R.A.

Plants have evolved mechanisms to tolerate the diverse stresses they may encounter. However, if plants constitutively expressed their anti-pathogen defenses or abiotic stress tolerances, the resulting metabolic drain would reduce their reproductive success. Thus, selection pressures to optimize the balance between growth and defenses have led plants to tightly regulate this tradeoff through complex signaling networks (Lozano-Durán and Zipfel 2015; Margalha et al. 2019). In order to reallocate resources from growth into defense or stress tolerance under the appropriate circumstances, signals cascade through complex networks of proteins via post-translational modifications such as phosphorylation (Chen et al. 2021; Jones and Dangl 2006). Protein kinases are a superfamily of proteins that phosphorylate at serine and threonine or tyrosine residues (Hanks and Hunter 1995). Phosphorylation is ubiquitous in cellular signaling and genes encoding predicted protein kinases make up a significant portion of plant genomes. For example, of the 25,498 protein coding genes in *Arabidopsis*, nearly 1,000 encode protein kinases (Arabidopsis Genome Initiative).

In order to perceive extracellular stimuli in apoplastic spaces, plants use a subfamily of protein kinases known as Receptor-Like Kinases (RLKs). RLKs are composed of three domains: an extracellular binding domain, a transmembrane domain, and an intracellular kinase domain. Receptor-Like Proteins (RLPs) have structural similarity to RLKs but lack a kinase domain. These receptors exhibit a high degree of specificity towards their elicitor ligands, and different receptor motifs enable the recognition of various classes of biomolecules, such as oligosaccharide-binding LysM domains and peptide-binding Leucine Rich Repeat domains. Following ligand binding, RLKs and RLPs often form heteromeric complexes with co-receptors to amplify

phosphorylation of downstream target proteins. For example, the RLK EFR must associate with the receptor kinase BAK1 to fully transduce its signal (Chinchilla et al. 2007).

These signaling mechanisms activate the innate immune system that plants use to defend themselves against diverse pests and pathogens. As part of a broad-spectrum defense pathway known as Pattern Triggered Immunity (PTI), plants first detect the presence of microbes in apoplastic spaces by means of RLKs. The subgroup of RLKs that act in PTI are known as Pattern Recognition Receptors (PRRs). These receptors detect specific molecular patterns associated with a potential threat. These patterns can be classified as either Damage Associated Molecular Patterns (DAMPs) or Microbe Associated Molecular Patterns (MAMPs), depending on their origin. MAMPs are ubiquitous, abundant, and broadly conserved within a taxonomic group; they are thus not specific. Known elicitors of PTI include DAMPs like plant cell wall fragments and MAMPs like chitin oligomers from fungal cell walls, bacterial flagellin, and bacterial Elongation Factor-Tu (EF-Tu).

When a PRR binds its target MAMP or DAMP elicitor, the kinase activity associated with the receptor complex phosphorylates proteins that in turn produce additional signaling molecules. For instance, calcium ion channels are phosphorylated to activate calcium-dependent protein kinases or NADPH oxidases to produce reactive oxygen species (ROS). Further phosphorylation of Mitogen-Activated Protein Kinases (MAPKs), produce phosphorylation cascades that ultimately lead to defensive changes in gene expression. Successful initiation of PTI can include behaviors like a measurable ROS burst, the deposition of callose to reinforce plant cell walls, stomatal closure to

exclude pathogens on the plant surface, production of antimicrobial compounds like phytoalexins, and transcriptional reprogramming of local and systemic defenses.

Despite their immense phylogenetic and morphological diversity, many plant pathogens share the general strategy of secreting a repertoire of virulence factors, collectively dubbed ‘effectors' as part of the host infection process. Plant pathogenic bacteria deliver effectors intracellularly via a molecular syringe that spans the host cell wall and plasma membranes, known as the Type 3 Secretion System. Because pathogenic bacteria risk detection by the plant innate immune system when they enter apoplastic spaces, they have evolved Type 3 effectors to suppress host defenses by disrupting immune signaling to evade detection. For example, 16 of 61 tested effectors produced by strain RS1000 of the bacterial wilt pathogen *Ralstonia solanacearum* suppressed ROS production in response to a single MAMP, a flagellin fragment (Nakano and Mukaihara 2019).

Determining the specific virulence contributions of individual effectors is complicated by the large and variable number of effectors produced by pathogens, even within species. For instance, *R. solanacearum* strains may make anywhere from 46 to 73 Type 3 effectors, with over 100 described in the species complex collectively (Landry et al. 2020). While underpinning molecular mechanisms of many effectors have yet to be elucidated, their relative contributions to fitness can sometimes be measured by assaying virulence of mutant strains lacking specific effector genes. In some extreme cases, like that of *Xanthomonas* effector *avrBs2*, deletion of the gene can result in pathogen populations 100-fold smaller in a susceptible host (Kearney and Staskawicz

1990). In other cases multiple effectors have redundant functions so mutants lacking a single effector retain full virulence.

In addition to using receptors that bind to broadly conserved molecular patterns and initiate a generalized lower-intensity PTI response, plants can also use intracellular receptors to detect specific pathogen effectors. In contrast to PTI, this Effector Triggered Immunity (ETI) generally occurs in a "gene-for-gene" manner, wherein a host Nucleotide Binding Leucine Rich Repeat Receptor (NLR) recognizes a specific pathogen effector. Upon recognition, the host plant initiates a rapid tissue collapse and desiccation known as the hypersensitive response. This localized cell death at the site of infection restricts pathogen proliferation and prevents spread of the disease. Effector recognition by NLRs can occur through direct binding between the effector and the NLR protein or indirectly. In the case of indirect detection of the effector, plant NLRs associate with other proteins and are activated when those associated elements are modified by the pathogen effector. The resulting recognition event leads to the activation of downstream signaling cascades, triggering strong defense responses, and ultimately conferring resistance against the pathogen. For example, the *Xanthomonas* effector *avrBs2* is recognized by the pepper plant NLR Bs2, but following effector recognition, Bs2 interacts with a helper NLR, NRC2, which in turn oligomerizes into a “resistasome” that acts as a calcium ion channel and initiates cell death (Contreras et al. 2023)**.** Bs2 is one of several NLRs that interact with NRC2 helper in this manner. Thus, not all ETI interactions occur in a strictly “gene-for-gene” fashion.

In addition to suppressing plant defenses, disruption of host metabolic functions is another common function of pathogen effectors. While effectors often interact directly

with host cytoplasmic elements to manipulate metabolism, some plant pathogenic *Ralstonia* and *Xanthomonas* strains produce Transcription Activator-Like effectors that enter the host nucleus and bind directly to promoters of host genes to influence their transcription (Boch et al. 2014; de Lange et al. 2013). *R*. *solanacearum* modifies the metabolic contents of xylem sap during the infection process in ways that increase its fitness *in planta* (Lowe-Power et al. 2018). Taken together, these findings offer a general model in which pathogens manipulate host metabolism to increase their fitness relative to other plant associated microbes.

While efforts to characterize the individual components of the plant immune system have identified the network of genes involved in several model and agriculturally important plant species, such approaches have clear limitations. The use of small *Arabidopsis* plantlets allows for quick experimentation, but induction of PTI defenses in this system leads to visible growth defects (Zipfel et al. 2006). Further, given that pathogen effectors commonly suppress PTI responses, the use of individual MAMPs as elicitors is preferred to natural infection in reductionist experimental systems. However, additional research has shown that exposure to individual MAMP elicitors or wounding does not cause the same magnitude of response as the combination of damage and MAMPs produced during natural infection (Zhou et al. 2020). Further, the contributions of PTI-mediated ROS events to ETI-mediated hypersensitivity has only recently been elucidated (Yuan et al. 2021) as has the role of ETI in re-potentiating the PTI signaling apparatus (Ngou et al. 2021).

While pathogens use effectors to subvert the plant immune system, we do not understand how plants interact with non-pathogenic microbes, which are abundant in

the natural plant environment. Nonpathogenic microbes also release MAMPS that could trigger PTI. MAMPs tend to be conserved and have important functions, so strong selection pressure maintains them in most microbes. Plant colonization by some nonpathogenic bacteria appears to elicit different plant transcriptional response patterns from those elicited by phytopathogenic bacteria (Garrido-Oter et al. 2018). Nonpathogenic bacteria may also have the ability to quench localized PTI responses through niche modification (Yu et al. 2019). Understanding plant responses to non-pathogenic microbes is further complicated by the distinct microbial communities found in different plant compartments (Ottesen et al. 2013). Despite the challenges of designing experiments to measure effects of nonpathogenic microbes on plant immune systems and vice-versa, this question is broadly important.

Plants can be engineered to resist pathogens by adding resistance genes to non-native backgrounds. The integration of additional PTI-related genes is of particular interest as a potential source of novel broad spectrum disease resistance. A notable example is the addition of a PRR gene from Brassicacaeae to tomato plants. Transgenic tomatoes expressing the Arabidopsis Elongation Factor-Tu Receptor (EFR) gene are remarkably resistant to multiple bacterial pathogens, including *R. solanacearum, X. perforans, Agrobacterium tumefaciens,* and *Pseudomonas syringae* (Lacombe et al. 2010). Transgenic *EFR*-based resistance to bacterial pathogens has also been explored in rice, wheat, and citrus (Schwessinger et al. 2015; Schoonbeek et al. 2015; Mitre et al. 2021). At present, commercial tomato growers in Florida USA have limited ways to control two major bacterial diseases: bacterial wilt (*R. solanacearum*) and bacterial leaf spot (*X. perforans*). Planting seedlings that have a resistant rootstock

grafted to a desirable scion is currently the best option for growers confronting high wilt disease pressure, but grafted seedlings are expensive (Suchoff et al. 2015). Control of *X. perforans* using copper sprays has led to the emergence of resistance to copper sulfate (Klein-Gordon et al. 2021).

There is interest in deploying transgenically engineered resistance to further improve disease management strategies. Expressing *EFR* in FL8000 tomatoes confers field level resistance under commercial production conditions to both the vascular pathogen *R. solanacearum* and the foliar pathogen *X. perforans* (Horvath et al. 2012; Kunwar et al. 2018). Transgenic plants expressing non-native NLRs can also gain ETI-based resistance to one or several pathogens based on their effector repertoires. For example, the insertion of the *Bs2* resistance gene from pepper has successfully controlled bacterial spot in tomato caused by *X. perforans* race (Horvath et al. 2012; Kunwar et al. 2018).

The term “microbiome” refers to “a characteristic microbial community occupying a reasonably well-defined habitat with distinct physio-chemical properties” (Whipps et al. 1988). The composition of microbial communities varies in association with different plant compartments (Ottesen et al. 2013). Given the unique properties associated with different plant compartments, these can be thought of as distinct phytobiomes. Some phytobiomes have been thoroughly studied, such as those of the rhizosphere (Berendsen et al. 2012; Qu et al. 2020) or the phyllosphere (Stone et al. 2018; Liu et al. 2020). However, xylem associated microbial communities are less well characterized.

The phyllosphere, or above-ground portion of plants, is a restrictive ecological niche for microbes. High levels of ultraviolet stress select for microbes that can produce

protective pigments or extracellular polymeric substances (Kadivar and Stapleton 2003). The hydrophobic, waxy cuticles of leaves limit the availability of moisture on the phylloplane (Beattie 2011). Bacteria are the most abundant members of the phyllosphere microbiome and can reach population densities as high as 10^7 cells per cm^2 or 10^8 cells per gram of leaf tissue (Lindow and Brandl 2003). Conditions in the phyllosphere are dynamic; prolonged high light and low humidity dramatically decrease bacterial phyllosphere populations (Wilson et al. 1999). A small number of taxa, including *Sphingomonas*, *Methylobacterium*, and *Pseudomonas*, have been shown to be core members of the phyllosphere bacterial community across plant species, including tomato, rice, *Arabidopsis*, clover, and soybean (Delmotte et al. 2009; Knief et al. 2012; Allard et al. 2016).

The rhizosphere is the interface between plant and soil where nutrient-rich rhizodeposits influence microbial communities in ways distinct from bulk soil. The rhizosphere is characterized by relative nutrient abundance and a degree of buffering from fluctuating environmental conditions, but it is also intensely competitive as many microbes seek to occupy this rich niche. Many rhizosphere microbes increase plant fitness by priming plant defenses, suppressing pathogen colonization, and sequestering water and nutrients for plants (Berendsen et al. 2012; Qu et al. 2020). While some root endophytes are seedborne and transmitted vertically, many microbes that eventually live inside plants, such as *R. solanacearum*, first colonize the rhizoplane before subsequently invading endophytic spaces. The endophytic microbial community is thus often a subset of the rhizosphere microbiome.

The microbial communities that inhabit the xylem tissues are less explored. Xylem sap is a moderately restrictive habitat for microbes: it is lower in nutrients, high-flow, and yet still subject to some plant defenses. It has frequently been proposed that endophytic xylem inhabitants could deliver probiotic benefits to plants, but this has not been fully explored empirically (Achari and Ramesh 2014; Lodewyckx et al. 2002). Several well studied major pathogens colonize plant xylem, including *Xylella fastidiosa, Ca*. Liberibacter spp., and *R. solanacearum*. However, because populations of xylem-dwelling pathogenic bacteria typically overwhelm the natural microbial community, analyses of these wilt pathogens in their xylem environment have not increased knowledge of healthy xylem microbiomes.

In addition to preventing crop losses to disease, the transgenic insertion of non-native immune receptors into plants also provides a powerful tool to explore interactions between plant compartments and their associated microbial communities. As described above, plants suffer reduced fitness if their defenses are constantly active, but we have learned that plants live bathed in microbes that produce PTI-triggering MAMPs like Elongation Factor Tu or flagellin. This presents a major paradox: how can plants distinguish between the millions of harmless bacteria in their microbiomes and a potentially threatening pathogen? Does the incorporation of an additional PRR and the resulting capacity to perceive an additional MAMP trigger increased basal defenses and thus alter the composition of plant associated microbial communities? Do microbial communities associated with plants expressing ETI- or PTI-based resistance differ from those of non-transgenic but otherwise similar plants? How do changes in plant-pathogen interactions alter the microbial ecology of disease?

These broad and widely relevant questions motivated my dissertation research. I took advantage of the demonstrated resistance of *EFR*-expressing transgenic tomatoes to both a leaf spot pathogen, *X. perforans*, and a soil-borne vascular wilt pathogen, *R. solanacearum*. These two contrasting pathosystems allowed me to measure the effects of EFR-mediated resistance on the bacterial communities on tomato leaf surfaces, in and near roots, and in xylem vessels. I used 16S metabarcoding to characterize the bacterial communities associated with phyllosphere, rhizosphere, and xylem sap in field-grown tomato plants under significant leaf spot or bacterial wilt disease pressure.

Specifically, I conducted a multi-year field study to assess the communities associated with tomato lines carrying the PTI-activating PRR EFR and/or the ETI-activating NLR Bs2. These genes were integrated into the widely planted commercial market tomato cultivar FL8000, with non-transgenic FL8000 serving as a control. Research was conducted under commercial production conditions at two Florida agricultural research stations under high disease pressure for bacterial wilt (Quincy) or bacterial leaf spot (Balm), respectively. Both the EFR and Bs2 receptors depend on other host elements to transduce their signals (Chinchilla et al. 2007; Contreras et al. 2023). Therefore, the insertion of these receptors alters how and when FL8000 plants deploy resistance, not the defense response itself.

In Chapter 2 I explore how transgenic EFR-based PTI resistance and Bs2-based resistance interact, and how susceptibility to *X. perforans* affects phyllosphere bacterial communities. In Chapter 3 I investigate how EFR-based PTI resistance interacts with *R. solanacearum* in communities associated with both whole roots and xylem sap. Finally,

in Chapter 4 I offer some general conclusions and discuss some approaches to address the many new questions that arose during this project.

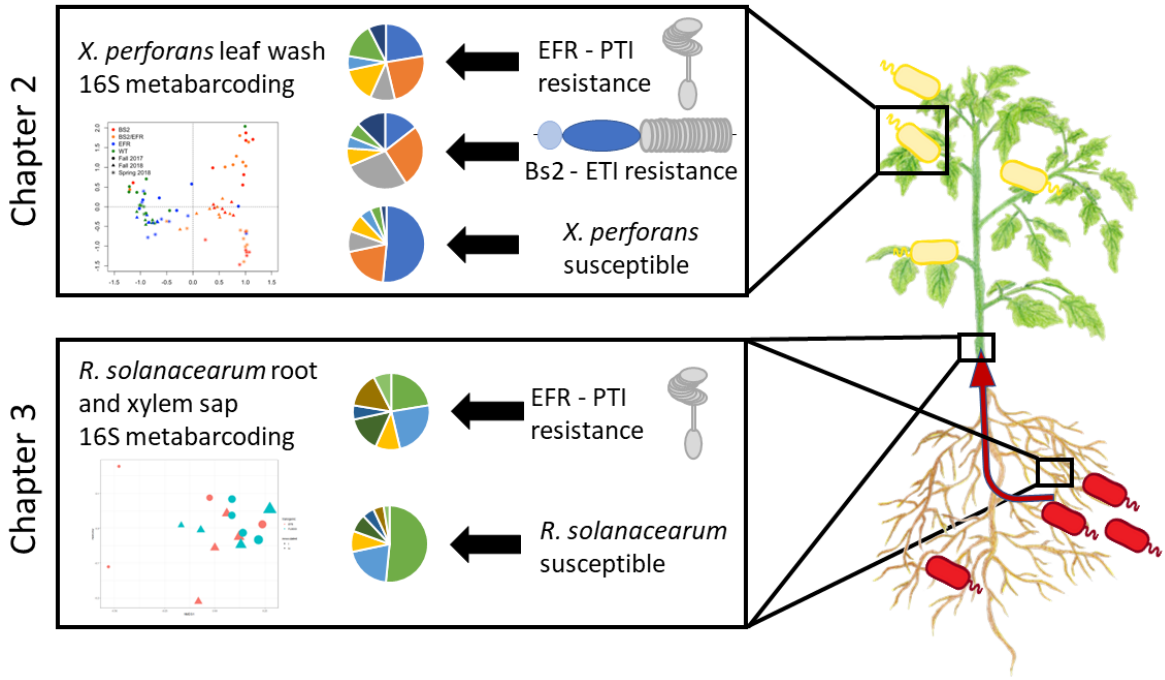

Figure 1: How does resistance change plant-associated microbial communites? A graphical abstract of 16S metabarcoding approaches to characterize phyllosphere communities with resistance and susceptiblity to *X. perforans* (Chapter 2) and root and xylem communities associated with with resistance and susceptiblity to *R. solanacearum* (Chapter 3).

Literature Cited

Achari, G. A., and Ramesh, R. 2014. Diversity, biocontrol, and plant growth promoting abilities of xylem residing bacteria from solanaceous crops. *Int. J. Microbiol*. 2014.

Allard, S. M., Walsh, C. S., Wallis, A. E., Ottesen, A. R., Brown, E. W., and Micallef, S. A. 2016. *Solanum lycopersicum* (tomato) hosts robust phyllosphere and rhizosphere bacterial communities when grown in soil amended with various organic and synthetic fertilizers. *Sci. Total Environ*. 573:555–563.

Arabidopsis Genome Initiative. 2000. Analysis of the genome sequence of the flowering plant Arabidopsis thaliana. *Nature*. 408:796–815.

Beattie, G. A. 2011. Water relations in the interaction of foliar bacterial pathogens with plants. *Annu. Rev. Phytopathol*. 49:533–555.

Berendsen, R. L., Pieterse, C. M. J., and Bakker, P. A. H. M. 2012. The rhizosphere microbiome and plant health. *Trends Plant Sci*. 17:478–486.

Boch, J., Bonas, U., and Lahaye, T. 2014. TAL effectors--pathogen strategies and plant resistance engineering. *New Phytol*. 204:823–832.

Chen, X., Ding, Y., Yang, Y., Song, C., Wang, B., Yang, S., et al. 2021. Protein kinases in plant responses to drought, salt, and cold stress. *J. Integr. Plant Biol*. 63:53–78.

Chinchilla, D., Zipfel, C., Robatzek, S., Kemmerling, B., Nürnberger, T., Jones, J. D. G., et al. 2007. A flagellin-induced complex of the receptor FLS2 and BAK1 initiates plant defense. *Nature*. 448:497–500.

Contreras, M. P., Pai, H., Tumtas, Y., Duggan, C., Yuen, E. L. H., Cruces, A. V., et al. 2023. Sensor NLR immune proteins activate oligomerization of their NRC helpers in response to plant pathogens. *EMBO J*. 42:e111519.

Delmotte, N., Knief, C., Chaffron, S., Innerebner, G., Roschitzki, B., Schlapbach, R., et al. 2009. Community proteogenomics reveals insights into the physiology of phyllosphere bacteria. *Proc. Natl. Acad. Sci*. U. S. A. 106:16428–16433.

Garrido-Oter, R., Nakano, R. T., Dombrowski, N., Ma, K.-W., McHardy, A. C., and Schulze-Lefert, P. 2018. Modular traits of the Rhizobiales root microbiota and their evolutionary relationship with symbiotic *Rhizobia*. *Cell Host Microbe*. 24:155–167.e5.

Hanks, S. K., and Hunter, T. 1995. The eukaryotic protein kinase superfamily: kinase (catalytic) domain structure and classification1. *The FASEB journal*.

Horvath, D. M., Stall, R. E., Jones, J. B., Pauly, M. H., Vallad, G. E., Dahlbeck, D., et al. 2012. Transgenic resistance confers effective field level control of bacterial spot disease in tomato. *PLoS One*. 7:e42036.

Jones, J. D. G., and Dangl, J. L. 2006. The plant immune system. *Nature*. 444:323–329.

Kadivar, H., and Stapleton, A. E. 2003. Ultraviolet radiation alters maize phyllosphere bacterial diversity. *Microb. Ecol*. 45:353–361.

Kearney, B., and Staskawicz, B. J. 1990. Widespread distribution and fitness contribution of *Xanthomonas campestris* avirulence gene *avrBs2. Nature*. 346:385–386.

Klein-Gordon, J. M., Xing, Y., Garrett, K. A., Abrahamian, P., Paret, M. L., Minsavage, G. V., et al. 2021. Assessing changes and associations in the *Xanthomonas perforans* population across Florida commercial tomato fields via a statewide survey. *Phytopathology*. 111:1029–1041.

Knief, C., Delmotte, N., Chaffron, S., Stark, M., Innerebner, G., Wassmann, R., et al. 2012. Metaproteogenomic analysis of microbial communities in the phyllosphere and rhizosphere of rice. *ISME J*. 6:1378–1390.

Kunwar, S., Iriarte, F., Fan, Q., Evaristo da Silva, E., Ritchie, L., Nguyen, N. S., et al. 2018. Transgenic expression of *EFR* and *Bs2* genes for field management of bacterial wilt and bacterial spot of tomato. *Phytopathology*. 108:1402–1411.

Lacombe, S., Rougon-Cardoso, A., Sherwood, E., Peeters, N., Dahlbeck, D., van Esse, H. P., et al. 2010. Interfamily transfer of a plant pattern-recognition receptor confers broad-spectrum bacterial resistance. *Nat. Biotechnol*. 28:365–369.

Landry, D., González-Fuente, M., Deslandes, L., and Peeters, N. 2020. The large, diverse, and robust arsenal of *Ralstonia solanacearum* type III effectors and their in planta functions*. Mol. Plant Pathol*. 21:1377–1388.

de Lange, O., Schreiber, T., Schandry, N., Radeck, J., Braun, K. H., Koszinowski, J., et al. 2013. Breaking the DNA-binding code of *Ralstonia solanacearum* TAL effectors provides new possibilities to generate plant resistance genes against bacterial wilt disease. *New Phytol*. 199:773–786.

Lindow, S. E., and Brandl, M. T. 2003. Microbiology of the phyllosphere. *Appl. Environ. Microbiol*. 69:1875–1883.

Liu, H., Brettell, L. E., and Singh, B. 2020. Linking the phyllosphere microbiome to plant health. *Trends Plant Sci*. 25:841–844.

Lodewyckx, C., Vangronsveld, J., Porteous, F., Moore, E. R. B., Taghavi, S., Mezgeay, M., et al. 2002. Endophytic bacteria and their potential applications. *CRC Crit. Rev*. *Plant Sci*. 21:583–606.

Lowe-Power, T. M., Hendrich, C. G., von Roepenack-Lahaye, E., Li, B., Wu, D., Mitra, R., et al. 2018. Metabolomics of tomato xylem sap during bacterial wilt reveals *Ralstonia solanacearum* produces abundant putrescine, a metabolite that accelerates wilt disease. *Environ. Microbiol*. 20:1330–1349.

Lozano-Durán, R., and Zipfel, C. 2015. Trade-off between growth and immunity: role of brassinosteroids. *Trends Plant Sci*. 20:12–19.

Margalha, L., Confraria, A., and Baena-González, E. 2019. SnRK1 and TOR: modulating growth–defense trade-offs in plant stress responses. *J. Exp. Bot*. 70:2261–2274.

Mitre, L. K., Teixeira-Silva, N. S., Rybak, K., Magalhães, D. M., de Souza-Neto, R. R., Robatzek, S., et al. 2021. The *Arabidopsis* immune receptor EFR increases resistance to the bacterial pathogens *Xanthomonas* and *Xylella* in transgenic sweet orange. *Plant Biotechnol. J.* 19:1294–1296.

Nakano, M., and Mukaihara, T. 2019. Comprehensive identification of PTI suppressors in type III effector repertoire reveals that *Ralstonia solanacearum* activates jasmonate signaling at two different steps. *Int. J. Mol. Sci*. 20:5992.

Ngou, B. P. M., Ahn, H.-K., Ding, P., and Jones, J. D. G. 2021. Mutual potentiation of plant immunity by cell-surface and intracellular receptors. *Nature*. 592:110–115.

Ottesen, A. R., González Peña, A., White, J. R., Pettengill, J. B., Li, C., Allard, S., et al. 2013. Baseline survey of the anatomical microbial ecology of an important food plant: *Solanum lycopersicum* (tomato). *BMC Microbiol*. 13:114.

Qu, Q., Zhang, Z., Peijnenburg, W. J. G. M., Liu, W., Lu, T., Hu, B., et al. 2020. Rhizosphere microbiome assembly and its impact on plant growth. J. Agric. Food Chem. 68:5024–5038.

Schoonbeek, H.-J., Wang, H.-H., Stefanato, F. L., Craze, M., Bowden, S., Wallington, E., et al. 2015. Arabidopsis EF-Tu receptor enhances bacterial disease resistance in transgenic wheat. New Phytol. 206:606–613.

Schwessinger, B., Bahar, O., Thomas, N., Holton, N., Nekrasov, V., Ruan, D., et al. 2015. Transgenic expression of the dicotyledonous pattern recognition receptor EFR in rice leads to ligand-dependent activation of defense responses. PLoS Pathog. 11:e1004809.

Stone, B. W. G., Weingarten, E. A., and Jackson, C. R. 2018. The role of the phyllosphere microbiome in plant health and function. *Ann. Plant Rev. Online.* :533–556.

Suchoff, D., Gunter, C., Schultheis, J., and Louws, F. J. 2015. On-farm grafted tomato trial to manage bacterial wilt. *Acta Hortic*. :119–127.

Whipps, J. M., Lewis, K., and Cooke, R. C. 1988. Mycoparasitism and plant disease control.

Wilson, M., Hirano, S. S., and Lindow, S. E. 1999. Location and survival of leaf-associated bacteria in relation to pathogenicity and potential for growth within the leaf. *Appl. Environ. Microbiol*. 65:1435–1443.

Wu, D., von Roepenack-Lahaye, E., Buntru, M., de Lange, O., Schandry, N., Pérez-Quintero, A. L., et al. 2019. A plant pathogen type III effector protein subverts translational regulation to boost host polyamine levels. *Cell Host Microbe*. 26:638–649.e5.

Yu, K., Liu, Y., Tichelaar, R., Savant, N., Lagendijk, E., van Kuijk, S. J. L., et al. 2019. Rhizosphere-Associated Pseudomonas Suppress Local Root Immune Responses by Gluconic Acid-Mediated Lowering of Environmental pH. *Curr. Biol*. 29:3913–3920.e4.

Yuan, M., Jiang, Z., Bi, G., Nomura, K., Liu, M., Wang, Y., et al. 2021. Pattern-recognition receptors are required for NLR-mediated plant immunity. *Nature*. 592:105–109.

Zhou, F., Emonet, A., Dénervaud Tendon, V., Marhavy, P., Wu, D., Lahaye, T., et al. 2020. Co-incidence of Damage and Microbial Patterns Controls Localized Immune Responses in Roots. *Cell*. 180:440–453.e18.

Zipfel, C., Kunze, G., Chinchilla, D., Caniard, A., Jones, J. D. G., Boller, T., et al. 2006. Perception of the bacterial PAMP EF-Tu by the receptor EFR restricts *Agrobacterium*-mediated transformation. *Cell*. 125:749–760.

Chapter 2: Narrow, but not Broad, Spectrum Resistance and Disease Reshape Phyllosphere Microbial Communities

A modified version of this chapter has been submitted for publication in *Phytobiomes* as: Narrow, but not broad, spectrum resistance and disease reshape phyllosphere microbial communities. Adam F. Bigott, Samuel F. Hutton, Gary Vallad, Richard Lankau, Jeri Barak.

This article will also be available as a BioRxiv pre-print under the same title.

Author Contributions:

This project was conceived by Barak, J.D. and Vallad, G. Field data was collected by Hutton S.F. and Bigott, A.F. and analyzed by Bigott, A.F. and Lankau, R.A. Bigott, A.F. was the lead author in writing the manuscript with help from by Barak, J.D. and editing contributions from Lankau, R.A.

Abstract: The phyllosphere is a restrictive environment for microbes, resulting in microbial communities typically dominated by select taxa with specific adaptations for success in this niche. However, biotic stress, especially from plant disease, could disrupt this environment in ways that alter the resulting phyllosphere community with potential consequences for both plant and human health. Additionally, plant disease resistance, through both broad-spectrum (pattern-triggered immunity) or specific (effector-triggered immunity) resistance, could affect non-pathogenic communities directly or indirectly by suppressing disease development. Here, we tested how transgenic ETI and PTI resistance genes in tomato affected the phyllosphere communities of plants in the presence of the pathogen *Xanthomonas perforans* and the resulting bacterial spot disease. We found that the presence of the *Bs2* transgene (ETI) had major effects on phyllosphere bacterial communities, while the *EFR* (PTI) transgene did not. The effect of the *Bs2* resistance gene could be largely attributed to the change in disease symptoms. Diseased leaves harbored reduced bacterial diversity and reductions in the relative abundance of common phyllosphere bacterial genera (e.g. *Sphinogmonas* and *Methylobacterium*), while a limited number of bacterial genera more closely associated with diseased leaves. These results suggest that phyllosphere communities are sensitive to the direct and indirect effects of plant disease and resistance, and the consequences of these shifts for plant and human health deserve further investigation.

Introduction

The phyllosphere, or above-ground portion of a plant, is a restrictive ecological niche for microbes. As such, phyllosphere microbial communities are typically dominated by a restricted set of taxa with specific adaptations to this challenging environment. However, phyllosphere environments are also dynamic, subjecting microbial communities to fluctuating physical conditions as leaves age, are buffeted by weather events, or are attacked by herbivores and pathogens. While a relatively consistent view of “healthy” phyllosphere has emerged from surveys across disparate plant species (Delmotte et al. 2009; Knief et al. 2012; Allard et al. 2016), how the phyllosphere microbial community changes in response to biotic stress from foliar pathogens is poorly understood. This aspect of phyllosphere ecology may be especially important these plant bacterial communities can contain rare and infrequent members, including potential human pathogens, whose populations may benefit from alterations to the phyllosphere environment.

Leaves are covered in waxy cuticles that limit the availability of moisture in the phylloplane, the leaf surface (Beattie 2011). Ultraviolet stress on the phylloplane leads to diversification of the associated bacterial communities favoring those with pigmentation and/or copious extra polymeric substance production (Kadivar and Stapleton 2003). High light and low humidity decrease bacterial phyllosphere populations (Wilson et al. 1999). Further, the availability of carbon sources in the phylloplane is limited and aggregated (Leveau and Lindow 2001). The aggregation of available nutrients results in few sites on the leaf surface where bacteria can replicate

and reward motility and chemotaxis towards a more hospitable oasis such as glandular trichomes or host cellular junctions (Remus-Emsermann et al. 2012).

Even in this restrictive environment, bacteria are the most abundant members of the phyllosphere microbiome and can reach population densities as high as 10^7 cells per cm^2 or 10^8 cells per gram of leaf tissue (Lindow and Brandl 2003). A small number of taxa, including *Sphingomonas*, *Methylobacterium*, and *Pseudomonas*, are common members of the phyllosphere bacterial community across plant species, including tomato, rice, *Arabidopsis*, clover, and soybean (Delmotte et al. 2009; Knief et al. 2012; Allard et al. 2016). Carbon availability limits epiphytic bacterial populations (Wilson and Lindow 1995); these taxa have made different adaptations primarily in carbon acquisition and/or utilization to succeed in the phyllosphere. A combined metagenomic and metaproteomic analysis assessing bacterial communities on *Arabidopsis*, clover, and soybean assinged a large number of TonB dependent transporters to *Sphingomonas* spp. that have a putative role in the uptake and utilization of a diverse array of carbon substrates (Delmotte et al. 2009). This suggests that the success of *Sphingomonas* in the phyllosphere is in part due to scavenging various substrates present at low amounts. Delmotte et al. (2009) also found *Methylobacterium* synethized greater quantities of the proteins required for methylotrophy while colonizing leaves than previously reported values when grown in culture.

Pseudomonas differs from cosmopolitan phyllosphere genera like *Sphingomonas* and *Methylobacterium* in that it contains both non-pathogenic and pathogenic members. In order to deal with waxy, hydrophobic leaf surfaces, *Pseudomonas* produces biosurfactants, increasing the wettability of the leaf for enhanced diffusion of nutrients

across the waxy cuticle and motility to favorable colonization sites (Burch et al. 2014). As a plant pathogen, *Pseudomonas syringae* has evolved different strategies for proliferation in the phyllosphere such as the production of coronatine to override plant defenses and prevent stomatal closure for apoplastic entry (Zheng et al. 2012) and, in some cases, conversion of the apoplastic space to an aqueous environment. Accessing the apoplast alleviates stresses associated with the phylloplane and may have more available free water and nutrients.

Yet as bacteria interact with plant cells in apoplastic spaces, they encounter an additional challenge to survival: the plant immune system. Plants possess a broad-spectrum defense pathway known as Pattern Triggered Immunity (PTI). Transmembrane Receptor-Like Kinases known as Pattern Recognition Receptors (PRRs) initiate PTI in the presence of both pathogenic and non-pathogenic bacteria in the apoplast. Bacterial pathogens often suppress host defenses by disruption of PTI signaling and other metabolic functions. During infection of tomato, *P*. *syringae* uses a type 3 (T3) effector (HopM1) to induce establishment of an aqueous apoplast, presumably increasing nutrient availability and potentially dampening pathogen associated molecular patterns (PAMP)-triggered immune (PTI) responses (Xin et al. 2016). Phyllosphere modification is not unique to pathogenic pseudomonads. On infection of tomato, *Xanthomonas gardneri* reprograms host pectate lyases by secretion of AvrHah1, a transcription activator-like T3 effector that also alters the apoplast to an aqueous environment (Schwartz et al. 2017). Furthermore, *X. translucens* infection of wheat leads to transcriptional reprogramming that converts infected leaves from carbohydrate sources to sinks (Garcia-Seco et al. 2017). In addition to modification of

the phyllosphere, *Xanthomonas* effectors also contribute directly to pathogen fitness. Following the deletion of *avrBS2*, inoculation of the susceptible pepper cultivar Early Calwonder with *X. vesicatoria* populations were 100 times smaller after four days than their wildtype counterparts (Kearney and Staskawicz 1990).

While pathogens use effectors to increase their own fitness *in planta*, the modifications to the phyllosphere that occur during disease development can alter colonization success for other bacteria. When *Xanthomonas* infects tomato, the survival and, in some cases, replication of *Salmonella enterica* in the phyllosphere increase (Potnis et al. 2014; Potnis et al. 2015). However, on hosts resistant to *Xanthomonas*, the human pathogen population decreased rapidly. Without changes to the phyllosphere caused by infection, *S. enterica* has limited success, fails to replicate, and immigrant populations decline over time (Islam et al. 2004a; Islam et al. 2004b; Potnis et al. 2014). How the bacterial community broadly responds to niche alterations due to disease or the triggering of host resistance by pathogens remains largely unknown.

Our aim in this study is to analyze how the bacterial phyllosphere community responds to host infection and disease resistance. We used a well-characterized pathosystem of *Xanthomonas perforans* and tomato. *X. perforans* causes bacterial spot of tomato and pepper, leading to disturbance of the phyllosphere, including establishment of an aqueous apoplast. There is little resistance in tomato to bacterial spot, but pepper, a close relative to tomato and fellow host to bacterial spot, has several resistance genes, including *Bs2* (Tai et al. 1999). *Bs2* confers resistance to *avrBs2*-carrying strains of *Xanthomonas* spp. in pepper in a highly specific, gene-for-gene interaction with the pathogen effector (Minsavage et al. 1990). This process, Effector-

Triggered Immunity (ETI), induces a hypersensitive response in the plant. The transgenic expression of *Bs2* from pepper into tomato was shown to both reduce disease severity and increase yield in field trials (Lacombe et al. 2010; Horvath et al. 2012). Plants can also initiate broad-spectrum PTI-based resistance to bacterial pathogens when PRRs are activated by binding with broadly conserved microbial epitopes, such as flagellin or Elongation Factor Tu (Jones and Dangl 2006, Boller and Felix 2009) (Jones and Dangl 2006; Boller and Felix 2009). Tomato lines expressing the *Arabidopsis thaliana* gene *EFR*, a PRR that recognizes Elongation Factor Tu, have been developed to resist multiple bacterial pathogens simultaneously. *EFR*-expressing plants are resistant to diseases caused by *P. syringae*, *Agrobacterium tumafaciens*, and *Ralstonia solanacearum* (Lacombe et al. 2010; Kunwar et al. 2018). Phyllosphere community assembly is partially shaped by early and influential colonizers (Debray et al. 2023). Disruption of this process by transgenic *EFR* could lead to distinct and unforeseen differences in phyllosphere community composition.

In this study, we characterized the phyllosphere bacterial community of tomato using 16S metabarcoding. We used isogenic lines of tomato varying in the presence or absence of resistance genes for both a narrow-spectrum ETI and a broad-spectrum PTI, grown in commercial production conditions under high disease pressure. To correlate bacterial community composition with disease, we also measured *Xanthomonas* disease severity and fruit yield. Using this information, we examined the importance of the pathogen and/or host resistance in shaping bacterial community structure. We calculated the relative abundance of bacterial community members to

examine how cosmopolitan genera, *Sphingomonas*, *Methylobacterium*, and *Pseudomonas*, were affected by host genotype and thus, disease.

Materials and Methods

Sampling and DNA Processing: The tomato plants used in these experiments were grown at and managed by the University of Florida Gulf Coast Research & Education Center in Balm, Florida. Fields were prepared according to standard commercial field production with fumigated (Pic-Clor 60, 336 kg/ha) raised beds (81.3 cm wide at the base, 71.1 cm wide at the crown and 20.3 cm in height) in groups of three at 91.4 m lengths, spaced on 1.5 m row spacing, and covered with either a white (fall) or black (spring) virtually impermeable film. Plots were arranged in a randomized complete block design with each treatment represented by four blocks of 10 plants per plot. The experimental design consisted of four plant genotypes (Fla. 8000, Fla. 8000 *BS2*, Fla. 8000 *BS2 EFR*, and Fla. 8000 *EFR*) crossed with an *Xanthomonas perforans* inoculation treatment. Inoculated treatment plots were inoculated with a cocktail of *Xanthomonas perforans* race T4 strains: GEV904, GEV917, GEV1001, and GEV1063. Inoculations and mock inoculations were performed two weeks after transplanting 4-week old seedlings at 45.7 cm spacing. Non-inoculated plots were mock inoculated with an equal volume of water. Leaf samples were collected at the end of the season and 2 mature leaves from the upper canopy of each of the 10 plants in a plot were binned for a single sample. Samples were shipped on ice and processed within 24 hours of collection. The experiment was repeated during three separate field seasons: fall 2017, spring 2018, and fall 2018.

Leaf fresh weights were recorded prior to leaf wash extraction. Leaves were double bagged in ziplock bags with 600 ml of water and 12 µl Hi-Wett (Loveland Products Inx., Greeley, CO). Leaves were washed in bags by vortexing on high for 30 seconds and then sonicated for 30 seconds using a Branson 5800 sonicator in two successive cycles. Leaf wash was then transferred to a Thermo Scientific Nalgene Analytical Test Filter Funnel and filtered with a vacuum pump. Filters containing leaf extract were cut into quarters and stored in 2 ml microcentrifuge tubes at -80C.

DNA extraction from the leaf extract filter paper was performed using the Omega Bio-Tek E.Z.N.A. Plant DNA Kit following the manufacturer's instructions. Extracted DNA was used as a template for an initial PCR amplification using 16S primer pair for the V5-V6 region (799F and 1115R) that do not amplify the chloroplast 16S sequences (Laforest-Lapointe et al. 2017; Redford et al. 2010). As previously described in Xue et al. 2019, a second PCR was performed while adding one of 8 variable length barcodes (5-8 bp) to each sample and space for the Nextera primer to bind. The external fusion PCR primers for the second PCR contained a 14 bp overlap with the end of the internal primer as well as one of two options: an 8-bp i7 index and P7 flow cell adapter sequence or a 7-bp spacer i5 index, and P5 flow cell adapter sequence.

The first PCR reaction used a total volume of 10 µL. Reactions used 0.2 µL of hot-start high fidelity Clonetech PrimeSTAR GLX polymerase (Takara Bio, Kusatusu, Japan), 2 µL of 5X buffer, 0.8 µL of 10 nM dNTPs, 0.25 µL of 10 nM forward and reverse primer, 0.7 µg T4 gene 32 protein, and 10 ng of template DNA. The Thermocycler protocol was as follows: a hot start at 98˚C for 5 minutes, 35 cycles of

denaturing at 98˚C for 45 seconds, annealing at 50˚C for 45 sec., extension at 68˚C for 1 min., and a final 15 min. extension at 68˚C.

The second PCR reaction used a total volume of 25 µL. Reactions contained 0.5 µL of hot-start high fidelity Clonetech PrimeSTAR GLX polymerase (Takara Bio, Kusatusu, Japan), 5 µL of 5X buffer, 1 µL of each 10 nM primer, and 1 µL of product from the previous PCR as template. The Thermocycler protocol was as follows: a hot start at 98˚C for 5 minutes, 15 cycles of denaturing at 98˚C for 30 seconds, annealing at 60˚C for 0:45, extension at 68˚C for 1:00, and a final extension of 10 minutes at 68˚C.

Successful amplification at each step was visually confirmed on a UV-transilluminator following gel electrophoresis of the product in 1% agarose and staining with gel red. Final amplification products were purified with the Omega BioTek E-Z 96 Cycle Pure kit and quantified using a Qubit 2.0 fluorometer with the Qubit dsDNA HS assay (Thermo Scientific, Grand Island, NY). DNA was pooled at equal concentration and sent for Illumina MiSeq sequencing at the University of Wisconsin Biotechnology Center (Madison, WI).

Processing of Sequencing Data: External barcodes were demultiplexed by the Wisconsin Biotech Center. Each set of matching external barcodes contained multiple samples distinguished by the third barcode sequence between the Nextera adapter and 16S primer sequence. This second demultiplexing was performed in Qiime2 (Boylen et al. 2018) using the cut-adapt plugin from the demux-paired function.

Denoising, replication, and chimera filtering were all performed in Qiime2 using the dada2 plugin's "denoise-paired" option using default settings. Taxonomic assignment was performed using naïve Bayesian classification. The Greengenes

database was used as a reference database for taxonomic identities (McDonald et al. 2012). Following assignment, a dataset for downstream analysis was created by combining amplicon sequence variants identified to the same genus. Sequences that could not be identified to a given taxonomic resolution were lumped into a single unclassified taxon with terminal identification at the next highest taxonomic rank.

Illumina sequencing of 16S amplicons are archived in the sequence read archive under BioProject accession number PRJNA604617. In order to address a potential bias in community diversity rooted in differential sequencing depth between plots, samples were assessed using rarefaction curves of the number of genera (Figure S1). In order to retain as many samples as possible, samples were rarefied to an even depth of 10,000 sequences. Each season of collected data contained 32 samples. Of the 96 total samples collected, 84 were retained at this sampling depth. The results of rarefaction show that not all samples exhibit a plateau in the number of genera present at the final sampling depth, suggesting that some samples may be underrepresented in more rare taxa. Across all three seasons of data, a total of 691 distinct genera were detected.

Yield Analysis: Tomatoes were harvested by making four separate picks between 10 to 12 weeks after transplanting. Fruit were graded and sorted into the following categories according to USDA grading standards: Culls, Small, Medium, Large, and Extra-large. Cull and small fruits were not incorporated into marketable yield estimates used in this analysis. Since the number of picks made to assess yield varied from season to season, the total yield for each season was analyzed independently.

Bacterial Spot Disease Rating: Individual plants within each plot were assessed for bacterial spot using the Horsfall-Barratt scale (Horsfall and Barratt 1945) and

transformed to the midpoint value of each interval prior to statistical analysis (Redman et al. 1964).

Statistical Analyses: All statistical analysis was performed in R (version 4.1.0). Transformed averages of disease severity per plot, average fruit yield, and alpha diversity metrics were analyzed by performing a mixed effects linear model using the lmer and lmerTest packages in R followed by post-hoc Tukey's HSD test in R using a value of $p < 0.05$. Mixed models included block nested within season-by-year as random effects. The assumptions of normality were assessed by visual inspection of residual value histograms to confirm a normal distribution of model residuals.

Permutational Multiple Analysis of Variance (PERMANOVA) was used to compare bacterial community composition among genotypes at the genus level. Bacterial community structure comparisons were visualized using distance-based redundancy analysis (db-RDA) of the Bray-Curtis dissimilarity matrix to visualize differences in community structure among bacterial phyllosphere communities.

We expected *Xanthomonas* to be a highly abundant taxa in our dataset, and to respond strongly to the presence of the *BS2* gene. To determine whether any effects seen on phylosphere community structure stemmed solely from changes to the *Xanthomonas* population, we created a subset of data that excluded *Xanthomonas* and rerarefied to a common sequence depth of 2,992 sequences. We then used the same PERMANOVA models as above to quantify the effect of the season, the *BS2* gene, and the *EFR* gene and their interactions on the composition of the non-*Xanthomonas* community.

The presence of the *BS2* gene could affect phyllosphere community composition due to the direct effects of *BS2* gene expression or due to indirect effects mediated through the Xanthomonas population and consequent disease symptoms. To disentangle these possibilities, we ran PERMANOVA models that included both the *BS2* gene treatment and the quantitative assessment of bacterial spot disease severity. We ran this model in two ways: once with the *BS2* gene treatment entered first in the model, and once with the disease severity term entered first. By comparing the resulting R^2 and P values associated with these terms when entered first or second in the model we can assess how much variation in bacterial community composition can be attributed uniquely to one or the other term, and how much of their effects cannot be distinguished. As before, we did this on the entire community dataset, as well as a subset that excluded *Xanthomonas*.

Individual taxonomic relationships were assessed using rarefied metabarcoding data. Taxa were tested whether they differed in their relative abundance based on the presence absence of a transgene by Wilcoxon Rank Sum test to determine if their abundance differed in *Bs2* and non-*Bs2* plants as well *EFR* and non-*EFR* plants. Wilcoxon Rank Sum P values were corrected using False Discovery Rate (FDR) based on the number of applicable rank sum comparisons.

In order to help determine the certainty of the assigned taxonomic identity of OTUs for *Salmonella*, sequences of closely related taxa were obtained from Greengenes database (https://greengenes.secondgenome.com/) and aligned in Mega 7.0. Aligned sequences were then used to construct a maximum likelihood phylogeny.

Identification of an OTU to genus was contingent on it being placed within a monophyletic clade of that genus.

Results

*Collection of field data***:** To assess how disease and resistance reshaped phyllosphere bacterial communities, 16S metabarcoding, disease rating, and yield assessments were conducted over the course of three seasons of field trials that mimicked commercial tomato production in Florida. Field trials consisted of four FL8000 tomato lines to assess the combinations of narrow-spectrum *Bs2* and a broad-spectrum *EFR* resistance to bacterial spot combined with supplemental *X*. *perforans* inoculation treatments. An initial analysis was conducted to test whether *X*. *perforans* inoculated and non-inoculated plots differed. ANOVA of yield, disease rating, proportion of *Xanthomonas* in the metabarcoding, and PERMANOVA testing bacterial community structure were not affected by the inoculation treatment ($p > 0.1$). Therefore, inoculated and non-inoculated treatment levels were combined in subsequent analyses.

*Transgenic resistance increased yield and lowered disease ratings***.** Bacterial spot disease severity differed based on the presence of *Bs2* and *EFR* (Figure 1, Table 1). In all three seasons sampled, *Bs2* expressing plants were rated as having less than 1% disease severity. Disease severity in *EFR* expressing plants ranged from as low as 12% in the fall of 2017 to 47% in spring 2018 whereas WT Fla. 8000 plants ranged from 24% to 68%. WT plants and plants only expressing *EFR* had significantly higher disease in the spring of 2018 than either fall season (Table 1; Tukey's HSD $p < 0.05$). Plants expressing either or both *Bs2* and *EFR* displayed reduced symptoms compared

to WT plants and no differences in symptoms were observed between *Bs2* and *Bs2*/*EFR* expressing plants (Table S1).

Due to differences in the number of fruit pickings between seasons, differences in yield were not compared between seasons. Yield differences were observed in plants expressing *Bs2* compared to non-*Bs2* plants (Table 1). Only in Fall 2017 did *Bs2* plants statistically yield higher than WT non-*Bs2* plants. No yield difference was observed between plants expressing only *EFR* and WT plants in that season, but *Bs2* plants consistently had higher yields than *EFR* plants. While clear differences were observed for disease severity among genotypes in both 2018 seasons, differences in bacterial leaf spot symptoms did not translate to a statistically significant difference in fruit yield.

Phyllosphere community structure differs by trial and Bs2 expression: The richness of bacterial genera in phyllosphere communities was influenced by the expression of *Bs2* and subsequent bacterial spot infection (Figure 2, Table S2). Plants expressing *Bs2* contained on average 54 more unique taxonomic identities than their non-*Bs2* counterparts. Communities associated with Bs2 plants had higher Shannon index values than their non-Bs2 counterparts (Figure 3).

A PERMANOVA of Bray-Curtis distances revealed community composition significantly differed based on sampling date, *Bs2*, and an interaction between those two terms ($p = 0.001$). Visualization of Bray-Curtis distances using distance-based redundancy analysis (db-RDA) clustered *EFR* and WT plants together (Figure 4). Combining the disease severity, represented by the size of points in the ordination, with visualization of the db-RDA ordination shows that similar communities on WT and *EFR* expressing plants were under high disease pressure (Figure 4). Plants expressing *Bs2*

and low disease severity were separate from the WT and *EFR* only communities. Furthermore, *Bs2* communities from spring 2018 clustered separately from those from fall samplings in 2017 and 2018. The composition of bacterial communities of WT and *EFR* expressing plants differed between sampling dates. PERMANOVA of community composition with *Xanthomonas* ASVs removed from the dataset still displayed strong significant differences in community composition with respect to the BS2 gene and season, and no consistent effects of the *EFR* gene (Table S3).

Individual genera of interest, *Xanthomonas* and *Pseudomonas*, were fit onto the ordination as vectors (Figure 5). Just as high disease pressure was found in WT and *EFR* expressing plants, an ASV with an identical sequence to *X. perforans* strains used for inoculation was also associated with those bacterial communities. We chose to examine the ordination of a *Pseudomonas* ASV because symptoms of bacterial speck, caused by *P. syringae* pv. Tomato, have been noted on *Bs2* expressing plants in spring plantings (G. Vallad, personal observation). The placement of the *Pseudomonas* ASV locates among the bacterial communities from *Bs2* expressing plants only in spring 2018. We found that 20 times more rain was recorded at the experimental site in May 2018 than either October 2017 or 2018, fall sampling months (Table S4). This increased rainfall likely influenced the increased bacterial spot severity recorded in the spring 2018 planting over the fall plantings (Figure 1).

Xanthomonas alters the phyllosphere in a way that only a small subset of taxa find conducive: We used a mediation analysis to determine if the effect of the *Bs2* gene on community composition could be attributed in whole or part to its effect on disease severity. After accounting for the effects of seasons, the presence of the *Bs2* gene

explained 23.7% of the variation in bacterial composition (Table S5). However, when disease severity was included first in the model, disease severity explained 25% of the variance in composition, and the *Bs2* gene explained only an additional 2.8% (Table S5). Very little of the variation in bacterial composition could be uniquely attributed to either the *Bs2* gene (2.8%) or disease severity (4%) – the vast majority of the effects of each of these two terms was shared with the other. As before, we repeated this analysis with a *Xanthomonas* filtered dataset. While the overall effect of the *Bs2* gene (and disease severity) was weaker (14.9 vs. 23.7% variation explained), the qualitative result was the same: most of the variation attributed to the *Bs2* gene could also be attributed to disease severity, with a small, but significant amount of variation attributed uniquely to each of the two terms (Table S4).

Individual taxa differ in relative abundance based on the presence or absence of Bs2: Because community structure was not altered by the expression of *EFR*, subsequent analysis of individual community members focuses on differences between *Bs2* and non-*Bs2* genotypes. In order to determine which taxa drive differences in community structure, Wilcoxon rank-sum tests were performed on all genera. Comparisons were made between *Bs2* genotypes (*Bs2, Bs2/EFR*) and non-*Bs2* (WT, *EFR*) genotypes. 604 genera were present in a sufficient number of samples to perform a Wilcox test. Of these 604 taxa, 119 differed in their rank sums between genotypes (FDR adjusted P value < 0.05). Taxa who differed by rank sum and had a greater relative abundance on *Bs2* genotypes were considered to be *Bs2* associated taxa (Figure 5, checkered colors) whereas those with a higher abundance on non-*Bs2* plants were considered non-*Bs2* associated (Figure 6). A total of 106 taxa were *Bs2*

associated; cumulatively, these taxa made up 51% of the community on *Bs2* plants and 13% on non-*Bs2* plants (Figure 6). Excluding *Xanthomonas*, 12 of the 13 non-*Bs2* associated taxa made up 3.5% of *Bs2* communities and 16.5% of non-*Bs2* communities. Unassociated taxa, those with an FDR adjusted P value > 0.05, had similar distributions among genotypes, making up 36% and 32% of the *Bs2* and non-*Bs2* communities respectively.

Across all genotypes, a small number of taxa made up the majority of the phyllosphere community. The twelve most relatively abundant genera represented 85% of the overall community (Figure 7). *Xanthomonas* was found on plants of all genotypes and was the most relatively abundant member of the community from non-*Bs2* expressing plants. The proportion of *Xanthomonas* in the community was 4 times greater in non-*Bs2* plants. Of the 12 most relatively abundant taxa, 8 were either *Bs2* or non-*Bs2* associated (Figure 7, denoted by asterisk). Common phyllosphere genera *Sphingomonas*, *Methylobacterium*, and *Pseudomonas* were among the most relatively abundant genera. Interestingly, *Pseudomonas* ranked as the third most relatively abundant genera across all genotypes and was not found associated with the presence or absence of *Bs2*, but made up 8.6% and 10.3% of *Bs2* and non-*Bs2* genotypes, respectively. Both *Sphigomonas* and *Methylobacterium* were among the most relatively abundant genera across all genotypes but were three times more relatively abundant on *Bs2* expressing plants. *Sphigomonas* and *Methylobacterium* relative abundance was negatively correlated with *Xanthomonas* relative abundance whereas *Agrobacterium* appears more abundant on non-*Bs2* plants along with *Xanthomonas*.

Salmonella enterica identified as a member of the tomato phyllosphere bacterial community: Three ASVs were identified as belonging to the genus *Salmonella.* In order to resolve the identity of these ASVs, sequences of closely related taxa were obtained from Genbank and the aligned sequences were used to construct a maximum likelihood phylogeny (Figure S2). While not all *Salmonella* spp. form a single monophyletic clade, all *S. enterica* accessions formed a monophyletic clade along with the three ASVs putatively identified as such, suggesting an appropriate taxonomic identification. ASV 1 was the sequence most often identified as *S. enterica* whereas ASV 3 was only found in a single sample in spring 2018 from *Bs2/EFR* plants (Table S7). ASV 1 and ASV 2 were commonly found concurrently and seldomly in fall 2017 with the exception of three samples. In contrast, they were found in every sample in fall 2018 and every sample of *Bs2* and *Bs2/EFR* expressing plants in spring 2018.

Discussion

Leaves support large populations of bacteria. The bacterial community of the tomato phyllosphere has previously been described as being similar to the airborne community (Ottesen et al. 2016) and stable, not prone to dramatic shifts from events such as irrigation (Telias et al. 2011). However, here we found that biotic stress, in the form of infection with *X*. *perforans* pathogenesis, resulted in dramatic restructuring of the phyllosphere community. The relative abundance of most bacterial genera was reduced in leaves, indicating that *Xanthomonas* infection alters the phyllosphere environment in ways that are largely detrimental to non-pathogenic microbial inhabitants.

The presence of *Xanthomonas*, as well as the resulting bacterial spot disease, was the dominant factor influencing the bacterial community in this study. Due to the prevalence of *Xanthomonas spp.* in the environment as well as our experimental design, we found that yield, disease rating, and proportion of *Xanthomonas* in the metabarcoding were not affected by our experimental inoculation. Thus, we were unable to assess differences between bacterial communities of truly healthy and diseased WT or *EFR*-expressing plants. The overlap in terms of disease rating and the *Bs2* transgene in explaining variation in the alpha and beta diversity among samples suggests *Xanthomonas* pathogenesis leads to a less complex community dominated by the pathogen. Most of the variation in bacterial community composition that could be attributed to the *BS2* gene could also be attributed to variation in disease severity. The consensus of alpha and beta diversity mediation suggest bacterial spot is more directly responsible for phyllosphere community modification than is the subsequent resistance response. We found that only a small subset of phyllosphere taxa benefited from the disease state of the leaves. This is reflected in the depression in alpha diversity in diseased leaves and the finding that many more individual taxa were significantly more associated with the *Bs2* expressing genotypes compared to the small number of non-*Bs2* associated taxa. Despite variation in healthy phyllosphere microbiomes from season to season, diseased microbiomes converged repeatedly into a similar community structure.

We found that while both *Bs2* and *EFR* expressing plants had significantly reduced bacterial spot, plants only expressing *EFR* had high levels of disease compared to *Bs2* expressing plants. Field-level resistance to bacterial spot has been

demonstrated by plants expressing *Bs2*, *EFR*, or both (Horvath et al. 2012; Kunwar et al. 2018); the differences we observed in disease severity between *EFR* and *Bs2* expressing plants match previously reported values. In addition to resistance against bacterial spot, *EFR* expressing plants are resistant to bacterial wilt caused by *Ralstonia solanacearum* (Kunwar et al. 2018). Instead of recognition of a specific pathogen effector, *EFR* recognizes one of the most widely conserved and abundant proteins in bacteria (Kunze et al. 2004) and leads to downstream flux in Ca^{2+} concentrations, oxidative burst, and activation of mitogen-activated protein kinases (Jones and Dangl 2006). Somewhat surprisingly, the presence of the *EFR* transgene on its own did not result in substantial changes to the phyllosphere community structure (i.e. diversity or composition) despite the ubiquitous synthesis of its elicitor by the bacterial community, perhaps because tomato plants expressing *EFR* do not appear to constitutively activate defense responses (Lacombe et al. 2010).

During infection, *Xanthomonas* fundamentally alters the phyllosphere. During disease development, *Xanthomonas* spreads from the point of entry and causes cell damage that extends beyond the site of infection (Ciardi et al. 2000). Cellular damage results in membrane instability and subsequent leakage of cellular constituents into the apoplast and onto the phylloplane. At the same time, leaves responsible for carbohydrate production through photosynthesis shift from carbohydrate sources to sinks (Garcia-Seco, Chiapello et al. 2017); infected leaves then receive carbohydrates from other source leaves instead of sending their own photosynthates away. These fundamental changes to the phyllosphere may in turn alter the distribution of nutrients across the infected leaf surface and the plant, in general. This change in carbon flow

means nutrient oases are no longer limited to glandular trichomes and cellular junctions, nutrient availability then follows *Xanthomonas* infection and phyllosphere colonization success may no longer be restricted to bacterial genera specialized in carbon scavenging and unique carbon utilization.

Changes to the available resource base in infected leaves may underlie the dramatic shifts in phyllosphere microbial composition. *Sphingomonas* and *Methylobacterium* are considered cosmopolitan members of the bacterial community due to their omnipresence in the phyllosphere across the plant kingdom. The dominance and commonality of *Sphingomonas* and *Methylobacterium* in phyllosphere bacterial communities of numerous plant species has been attributed to these taxa's capacity in carbon acquisition and/or utilization(Wilson and Lindow 1994; Delmotte et al. 2009). We found *Sphingomonas* and *Methylobacterium* among the most abundant genera on *Bs2* expressing plants, which had little disease and smaller *Xanthomonas* relative abundance. *Sphingomonas* and *Methylobacterium* were not among the most abundant bacteria in the phyllosphere of non-*Bs2* plants to the same extent that they were on healthy *Bs2* plants. On the other hand, *Agrobacterium* relative abundance increased and was a similar percentage to *Sphingomonas* and five times larger than *Methylobacterium* on the diseased plants without the *Bs2* gene. This community structure shift suggests that on a diseased host, previously viable strategies in the phyllosphere such as the use single carbon sugars no longer provided the same advantages as the do on healthy hosts.

Previous studies have examined how disease can alter the bacterial community of tomato, focusing on the root-associated communities, rhizoplane and rhizosphere,

and effects of disease caused by *R. solanacearium* (Gu et al. 2016, Hu et al. 2016). In addition to the direct effects of disease on the plant, *R. solanacearium* infection alters root exudates which in turn directly affects the rhizosphere bacterial community.

Other investigations of the tomato phyllosphere have also found an abundance of Xanthomonadaceae family members (Allard et al. 2018) and identified *Xanthomonas* as a core member of plants grown in Maryland, Virginia, and North Carolina, but not California (Ottesen et al. 2015, Ottesen et al. 2019). During the tomato growing season, weather conditions between California and the East Coast of the United States are distinct with low relative humidity and no rain events in California (https://www.wunderground.com/history). Environmental factors appear to strongly influence phyllosphere bacterial community structure.

Rain events have long been accepted to increase plant disease and food safety risks by enhanced dissemination of pathogens or creating a more favorable phyllosphere environment (Cevallos-Cevallos et al. 2012, Thompson et al. 2013). As the tomato grows and the phyllosphere physically moves up and away from the soil, the phyllosphere resembles the airborne community as opposed to the soil or rhizosphere community (Ottesen et al. 2013, Ottesen et al. 2016). A recent examination of airborne bacterial communities over a 7-year period found *Pseudomonas* as a core member and that consistent seasonal fluctuations of the airborne community can lead to bacterial introductions via rain events (Cáliz et al. 2018). We found that *Pseudomonas* was the third most abundant genera regardless of host genotype. A correlation unique to the tomato phyllosphere bacterial community was shown among members of *Pseudomonas* and *Methylobacterium* (Ottesen et al. 2016). We found the overall abundance of

Methylobacterium associated with plants expressing *Bs2* but overall, we did not find *Pseudomonas* associated with host genotype when the fall samples were included. In spring 2018, we found a distinct community structure for plants possessing *Bs2* that were associated with a unique ASV, identified by 16S sequence as *P. syringae*, concurrently with a reported bacterial speck outbreak. A deluge of rainfall occurred during the month the spring samples were taken and the appearance of bacterial speck, caused by *Pseudomonas syringae* pv. *tomato*, was observed on *Bs2* expressing plants that season. While *Bs2* confers resistance against *Xanthomonas* infection, these plants are susceptible to *P. syringae* pv. *tomato* infection. In addition to a virulent pathogen and susceptible host, disease requires conducive environmental conditions such as optimal temperature and humidity (Horsfall and Dimond 1959) and microbial community (Hacquard et al. 2017). Plants resistant to *Xanthomonas* infection had a more diverse bacterial community and a second pathogen appeared to thrive under conducive environmental conditions and may have had its own impacts on phyllosphere bacterial communities.

Several ASVs identified as *Salmonella. enterica* were found in samples from in fall 2018 and across all genotypes in spring 2018. We were surprised that the incidence of *S. enterica* was not correlated with plant disease as previous studies have identified plant disease as a food safety risk factor with larger populations of *S. enterica* found on diseased plants (Meng et al. 2013, Potnis et al. 2014, Potnis et al. 2015). Given the capacity of *S. enterica* to thrive in the phyllosphere of *Xanthomonas*-infected tomato plants, we might have expected that genotypes without *Bs2* would be more likely hosts of *S. enterica.* However, in spring 2018 *Bs2* expressing plants were not disease free as

bacterial speck was observed. Since we were unable to quantify the absolute abundance of *S. enterica* populations in the current study and only a single time point was sampled, it is unclear the fate of the *S. enterica* populations among the host genotypes and whether plant disease affected them. It is also possible that our greater ability to detect Salmonella ASVs in the Bs2 genotypes may simply reflect the overwhelming abundance of *Xanthomonas* on the non-Bs2 genotypes, which inevitably reduces the relative abundance of the other microbial populations and can result in rarer taxa falling below our detection limit.

In conclusion, we found effector-triggered immunity controlled the targeted plant disease while maintaining a diverse bacterial community. In fact, *Bs2* expressing plants consistently hosted *S. enterica* as a phyllosphere bacterial community member throughout two growing seasons and under conducive environmental conditions that permitted infection and disease by a second phytobacterial pathogen, *P. syringae* pv. tomato. Plants lacking this specific resistance suffered high pathogen loads and severe disease symptoms; these, in turn, led to a dramatic restructuring of the phyllosphere microbial community and a reduction in taxa adapted to life as leaf epiphytes.

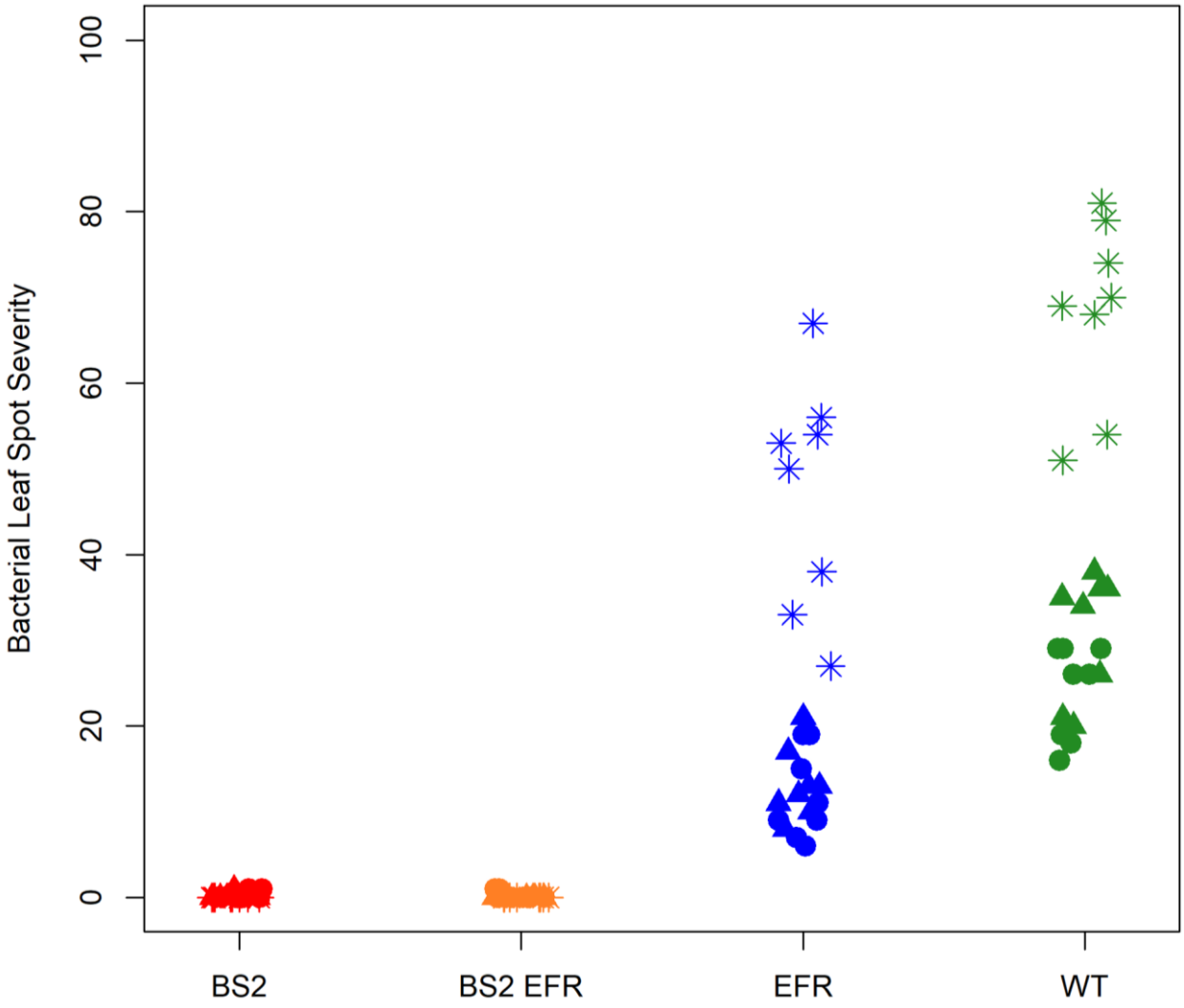

Figure 1. **Little to no bacterial leaf spot was found on *Bs2* expressing plants and more disease occurred during the spring crop.** Bacterial leaf spot severity average per plot. Color designates genotype (green, WT; blue, *EFR*; yellow *Bs2*/*EFR*; red, *Bs2*) and symbol sampling date (circle, fall 2017; asterisk, spring 2018; triangle, fall 2018). A one-way, analysis of variance (ANOVA) was used to assess transformed averages of disease severity per plot and average fruit yield, Tukey's HSD $p < 0.05$.

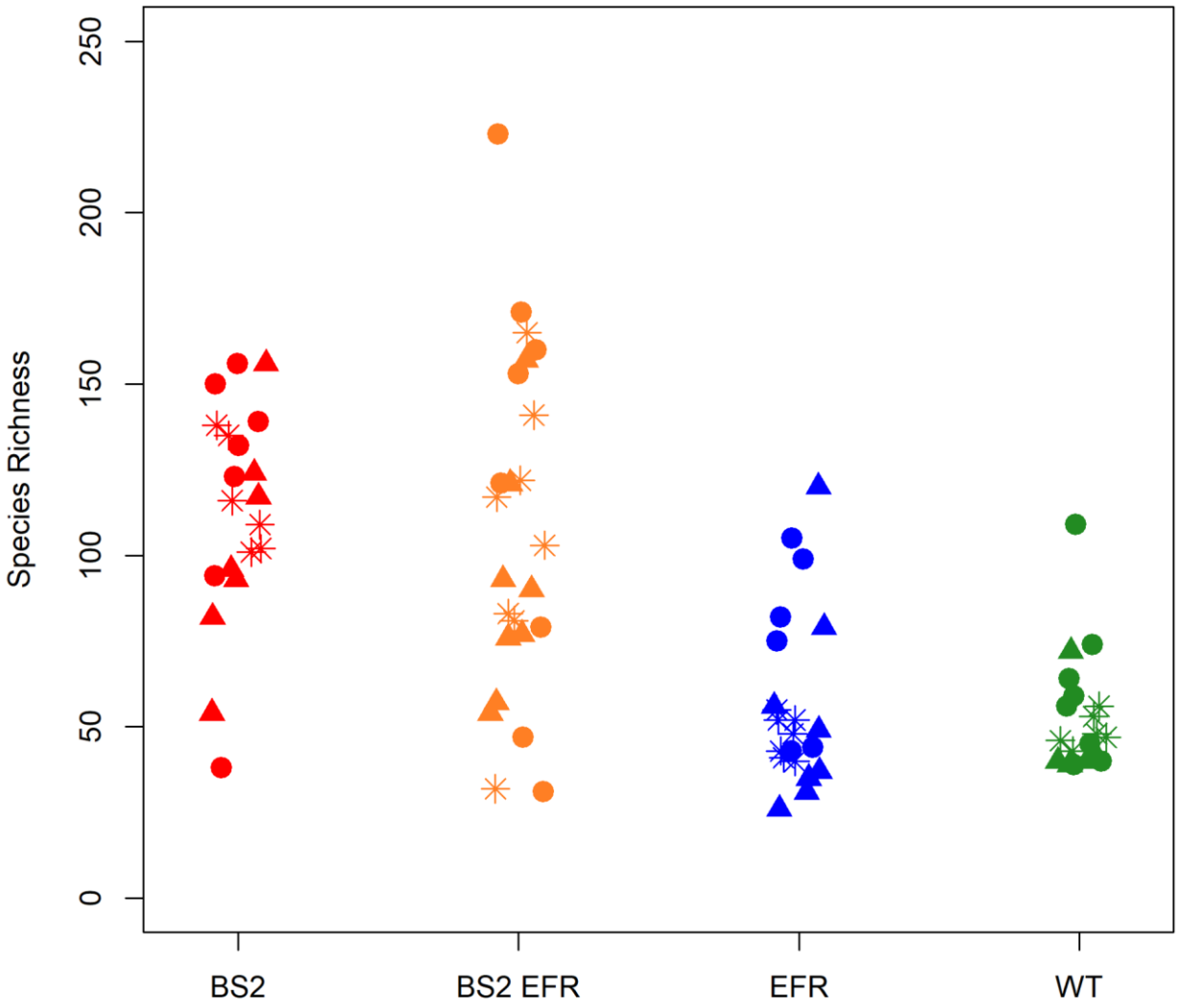

Figure 2. **Richness is greater in plants expressing *Bs2*.** A one-way, analysis of variance (ANOVA) was used to assess species richness. Color designates genotype (green, WT; blue, *EFR*; yellow *Bs2*/*EFR*; red, *Bs2*) and symbol sampling date (circle, fall 2017; asterisk, spring 2018; triangle, fall 2018).

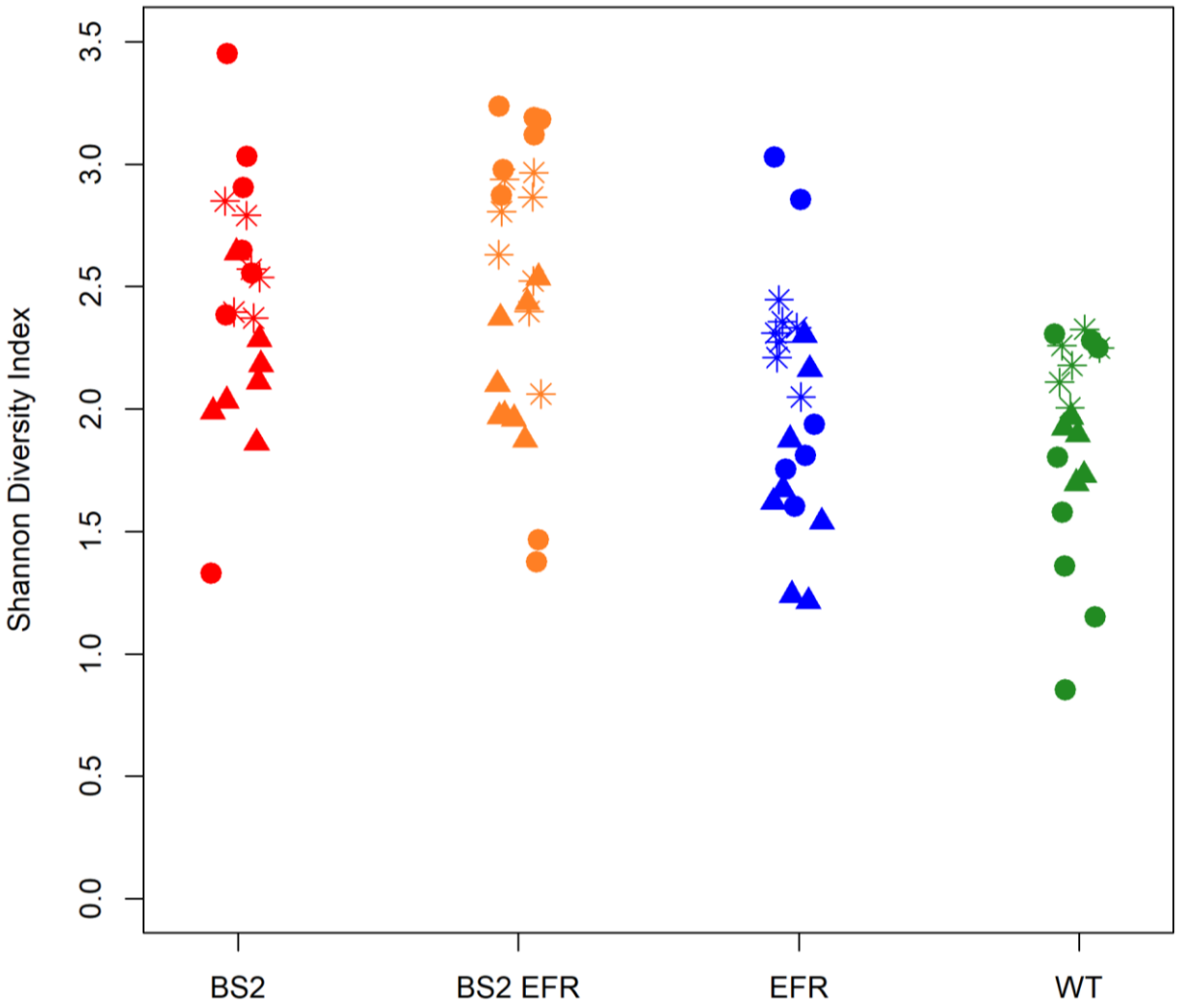

Figure 3. **Shannon Diversity is greater in plants expressing Bs2.** A one-way, analysis of variance (ANOVA) was used to assess Shannon Diversity. Color designates genotype (green, WT; blue, *EFR*; yellow *Bs2*/*EFR*; red, *Bs2*) and symbol sampling date (circle, fall 2017; asterisk, spring 2018; triangle, fall 2018).

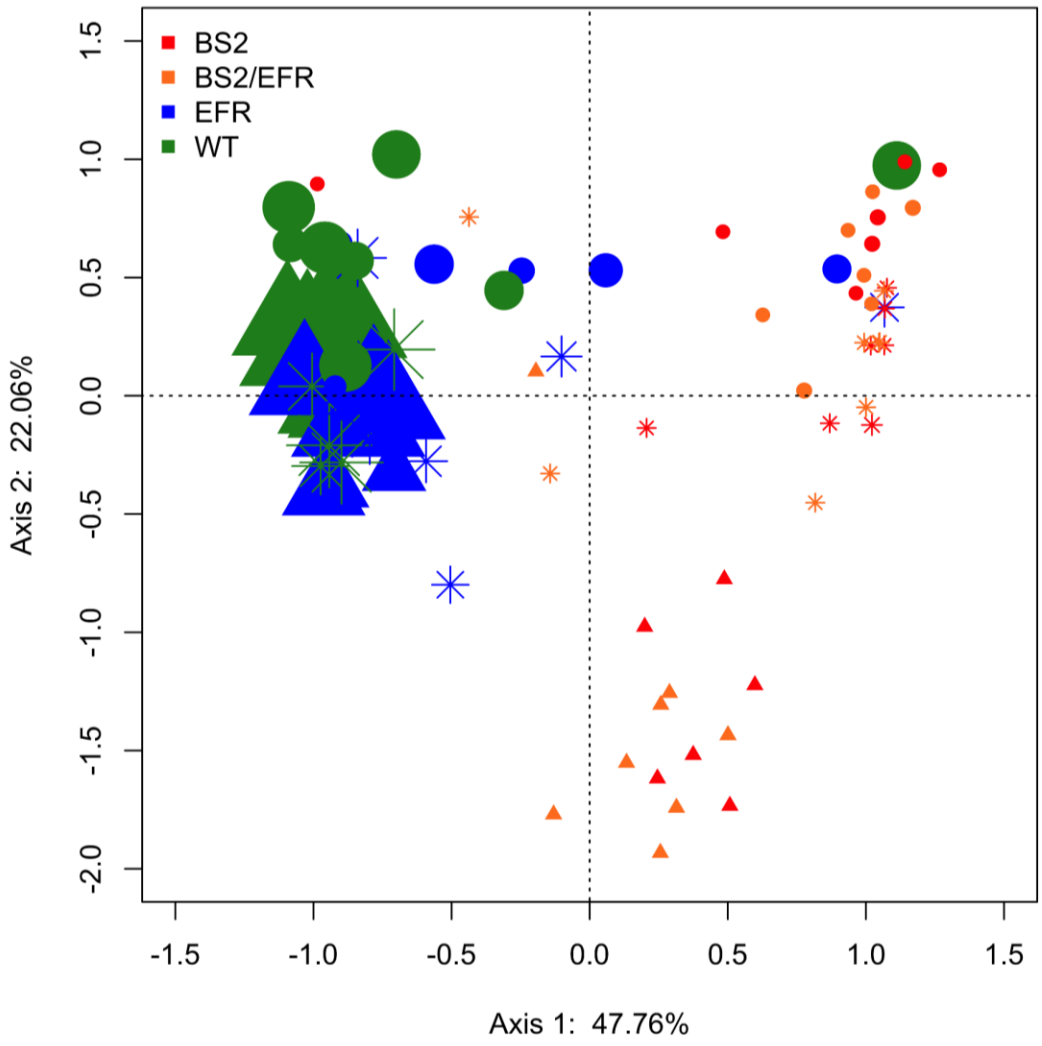

Figure 4. ***Bs2* expression and season affect phyllosphere community structure.** Pairwise comparisons in the overall structure of bacterial phyllosphere communities were made into a Bray-Curtis distance matrix and visualized using distance-based redundancy analysis. A) Disease severity results were combined with the Bray-Curtis distances to display disease pressure on bacterial communities of each genotype. B) Individual ASVs of interest, *Xanthomonas* and *Pseudomonas*, were fit onto the ordination as vectors. Color designates genotype (green, WT; blue, *EFR*; yellow *Bs2*/*EFR*; red, *Bs2*) and symbol sampling date (circle, fall 2017; asterisk, spring 2018; triangle, fall 2018).

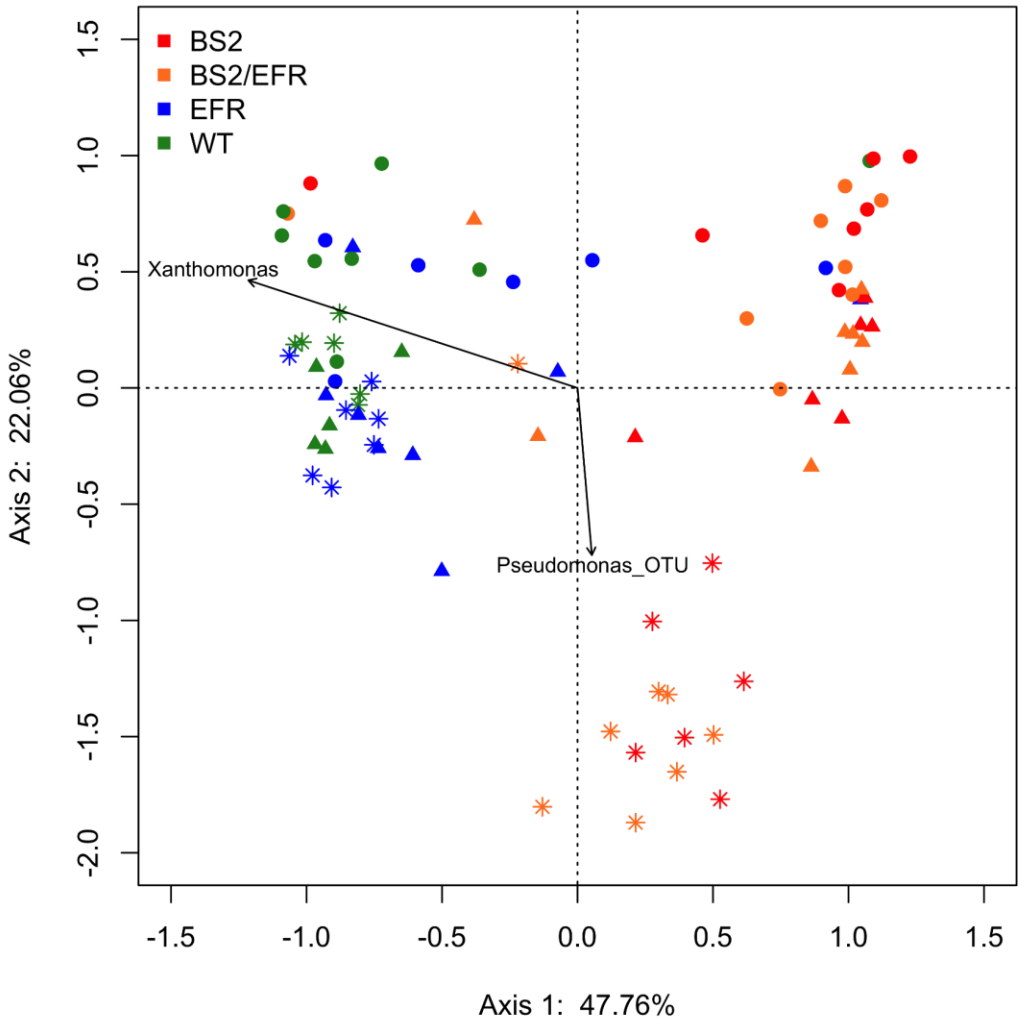

Figure 5. ***Xanthomonas, Pseudomonas* ASVs Correlate with Ordination of Phyllosphere Community.** Pairwise comparisons in the overall structure of bacterial phyllosphere communities were made into a Bray-Curtis distance matrix and visualized using distance-based redundancy analysis. Individual ASVs of interest, *Xanthomonas* and *Pseudomonas*, were fit onto the ordination as vectors. Color designates genotype (green, WT; blue, *EFR*; yellow *Bs2*/*EFR*; red, *Bs2*) and symbol sampling date (circle, fall 2017; asterisk, spring 2018; triangle, fall 2018).

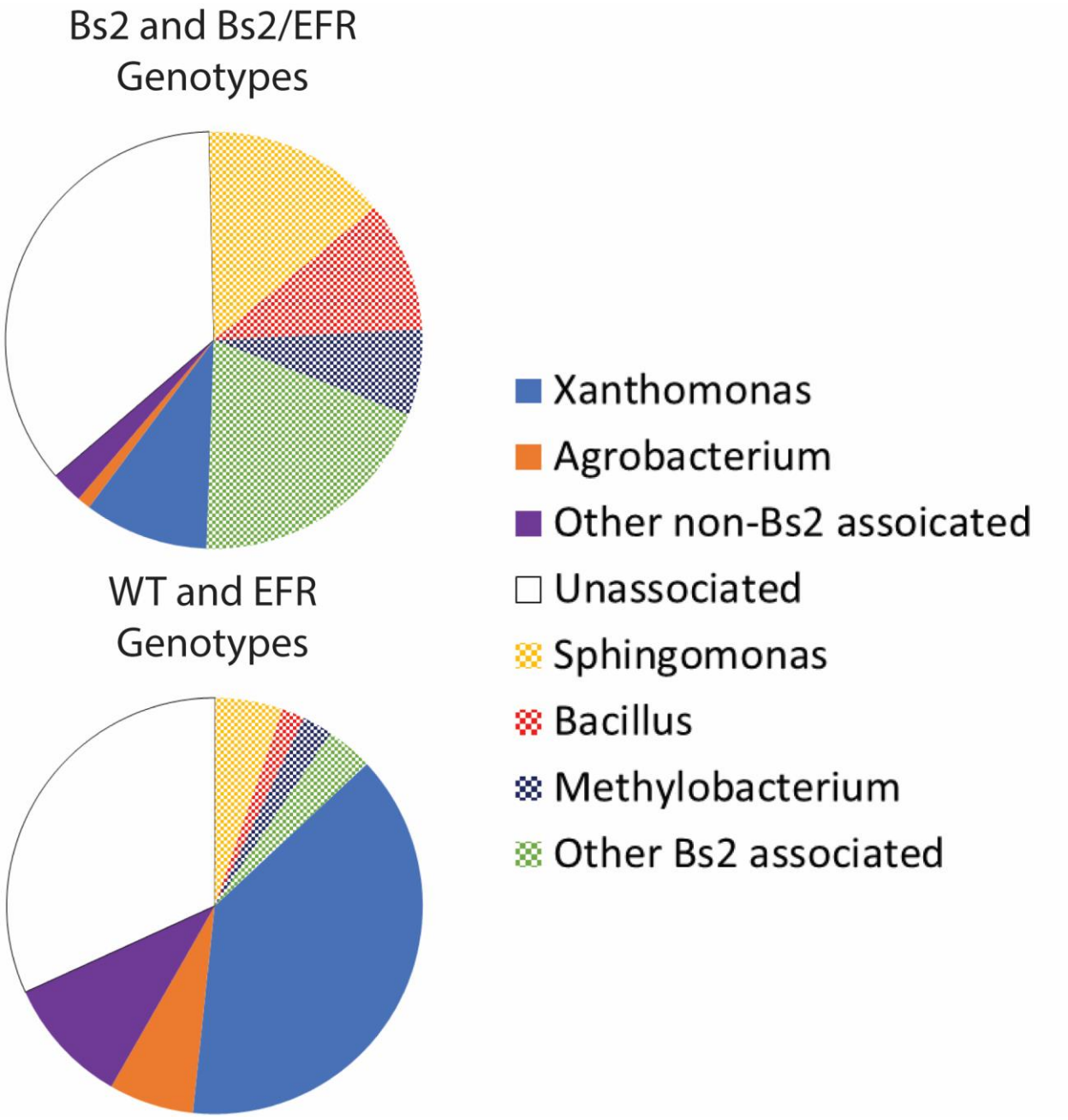

Figure 6. ***Bs2* expression influenced individual taxa relative abundance**. Wilcoxon rank-sum tests were performed on all genera and comparisons were made between *Bs2* and non-*Bs2* genotypes. Upper pie represents the proportion of taxa relative abundance found on *Bs2* and *Bs2*/*EFR* expressing plants while the lower pie is WT and *EFR* expressing plants. Taxa who differed by rank sum and had a greater relative abundance on *Bs2* genotypes labelled as *Bs2* associated (checkered colors) and those with a higher abundance on non-*Bs2* plants labelled non-*Bs2* associated (solid colors).

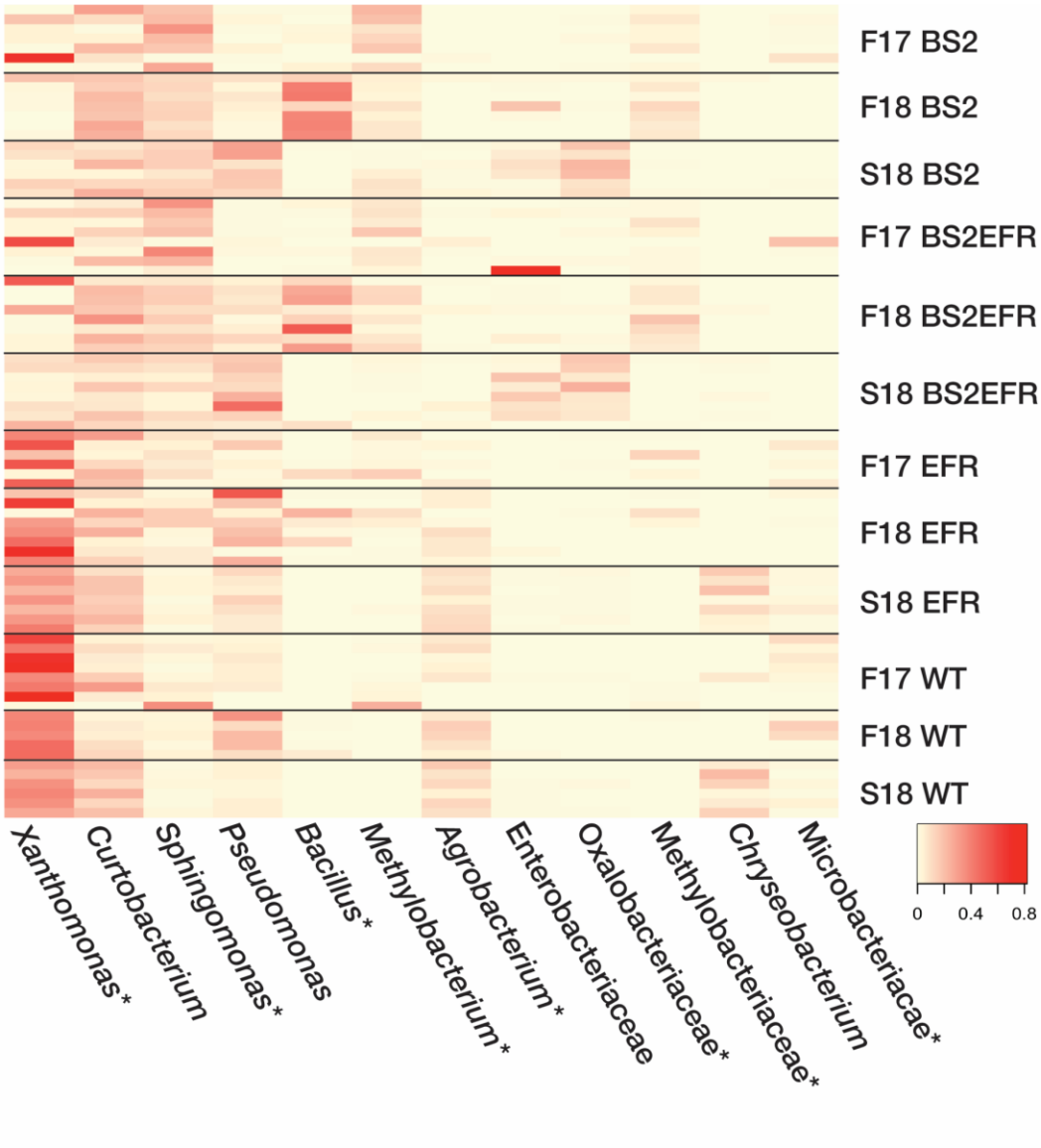

Figure 7. **The twelve most abundant genera represented 85% of the overall phyllosphere bacterial community.** Wilcoxon rank-sum tests were performed to determine general abundance; color intensity denotes relative abundance of each genera for each plot sampled.

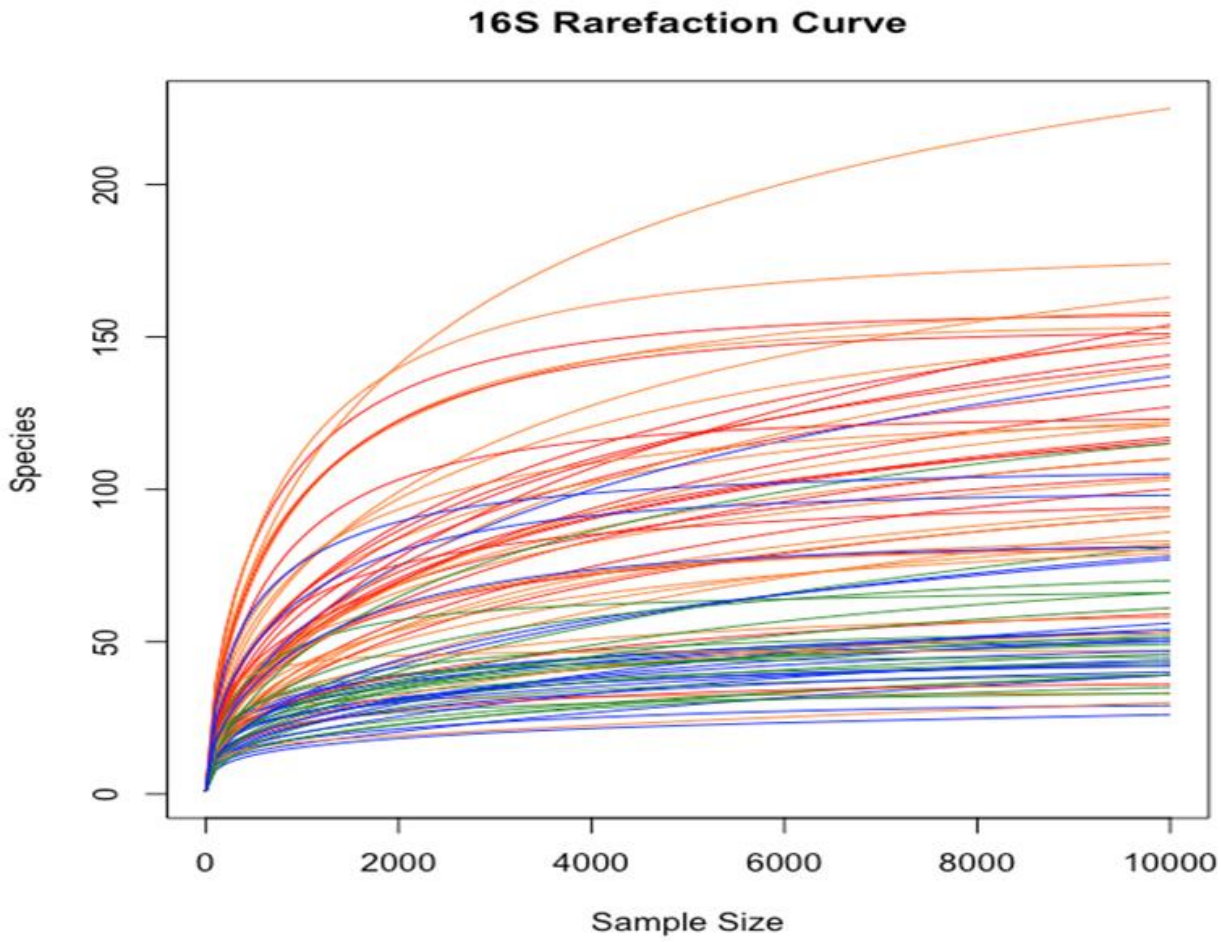

Figure S1: Rarefaction curves of the number of genera identified per sample at increasing sampling depths up to 10,000 reads. Color designates genotype (green, WT; blue, *EFR*; yellow *Bs2*/*EFR*; red, *Bs2*)

Figure S2: Maximum likelihood phylogeny of *Salmonella* enterica sequences and three ASVs identified as belonging to the genus *Salmonella*.

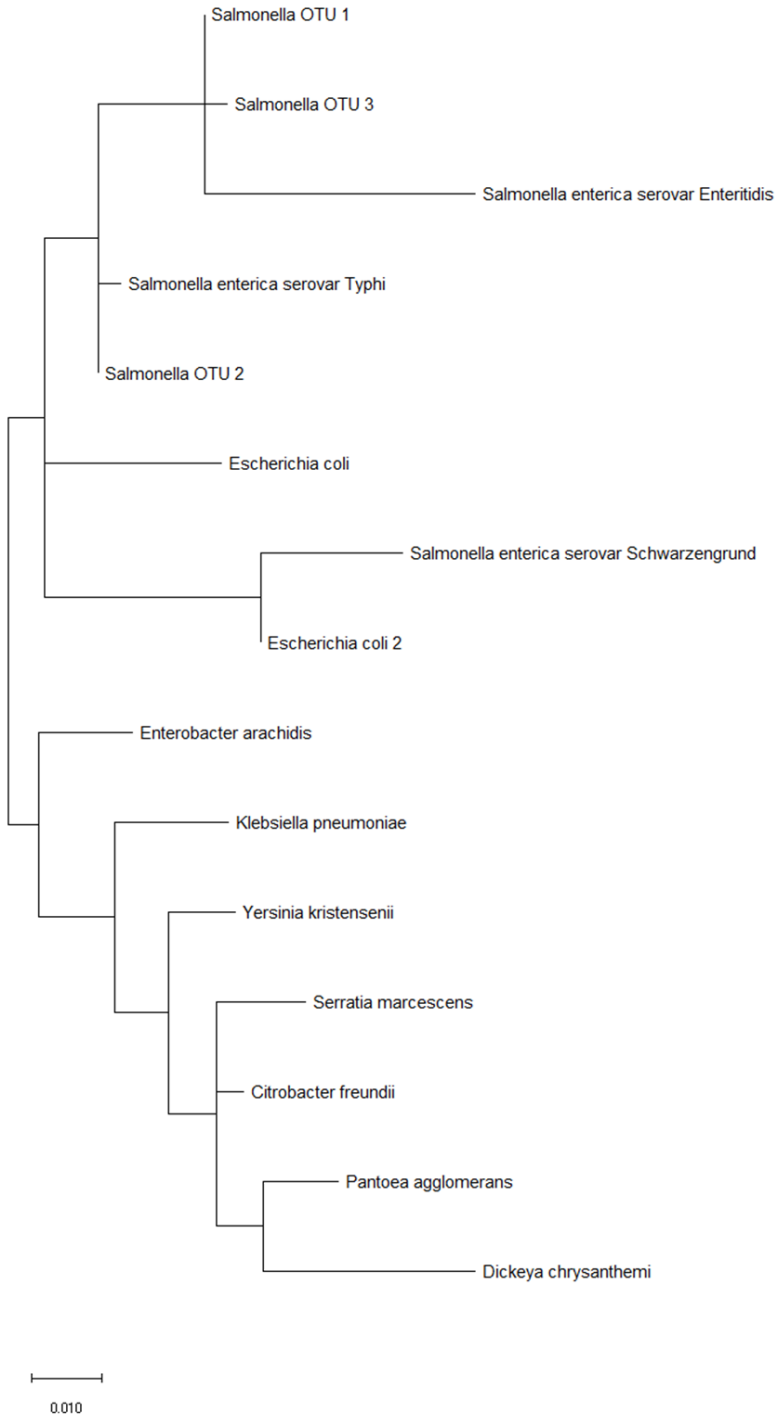

Supplemental Tables

Table 1: Little to no bacterial leaf spot was found on *Bs2* expressing plants and more disease occurred during the spring crop. The Horsfall-Barrat scale was used to estimate the severity of disease based on lesion size, number, and damage from disease progression to the leaf understory. Scores of individual plants were transformed to the midpoint of that interval before being averaged to produce disease severity values per plot. Letters assignments represent Tukey HSD significance groupings within a given season ($p < 0.05$).

Year	Season	Genotype	Disease Severity	Fruit Yield (kg)
2017	Fall	WT	24.0 A	18.1 B
		EFR	11.9 B	18.5 B
		Bs2	0.3 C	42.6 A
		Bs2/EFR	0.3 C	40.4 A
2018	Spring	WT	68.3 a	44.5 ab
		EFR	47.3 b	41.7 b
		Bs2	0.0 c	54.6 a
		Bs2/EFR	0.0 c	55.8 a
2018	Fall	WT	30.8 α	13.8 αβ
		EFR	13.1 β	8.3 β
		Bs2	0.1 χ	20.1 α
		Bs2/EFR	0.0 χ	17.6 α

Table S1: ANOVA results for bacterial spot disease severity ratings.

3 Seasons Disease Severity Analysis						
	Sum of Squares	Mean of Squares	Numerator DF	Denominator DF	F Value	Pr(>F)
BS2	24959	24959	1	81	200.922	2.20E-16
EFR	1704.2	1704.2	1	81	13.719	0.000386
BS2:EFR	1711	1711	1	81	13.773	0.000377
Fall 2017 Disease Severity Analysis						
	Sum of Squares	Mean of Squares	Numerator DF	Denominator DF	F Value	Pr(>F)
BS2	2083.63	2083.63	1	22.484	161.26	9.78E-12
EFR	289.49	289.49	1	22.484	22.404	9.55E-05
BS2:EFR	311.01	311.01	1	22.871	24.07	5.97E-05
Fall 2018 Disease Severity Analysis						
	Sum of Squares	Mean of Squares	Numerator DF	Denominator DF	F Value	Pr(>F)
BS2	3163.4	3163.4	1	24	264.632	1.83E-14
EFR	508.3	508.3	1	24	42.525	9.60E-07
BS2:EFR	495	495	1	24	41.412	1.18E-06
Spring 2018 Disease Severity Analysis						
	Sum of Squares	Mean of Squares	Numerator DF	Denominator DF	F Value	Pr(>F)
BS2	21097.4	21097.4	1	20.183	3.54E+02	2.84E-14
EFR	654.2	654.2	1	20.327	1.10E+01	0.0034
BS2:EFR	703.2	703.2	1	20.183	1.18E+01	0.002584

Table S2. P-values for alpha diversity analyses.

	Effects of genotype across all sampling dates		Effects of *Bs2* expression for individual seasons		
	Bs2	*EFR*	Fall 17	Spring 18	Fall 18
Species Richness	5.8e-10	0.997	2.25e-03	1.18e-06	1.03e-03
Shannon Diversity	1.07e-06	0.295	5.13e-03	8.35e-05	8.01e-04

Table S3. perMANOVA results of phyllosphere bacterial community composition excluding *Xanthomonas.*

	Df	Sums of Sqs	Mean Sps	F. Model	R2	Pr(>F)	
Season	2	3.1811	1.59057	15.0964	0.20376	0.001	***
BS2	1	2.3327	2.33274	22.1406	0.14942	0.001	***
EFR	1	0.0653	0.0653	0.6198	0.00418	0.75	
Season:BS2	2	1.9227	0.96136	9.1245	0.12316	0.001	***
Season:EFR	2	0.1658	0.08289	0.7867	0.01062	0.666	
BS2:EFR	1	0.1626	0.16259	1.5432	0.01041	0.129	
Season:BS2	2	0.1956	0.0978	0.9282	0.01253	0.508	
Residuals	72	7.586	0.10536	0.48591			
Total	83	15.6118	1				
Fall 2017							
BS2	1	0.7584	0.75838	4.3351	0.14234	0.006	**
EFR	1	0.0803	0.08031	0.4591	0.01507	0.889	
BS2:EFR	1	0.1156	0.11563	0.6609	0.0217	0.657	
Residuals	25	4.3735	0.17494	0.82088			
Total	28	5.3278	1				
Spring 2018							
BS2	1	2.0744	2.07443	30.1523	0.53921	0.001	***
EFR	1	0.0794	0.07944	1.1546	0.02065	0.268	
BS2:EFR	1	0.1109	0.11093	1.6123	0.02883	0.183	
Residuals	23	1.5824	0.0688	0.41131			
Total	26	3.8472	1				
Fall 2018							
BS2	1	1.4253	1.42534	20.9855	0.4378	0.001	***
EFR	1	0.0686	0.06864	1.0106	0.02108	0.34	
BS2:EFR	1	0.1316	0.13164	1.9381	0.04043	0.121	
Residuals	24	1.6301	0.06792	0.50069			
Total	27	3.2557	1				

Table S4. Monthly rainfall (mm) measured at 2 m height at the Gulf Coast Research Center in Balm, FL. https://fawn.ifas.ufl.edu/data/

	2017	2018
March	17.78	29.21
April	69.85	85.34
May	44.96	**328.68**
June	261.62	175.01
July	247.14	277.37
August	199.14	201.42
September	226.57	116.33
October	14.73	13.97
November	3.302	55.37

Table S5. Mediation of effects of BS2 gene versus bacterial spot disease severity on bacterial community composition.

	Effect	Df	SS	PseudoF	R^2	P
Model 1	Season	2	2.7316	11.96	0.16876	0.001
	Disease Severity	1	4.0417	35.392	0.24971	0.001
	BS2	1	0.45	3.941	0.0278	0.011
	EFR	1	0.055	0.482	0.0034	0.807
	Residuals	78	8.9076		0.55033	
	Total	83	16.186		1	
Model 2	Season	2	2.7316	11.96	0.16876	0.001
	BS2	1	0.651	5.701	0.04022	0.002
	Disease Severity	1	3.8407	33.632	0.23729	0.001
	EFR	1	0.055	0.482	0.0034	0.807
	Residuals	78	8.9076		0.55033	
	Total	83	16.186		1	
Non-*Xanthomonas* community						
Model 1	Season	2	3.1811	13.4919	0.20376	0.001
	Disease Severity	1	2.6317	22.3233	0.16857	0.001
	BS2	1	0.5248	4.4513	0.03361	0.001
	EFR	1	0.0787	0.6678	0.00504	0.676
	Residuals	78	9.1955		0.58901	
	Total	83	15.6118		1	
Model 2	Season	2	3.1811	13.4919	0.20376	0.001
	BS2	1	2.3327	19.7873	0.14942	0.001
	Disease Severity	1	0.8237	6.9873	0.05276	0.001
	EFR	1	0.0787	0.6678	0.00504	0.708
	Residuals	78	9.1955		0.58901	
	Total	83	15.6118		1	

Table S6. Accessions of full-length 16S rRNA genes from Greengenes used to construct a maximum likelihood phylogeny. http://greengenes.secondgenome.com

Accession	Taxonomy
4475936	*Salmonella enterica* serovar Typhi
4350788	*Salmonella ente*rica serovar Schwarzengrund
4306121	*Salmonella enterica* serovar Enteritidis
558281	*Serratia marcescens*
291478	*Klebsiella pneumonia*
737912	*Citrobacter freundii*
687940	*Enterobacter arachidis*
4359731	*Pantoea agglomerans*
656881	*Escherichia coli*
114510	*Escherichia coli*
775089	*Dikeya chrysanthemi*
274754	*Yersinia kristensenii*

Table S7. Percentage of specific sequences from the bacterial community identified as *Salmonella enterica*.

Sample	ASV 1	ASV 2	ASV 3
F17 Bs2	0	0	0
F17 Bs2	0	0	0
F17 Bs2	0	0	0
F17 Bs2	0	0	0
F17 Bs2	0	0	0
F17 Bs2	0	0	0
F17 Bs2	0	0	0
F17 Bs2/EFR	0	0	0
F17 Bs2/EFR	0	0	0
F17 Bs2/EFR	0	0	0
F17 Bs2/EFR	0	0	0
F17 Bs2/EFR	0	0	0
F17 Bs2/EFR	0	0	0
F17 Bs2/EFR	0	0	0
F17 Bs2/EFR	0	0	0
F17 EFR	0	0	0
F17 EFR	0	0	0
F17 EFR	0	0	0
F17 EFR	0.0019	0.0029	0
F17 EFR	0.0049	0.0016	0
F17 EFR	0	0	0
F17 EFR	0	0	0
F17 WT	0	0	0
F17 WT	0	0	0
F17 WT	0	0	0
F17 WT	0	0	0
F17 WT	0.0007	0	0
F17 WT	0	0	0
F17 WT	0	0	0
F17 WT	0	0	0
S18 Bs2	0.0082	0.0027	0
S18 Bs2	0.0103	0.0024	0
S18 Bs2	0.0095	0.0021	0
S18 Bs2	0.0089	0.0024	0
S18 Bs2	0.0138	0.008	0
S18 Bs2	0.0054	0.0016	0
S18 Bs2/EFR	0.0005	0.0001	0
S18 Bs2/EFR	0.0009	0.0003	0
S18 Bs2/EFR	0.0019	0.0003	0
S18 Bs2/EFR	0.0001	0.0001	0
S18 Bs2/EFR	0.0047	0.0009	0
S18 Bs2/EFR	0.0004	0.0002	0

S18 Bs2/EFR	0.0015	0.0012	0
S18 Bs2/EFR	0.1594	0.0531	0.0045
S18 EFR	0	0	0
S18 EFR	0	0	0
S18 EFR	0	0	0
S18 EFR	0.0002	0.0001	0
S18 EFR	0.0004	0.0001	0
S18 EFR	0	0	0
S18 WT	0	0	0
S18 WT	0	0	0
S18 WT	0	0	0
S18 WT	0	0.0001	0
S18 WT	0	0	0
S18 WT	0	0	0
F18 Bs2	0.0122	0.004	0
F18 Bs2	0.0177	0.0063	0
F18 Bs2	0.0142	0.0049	0
F18 Bs2	0.0018	0.0006	0
F18 Bs2	0.0041	0.0048	0
F18 Bs2	0.0033	0.0013	0
F18 Bs2	0.0027	0.002	0
F18 Bs2/EFR	0.017	0.0006	0
F18 Bs2/EFR	0.0034	0.0019	0
F18 Bs2/EFR	0.0005	0	0
F18 Bs2/EFR	0.0079	0.0036	0
F18 Bs2/EFR	0.0105	0.0018	0
F18 Bs2/EFR	0.0084	0.0043	0
F18 Bs2/EFR	0.0041	0.0015	0
F18 Bs2/EFR	0.0026	0.0012	0
F18 EFR	0.0002	0	0
F18 EFR	0.0003	0	0
F18 EFR	0.0023	0	0
F18 EFR	0.0012	0.0003	0
F18 EFR	0.0003	0	0
F18 EFR	0.0002	0.0001	0
F18 EFR	0.0006	0	0
F18 EFR	0.0002	0	0
F18 WT	0.0001	0.0002	0
F18 WT	00.002	0	0
F18 WT	0	0.0006	0
F18 WT	0.0001	0.0001	0
F18 WT	0.0019	0.0004	0

Literature Cited:

Allard, S. M., Walsh, C. S., Wallis, A. E., Ottesen, A. R., Brown, E. W., and Micallef, S. A. 2016. *Solanum lycopersicum* (tomato) hosts robust phyllosphere and rhizosphere bacterial communities when grown in soil amended with various organic and synthetic fertilizers. Sci. Total Environ. 573:555–563.

Allard, S. M., Ottesen, A. R., Brown, E. W., and Micallef, S. A. 2018. Insect exclusion limits variation in bacterial microbiomes of tomato flowers and fruit. J. Appl. Microbiol. Available at: http://dx.doi.org/10.1111/jam.14087.

Beattie, G. A. 2011. Water relations in the interaction of foliar bacterial pathogens with plants. Annu. Rev. Phytopathol. 49:533–555.

Boller, T., and Felix, G. 2009. A renaissance of elicitors: perception of microbe-associated molecular patterns and danger signals by pattern-recognition receptors. Annu. Rev. Plant Biol. 60:379–406.

Burch, A. Y., Zeisler, V., Yokota, K., Schreiber, L., and Lindow, S. E. 2014. The hygroscopic biosurfactant syringafactin produced by *Pseudomonas syringae* enhances fitness on leaf surfaces during fluctuating humidity. Environ. Microbiol. 16:2086–2098.

Cáliz, J., Triadó-Margarit, X., Camarero, L., and Casamayor, E. O. 2018. A long-term survey unveils strong seasonal patterns in the airborne microbiome coupled to general and regional atmospheric circulations. Proc. Natl. Acad. Sci. U. S. A. 115:12229–12234.

Cevallos-Cevallos, J. M., Danyluk, M. D., Gu, G., Vallad, G. E., and van Bruggen, A. H. C. 2012. Dispersal of *Salmonella typhimurium* by rain splash onto tomato plants. J. Food Prot. 75:472–479.

Ciardi, J. A., Tieman, D. M., Lund, S. T., Jones, J. B., Stall, R. E., and Klee, H. J. 2000. Response to *Xanthomonas campestris* pv. *vesicatoria* in tomato involves regulation of ethylene receptor gene expression. Plant Physiol. 123:81–92.

Debray, R., Conover, A., Zhang, X., Dewald-Wang, E. A., and Koskella, B. 2023. Within-host adaptation alters priority effects within the tomato phyllosphere microbiome. Nature Ecology & Evolution. 7:725–731.

Delmotte, N., Knief, C., Chaffron, S., Innerebner, G., Roschitzki, B., Schlapbach, R., et al. 2009. Community proteogenomics reveals insights into the physiology of phyllosphere bacteria. Proc. Natl. Acad. Sci. U. S. A. 106:16428–16433.

Garcia-Seco, D., Chiapello, M., Bracale, M., Pesce, C., Bagnaresi, P., Dubois, E., et al. 2017. Transcriptome and proteome analysis reveal new insight into proximal and distal responses of wheat to foliar infection by *Xanthomonas translucens*. Sci. Rep. 7:10157.

Gassmann, W., Dahlbeck, D., Chesnokova, O., Minsavage, G. V., Jones, J. B., and Staskawicz, B. J. 2000. Molecular evolution of virulence in natural field strains of *Xanthomonas campestris* pv. *vesicatoria*. J. Bacteriol. 182:7053–7059.

Gu, Y., Wei, Z., Wang, X., Friman, V.-P., Huang, J., Wang, X., et al. 2016. Pathogen invasion indirectly changes the composition of soil microbiome via shifts in root exudation profile. Biol. Fertil. Soils. 52:997–1005.

Hacquard, S., Spaepen, S., Garrido-Oter, R., and Schulze-Lefert, P. 2017. Interplay Between Innate Immunity and the Plant Microbiota. Annu. Rev. Phytopathol. 55:565–589.

Horsfall, J. G., and Barratt, R. W. 1945. An improved grading system for measuring plant disease. Phytopathology. 35:655.

Horsfall, J. G., Dimond, A. E., and Others. 1959. Plant pathology: an advanced treatise. Vol. I: the diseased plant. Plant pathology: an advanced treatise. Vol. I: the diseased plant. Available at: https://www.cabdirect.org/cabdirect/abstract/19601602147.

Horvath, D. M., Stall, R. E., Jones, J. B., Pauly, M. H., Vallad, G. E., Dahlbeck, D., et al. 2012. Transgenic resistance confers effective field level control of bacterial spot disease in tomato. PLoS One. 7:e42036.

Hu, J., Wei, Z., Friman, V.-P., Gu, S.-H., Wang, X.-F., Eisenhauer, N., et al. 2016. Probiotic Diversity Enhances Rhizosphere Microbiome Function and Plant Disease Suppression. MBio. 7 Available at: http://dx.doi.org/10.1128/mBio.01790-16.

Islam, M., Morgan, J., Doyle, M. P., Phatak, S. C., Millner, P., and Jiang, X. 2004a. Fate of *Salmonella enterica* serovar Typhimurium on carrots and radishes grown in fields treated with contaminated manure composts or irrigation water. Appl. Environ. Microbiol. 70:2497–2502.

Islam, M., Morgan, J., Doyle, M. P., Phatak, S. C., Millner, P., and Jiang, X. 2004b. Persistence of *Salmonella enterica* serovar typhimurium on lettuce and parsley and in soils on which they were grown in fields treated with contaminated manure composts or irrigation water. Foodborne Pathog. Dis. 1:27–35.

Jones, J. D. G., and Dangl, J. L. 2006. The plant immune system. Nature. 444:323–329.

Kadivar, H., and Stapleton, A. E. 2003. Ultraviolet radiation alters maize phyllosphere bacterial diversity. Microb. Ecol. 45:353–361.

Kearney, B., and Staskawicz, B. J. 1990. Widespread distribution and fitness contribution of *Xanthomonas campestris* avirulence gene avrBs2. Nature. 346:385–386.

Knief, C., Delmotte, N., Chaffron, S., Stark, M., Innerebner, G., Wassmann, R., et al.

2012. Metaproteogenomic analysis of microbial communities in the phyllosphere and rhizosphere of rice. ISME J. 6:1378–1390.

Kunwar, S., Iriarte, F., Fan, Q., Evaristo da Silva, E., Ritchie, L., Nguyen, N. S., et al. 2018. Transgenic Expression of EFR and Bs2 Genes for Field Management of Bacterial Wilt and Bacterial Spot of Tomato. Phytopathology. 108:1402–1411.

Kunze, G., Zipfel, C., Robatzek, S., Niehaus, K., Boller, T., and Felix, G. 2004. The N terminus of bacterial elongation factor Tu elicits innate immunity in Arabidopsis plants. Plant Cell. 16:3496–3507.

Lacombe, S., Rougon-Cardoso, A., Sherwood, E., Peeters, N., Dahlbeck, D., van Esse, H. P., et al. 2010. Interfamily transfer of a plant pattern-recognition receptor confers broad-spectrum bacterial resistance. Nat. Biotechnol. 28:365–369.

Laforest-Lapointe, I., Paquette, A., Messier, C., and Kembel, S. W. 2017. Leaf bacterial diversity mediates plant diversity and ecosystem function relationships. Nature. 546:145–147.

Leveau, J. H., and Lindow, S. E. 2001. Appetite of an epiphyte: quantitative monitoring of bacterial sugar consumption in the phyllosphere. Proc. Natl. Acad. Sci. U. S. A. 98:3446–3453.

Lindow, S. E., and Brandl, M. T. 2003. Microbiology of the phyllosphere. Appl. Environ. Microbiol. 69:1875–1883.

McDonald, D., Price, M. N., Goodrich, J., Nawrocki, E. P., DeSantis, T. Z., Probst, A., et al. 2012. An improved Greengenes taxonomy with explicit ranks for ecological and evolutionary analyses of bacteria and archaea. ISME J. 6:610–618.

Meng, F., Altier, C., and Martin, G. B. 2013. Salmonella colonization activates the plant immune system and benefits from association with plant pathogenic bacteria. Environ. Microbiol. 15:2418–2430.

Minsavage, G. V., Dahlbeck, D., Whalen, M. C., Kearney, B., Bonas, U., Staskawicz, B. J., et al. 1990. Gene-for-gene relationships specifying disease resistance in *Xanthomonas campestris* pv. *vesicatoria*-pepper interactions. Mol. Plant. Microbe. Interact. 3:41–47.

Ottesen, A. R., González Peña, A., White, J. R., Pettengill, J. B., Li, C., Allard, S., et al. 2013. Baseline survey of the anatomical microbial ecology of an important food plant: *Solanum lycopersicum* (tomato). BMC Microbiol. 13:114.

Ottesen, A. R., Gorham, S., Pettengill, J. B., Rideout, S., Evans, P., and Brown, E. 2015. The impact of systemic and copper pesticide applications on the phyllosphere microflora of tomatoes. J. Sci. Food Agric. 95:1116–1125.

Ottesen, A. R., Gorham, S., Reed, E., Newell, M. J., Ramachandran, P., Canida, T., et al. 2016. Using a control to better understand phyllosphere microbiota. PLoS One. 11:e0163482.

Ottesen, A., Ramachandran, P., Reed, E., Gu, G., Gorham, S., Ducharme, D., et al. 2019. Metagenome tracking biogeographic agroecology: Phytobiota of tomatoes from Virginia, Maryland, North Carolina and California. Food Microbiol. 79:132–136.

Potnis, N., Soto-Arias, J. P., Cowles, K. N., van Bruggen, A. H. C., Jones, J. B., and Barak, J. D. 2014. *Xanthomonas perforans* colonization influences *Salmonella enterica* in the tomato phyllosphere. Appl. Environ. Microbiol. 80:3173–3180.

Potnis, N., Colee, J., Jones, J. B., and Barak, J. D. 2015. Plant pathogen-induced water-soaking promotes *Salmonella enterica* growth on tomato leaves. Appl. Environ. Microbiol. 81:8126–8134.

Redford, A. J., Bowers, R. M., Knight, R., Linhart, Y., and Fierer, N. 2010. The ecology of the phyllosphere: geographic and phylogenetic variability in the distribution of bacteria on tree leaves. Environ. Microbiol. 12:2885–2893.

Redman, C. E., King, E. P., and Brown, I. F. 1964. Tables for converting Barratt and Horsfall rating scores to estimated mean percentages. Available at: https://agris.fao.org/agris-search/search.do?recordID=US201300121787 [Accessed March 30, 2023].

Remus-Emsermann, M. N. P., Tecon, R., Kowalchuk, G. A., and Leveau, J. H. J. 2012. Variation in local carrying capacity and the individual fate of bacterial colonizers in the phyllosphere. ISME J. 6:756–765.

Schwartz, A. R., Morbitzer, R., Lahaye, T., and Staskawicz, B. J. 2017. TALE-induced bHLH transcription factors that activate a pectate lyase contribute to water soaking in bacterial spot of tomato. Proc. Natl. Acad. Sci. U. S. A. 114:E897–E903.

Tai, T. H., Dahlbeck, D., Clark, E. T., Gajiwala, P., Pasion, R., Whalen, M. C., et al. 1999. Expression of the Bs2 pepper gene confers resistance to bacterial spot disease in tomato. Proc. Natl. Acad. Sci. U. S. A. 96:14153–14158.

Telias, A., White, J. R., Pahl, D. M., Ottesen, A. R., and Walsh, C. S. 2011. Bacterial community diversity and variation in spray water sources and the tomato fruit surface. BMC Microbiol. 11:81.

Thompson, S., Levin, S., and Rodriguez-Iturbe, I. 2013. Linking plant disease risk and precipitation drivers: a dynamical systems framework. Am. Nat. 181:E1–16.

Wilson, M., and Lindow, S. E. 1994. Coexistence among epiphytic bacterial populations

mediated through nutritional resource partitioning. Appl. Environ. Microbiol. 60:4468–4477.

Wilson, M., and Lindow, S. E. 1995. Enhanced epiphytic coexistence of near-isogenic salicylate-catabolizing and non-salicylate-catabolizing *Pseudomonas putida* strains after exogenous salicylate application. Appl. Environ. Microbiol. 61:1073–1076.

Wilson, M., Hirano, S. S., and Lindow, S. E. 1999. Location and survival of leaf-associated bacteria in relation to pathogenicity and potential for growth within the leaf. Appl. Environ. Microbiol. 65:1435–1443.

Xin, X.-F., Nomura, K., Aung, K., Velásquez, A. C., Yao, J., Boutrot, F., et al. 2016. Bacteria establish an aqueous living space in plants crucial for virulence. Nature. 539:524–529.

Zheng, X.-Y., Spivey, N. W., Zeng, W., Liu, P.-P., Fu, Z. Q., Klessig, D. F., et al. 2012. Coronatine promotes *Pseudomonas syringae* virulence in plants by activating a signaling cascade that inhibits salicylic acid accumulation. Cell Host Microbe. 11:587–596

Chapter 3: PTI-Based Transgenic Resistance Has Little Effect on Tomato Microbiomes in the Field

A modified version of this chapter has been submitted for publication in *Phytobiomes* as: PTI-Based Transgenic Resistance Has Little Effect on Tomato Microbiomes in the Field**.** Adam F. Bigott, Sanju Kunwar, Mathews Paret, Richard Lankau, and Caitilyn Allen

This article will also be available as a BioRxiv pre-print under the same title.

Author Contributions:

This project conceived by S., Paret, M., Allen, C., and Lankau R.A. Field data was collected by Kunwar, S. and Bigott, A.F. and analyzed by Bigott, A.F. and Lankau, R.A. Bigott, A.F. was the primary author of this work with writing and editing contributions from Lankau, R.A. and Allen, C.

Abstract

Plants associate with complex microbial communities that play diverse but poorly understood roles in plant health. Pattern Triggered Immunity (PTI) is an immune response pathway elicited when Microbe Associated Molecular Patterns (MAMPs) bind to host Pattern Recognition Receptors (PRRs). Transgenic PTI genes can confer novel broad-spectrum disease resistance. Specifically, incorporating the *Arabidopsis* PRR Elongation Factor Tu Receptor (EFR) into the tomato genome dramatically increases resistance to bacterial wilt in the field. But how does this transgenic immunity affect the broader, non-pathogenic bacterial communities of these plants? Using 16S metabarcoding, we characterized and compared bacterial communities associated with roots and xylem of isogenic lines of FL8000 tomatoes with and without the *EFR* transgene to determine if EFR-based PTI changed bacterial community composition under commercial field conditions. While EFR largely prevents *Ralstonia solanacearum* from causing bacterial wilt on transgenic tomatoes, it had only subtle effects on xylem and rhizosphere microbiomes. Neither alpha diversity nor composition of root-associated bacterial communities was affected by the *EFR* gene, while diversity in xylem actually increased in *EFR* genotypes when combined with experimental *R. solanacearum* inoculation. The *EFR* gene altered bacterial community assembly in roots only when combined with experimental pathogen inoculation; root-associated bacterial composition was more variable in inoculated EFR than in inoculated wildtype plants. These encouraging results suggest that deploying broad-spectrum disease resistance using transgenic PRR genes will not have detrimental effects on plant microbiomes.

However, the effects of subtle interactions between PRR transgenes and pathogen populations on phytobiomes deserve further investigation.

Introduction

Eukaryotes use an innate immune system called Pattern-Triggered Immunity or PTI to defend themselves against diverse pathogens. The PTI defense signaling pathway is activated when membrane bound Pattern Recognition Receptors (PRRs) encounter broadly conserved extracellular ligands known as microbe associated molecular patterns (MAMPs) such as flagellin or chitin (Jones and Dangl 2006; Boller and Felix 2009). Detection of the microbial signatures enacts the first line of defense. PRRs are receptor-like kinases that transduce their signal through phosphorylation or form complexes with host kinases to rapidly initiate basal defenses (Ngou et al. 2022).

Genetic engineering can integrate resistance genes into non-native backgrounds to create novel pathogen resistance. The *Arabidopsis thaliana EFR* gene encodes a PRR that recognizes a peptide from the abundant and conserved bacterial protein Elongation Factor Tu (EF-Tu). Tomato plants expressing *EFR* are resistant to multiple bacterial pathogens in the growth chamber experiments, including *Pseudomonas syringae, Xanthomonas perforans, Agrobacterium tumefaciens,* and *Ralstonia solanacearum* (Lacombe et al. 2010). Transgenic *EFR*-based resistance to bacterial pathogens has also been explored in rice, wheat, and citrus (Schwessinger et al. 2015; Schoonbeek et al. 2015; Mitre et al. 2021)

EFR-expressing tomato plants were also resistant to *R. solanacearum* in the field under commercial production conditions (Kunwar et al. 2018). *R. solanacearum* belongs to the *R. solanacearum* species complex (RSSC), a group of related Proteobacteria that

cause bacterial wilt disease of plants in over 80 families, including economically important crops such as potato, banana, and tomato (Allen et al. 2005; Mansfield et al. 2012). Plant pathogenic *R. solanacearum* strains are typically soilborne, invading plant roots through wounds and natural openings. Wilting occurs due to bacteria colonizing the water-transporting xylem vessels at high cell densities and obstructing transport (Lowe-Power et al. 2018). During pathogenesis, *R. solanacearum* deploys dozens of Type III-secreted effector proteins, including many that suppress plant PTI defenses (Landry et al. 2020). Transient expression studies found *R. solanacearum* has many functionally redundant PTI-suppressing effectors, suggesting that overcoming host PTI is important for bacterial fitness (Nakano and Mukaihara 2019)

The transgenic expression of PRRs to confer novel resistance to bacterial wilt in the field is exciting because tomato growers have no commercially desirable wilt resistant cultivars (Lopes et al. 2022). Planting grafted seedlings consisting of a resistant rootstock and a desirable scion is currently the best option for growers confronting high wilt disease pressure (Suchoff et al. 2015), but with limited commercial viability in open field conditons. Although the effectiveness of rootstock grafting demonstrates that wilt resistance can operate in plant roots, reciprocal grafting experiments unexpectedly found that resistant scions reduced bacterial colonization of aboveground xylem elements, suggesting that resistance functions in xylem as well (Planas-Marquès et al. 2019). Grafting *EFR*-expressing scions onto isogenic susceptible rootstocks similarly limited *R. solanacearum* colonization of the upper stem above the grafting scar as compared to susceptible self-grafted plants (Kunwar, unpublished).

Plant diseases may also be controlled indirectly. In particular, the tomato-associated microbiota has the potential to suppress bacterial wilt disease. Mesocosm experiments comparing the susceptible Moneymaker and resistant Hawaii 7996 cultivars revealed compositionally different rhizosphere-associated microbial communities and cultivation of the susceptible Moneymaker in soil previously used to grow the resistant Hawaii 7996 cultivar reduced wilting symptoms (Kwak et al. 2018). This reduced disease development correlated with increased relative abundance of *R. solanacearum*-antagonistic strains of Flavobacterium, suggesting resistance may be in part due to the ability of tomato cultivars to recruit mutualistic microbes (Choi et al. 2020; Jousset and Lee 2023) Conversely, *R. solanacearum* invasion of a susceptible tomato host corresponds with modification of rhizosphere-associated communities (Wei et al. 2018).

While the *EFR* transgene provides resistance to multiple pathogens, it also raises concerns about what the effect of constitutively expressing a novel PRR will have on the non-pathogenic and beneficial members of the tomato microbiome. Tomato-associated communities with highly connected trophic architecture and pathogen niche overlap can suppress bacterial wilt development in the greenhouse (Wei et al. 2015). Probiotic applications of *Pseudomonas* communities prior to *R. solanacearum* inoculation was best able to maintain high rhizosphere populations and subsequently suppress disease development and improve plant growth in a diversity-dependent fashion. (Hu and Wei et al. 2016; Hu et al. 2021). The importance of the initial composition of tomato-associated rhizosphere communities on bacterial wilt has also been demonstrated at the field level (Wei et al. 2019). Since both pathogen and non-pathogenic microbes produce the

broadly conserved MAMP signals, enhancing MAMP reception could potentially affect the abundance, diversity, and composition of the whole plant microbiome.

Thus, in addition to increasing resistance to challenging pathogens like *R. solanacearum*, transgenic EFR plants provide an opportunity to investigate an important broader question in plant-microbial interactions: If plants activate defenses whenever their PRRs detect MAMPs, how does this affect the diverse microbial community that naturally associates with plants? Does the incorporation of an additional PRR and the resulting capacity to perceive an additional MAMP alter the tomato microbiome? Specifically, we hypothesize that *EFR* expressing tomato lines will harbor less diverse communities composed of fewer members and a lower relative abundance of *R. solanacearum*.

To test this hypothesis, we characterized bacterial communities in whole roots and xylem sap samples from tomato plants in the field under *R. solanacearum* disease pressure. We compared root and xylem microbiomes from two tomato lines, wild type FL8000 and an isogenic *EFR*-expressing FL8000 genotype, under either natural disease pressure or with supplemental *R. solanacearum* inoculation.

Methods

Experimental Design and sampling

Field trials were conducted in the falls of 2017 and 2018. Trials were managed by the University of Florida North Florida Research and Education Center in Quincy, Florida. Seeds were germinated in greenhouses in July and transplanted to the field in late August. Fields were prepared for standard commercial field production with

fumigated (Pic-Clor 60, 336 kg/ha) raised beds (81.3 cm wide at the base, 71.1 cm wide at the crown and 20.3 cm in height) at 91.4 m lengths, spaced on 1.5 m row spacing, and covered with an impermeable white film.

The experimental design consisted of two plant genotypes (FL 8000, and FL 8000 *EFR*) inoculated with *Ralstonia solanacearum*. Each transplant hole was inoculated with 50 ml of 10^5 CFU/ml of the Rs5 strain (R1B1 phyloytype II sequevar 7) in 2017 and 10^6 CFU/ml in 2018. Plots were arranged in a randomized complete block design with individual plots consisting of 10 plants each. In 2017, each combination of genotype and inoculation treatments was represented by 5 blocks whereas in 2018 each treatment was represented by 4 blocks.

Field samples were collected in October as plants approached harvesting age. For the collection of whole roots, soil cores were collected from the base of every plant in a plot and homogenized by plot. In order to collect xylem sap, plants were detopped (? cm from the crown region or from the soil surface) and fitted with clear vinyl tubing. Sap was collected from three plants per plot. In 2017, poor plant health prevented us from successfully collecting xylem sap from a sufficient number of individuals to allow statistical analysis, so only data from the 2018 xylem collections are presented here.

Characterization of bacterial communities

Extracted xylem sap and soil cores were shipped overnight to Madison, WI for processing. Roots were manually separated from soil cores and cleared of loosely adhering soil. To prepare whole roots for DNA extraction, 25 mg of tissue was flash frozen with liquid nitrogen and ground using metal beads and a Genogrinder set to 1500 rpm for 3 minutes. DNA extraction on xylem sap and ground up roots was performed

using the Omega Bio-Tek E.Z.N.A. Plant DNA Kit following the manufacturer's instructions.

Extracted DNA was used as a template for an initial PCR amplification using a 16S primer pair for the V5-V6 region (799F and 1115R) that does not amplify the chloroplast 16S sequences (Laforest-Lapointe et al. 2017; Redford et al. 2010). As previously described in Xue et al. 2018, a second PCR was performed while adding one of 8 variable length barcodes (5-8 bp) to each sample and space for the Nextera primer to bind. The external fusion PCR primers for the second PCR contained a 14 bp overlap with the end of the internal primer as well as one of two options: an 8-bp i7 index and P7 flow cell adapter sequence or a 7-bp spacer i5 index, and P5 flow cell adapter sequence.

The first PCR reaction used a total volume of 10 µL. Reactions used 0.2 µL of hot-start high fidelity Clonetech PrimeSTAR GLX polymerase (Takara Bio, Kusatusu, Japan), 2 µL of 5X buffer, 0.8 µL of 10 nM dNTPs, 0.25 µL of 10 nM forward and reverse primer, 0.7 µg T4 gene 32 protein, and 10 ng of template DNA. The Thermocycler protocol was as follows: a hot start at 98˚C for 5 minutes, 35 cycles of denaturing at 98˚C for 45 seconds, annealing at 50˚C for 45 sec., extension at 68˚C for 1 min., and a final 15 min. extension at 68˚C.

The second PCR reaction used a total volume of 25 µL. Reactions contained 0.5 µL of hot-start high fidelity Clonetech PrimeSTAR GLX polymerase (Takara Bio, Kusatusu, Japan), 5 µL of 5X buffer, 1 µL of each 10 nM primer, and 1 µL of product from the previous PCR as template. The Thermocycler protocol was as follows: a hot

start at 98˚C for 5 minutes, 15 cycles of denaturing at 98˚C for 30 seconds, annealing at 60˚C for 0:45, extension at 68˚C for 1:00, and a final extension of 10 minutes at 68˚C.

Successful amplification at each step was visually confirmed on a UV-transilluminator following gel electrophoresis of the product in 1% agarose and staining with gel red. Final amplification products were purified with the Omega BioTek E-Z 96 Cycle Pure kit and quantified using a Qubit 2.0 fluorometer with the Qubit dsDNA HS assay (Thermo Scientific, Grand Island, NY). DNA was pooled at equal concentration and sent for Illumina MiSeq sequencing at the University of Wisconsin Biotechnology Center (Madison, WI), using a paired end, 300 cycle run. Separate Miseq runs were performed for each sampling year.

Bioinformatic processing

External barcodes were demultiplexed by the Wisconsin Biotech Center. Each set of matching external barcodes contained multiple samples distinguished by the third barcode sequence between the Nextera adapter and 16S primer sequence. This second demultiplexing was performed in Qiime2 (Bolyen et al. 2019) using the cut-adapt plugin from the demux-paired function.

Denoising, replication, and chimera filtering were all performed in Qiime2 using the dada2 plugin's "denoise-paired" option using default settings. Taxonomic assignment was performed using naïve Bayesian classification. The Greengenes database was used as a reference database for taxonomic identities (McDonald et al. 2012). Following assignment, a dataset for downstream analysis was created by combining amplicon sequence variants identified to the same genus. Sequences that

could not be identified to a given taxonomic resolution were lumped into a single unclassified taxon with terminal identification at the next highest taxonomic rank.

Statistical analysis

All statistical analysis was performed in R (version 4.1.0). To determine how an ectopic pattern recognition receptor affects tomato microbiomes, we compared bacterial communities associated with wild-type and isogenic *EFR*-expressing plants growing under commercial production conditions in the Florida panhandle over two years. One set of plants were exposed to moderate bacterial wilt pressure from endemic *R. solanacearum* populations, while the second set were supplementally inoculated with the endemic strain at the time of seedling transplant. Our dataset consists of root samples from 2017 and 2018 and xylem sap samples from 2018 (field conditions in 2017 did not allow for the collection of xylem sap). The number of samples collected from each plant part, their sequencing depths, and rarefaction depths are listed for whole root (Table S1) and xylem sap (Table S2) samples.

To test whether plant genotype and *R. solanacearum* inoculation affect the alpha genera diversity and richness of root- and xylem-associated bacterial communities, we used linear models with plant genotype (presence or absence of the *EFR* transgene), the inoculation treatments (supplementally inoculated or not) and their interaction as dependent variables using the lm function in the R statistical package. We calculated diversity using the Shannon-Weaver diversity index.

Rarefaction revealed that the sequencing depth of a given sample and the number of observed unique ASVs were correlated in a subset of our data (Supplemental Figure 1). In order to distinguish between meaningful biological

differences and this technical artifact of the sequencing data, we included sequencing depth as a covariate in our linear models. Additionally, there was high variation in metabarcoding profiles of root associated communities from different years, independent of tomato genotype or experimental treatments, likely due to environmental differences. Therefore, we analyzed the two years of root associated data separately while still asking the same questions about the relationships among EFR, *R. solanacearum* inoculation, and the plant associated microbial communities.

In order to assess differences in community composition, we performed perMANOVA tests to assess the effects of the expression of *EFR*, supplemental *R. solanacearum* inoculation, and their interaction on roots and xylem sap communities, using the adonis function in the vegan package in the R statistical program. Again, we analyzed the composition of root-associated communities separately by year. Additionally, we tested whether replicated communities within a given experimental treatment (combination of plant genotype and inoculation treatment) displayed differences in compositional variability (dispersion) using the betadisper package in the vegan package in R, followed by an analysis of variance of within-group dispersion.

Variation in the endemic pathogen populations within plots had the potential to undermine the effects of supplemental field inoculation intended to increase disease pressure. Relative abundance of *R. solanacearum* ASVs in our datasets provided internal validation. Thus, to better characterize the effects of *R. solanacearum* on the overall community composition in communities associated with *EFR* and non-*EFR* expressing plants, we removed *R. solanacearum* reads from the community composition data and re-rarified the remaining communities to a standard sequence

depth. The relative abundance of *R. solanacearum* in the full community was then used as an explanatory variable in linear models analyzing diversity and richness, and perMANOVA analyses of the composition of the remaining members of the community. Using this newly trimmed dataset, we reexamined our original questions about the effects of resistance and disease pressure on the rest of the plant associated bacterial community.

Results

Composition of tomato root and xylem sap communities

Root associated microbial communities were dominated by Proteobacteria and Actinobacteria in both 2017 and 2018 (Figure 1A, B). Root associated communities differed substantially between years. In 2017, the Actinobacteria phyla were a much more substantial component of the community, with a relatively equal abundance compared to the Proteobacteria. In 2018 the Proteobacteria, including *R. solanacearum* specifically, comprised the vast majority of the community. The relative abundance of *R. solanacearum* in roots was not affected by inoculation or EFR, but did differ by year (Figure 1, p=2.00E-13, Table S3). Xylem communities were again dominated by Proteobacteria, but had Bacteroidetes as the second most abundant phyla over Actinobacteria (Figure 2).

The *EFR* transgene did not affect alpha diversity of root-associated bacterial communities, but increased xylem sap alpha diversity

We compared the relative diversity of communities associated with roots and xylem sap using total richness and the Shannon-Weaver diversity index analyses. In all

root communities, species richness varied by year. The 2017 root samples had an average richness of 110 genera per plant, which was less than half the average of 231 genera observed in 2018 (Figure 3A, p = 3.48e-05, Table 1A). However, the Shannon index of root communities did not differ between the two field seasons (Figure 3B, p = 0.1047, Table 2A).

Because alpha richness levels of roots between years, we performed separate analyses within each year to test the effects of experimental treatments on richness. Supplemental inoculation of plants with *R. solanacearum* increased the total richness, but not Shannon-Weaver diversity, in root associated communities in 2017 (Figure 3A, p = 0.00952, Table 1B,C). In contrast, supplemental *R. solanacearum* inoculation did not affect the two alpha diversity metrics in 2018 (Table 2B,C). The *EFR* transgene did not affect either the number of genera present or the Shannon-Weaver diversity index in roots in either field season (p> 0.05, Table 1, Table 2).

The diversity of xylem sap communities was generally lower than in the root associated communities from the same field season. Xylem sap total richness was the lowest in susceptible FL8000 plants supplementally inoculated with *R. solanacearum,* while EFR-based resistance was associated with richer xylem sap communities (Figure 4A, p = 0.004621, Table 1D). In order to further investigate the effects of EFR on richness, Tukey's HSD testing of combinations of genotype and inoculation revealed specifically that supplementally inoculated EFR plants contained a significantly more genera than their FL8000 counterparts (Figure 4A, p = 0.0233). Further, inoculation of both FL8000 and EFR plants decreased the associated Shannon index of xylem

communities compared to their non-inoculated counterparts (Figure 4B, p = 0.028, Table 2D).

Isogenic *EFR* and non-*EFR* plants harbor similar bacterial communities on average, but differ in the variability of their communities

Root associated community composition did not differ with respect to genotype or supplemental *R. solanacearum* inoculation in either 2017 (Supplemental Figure 2, p > 0.05, Table 3B) or 2018 (Figure 5, p > 0.05, Table 3C). Similarly, the composition of bacterial communities in xylem sap did not differ in response to the *EFR* transgene or supplemental inoculation with *R. solanacearum* (Figure 6, p > 0.05, Table 3D).

While community composition did not display consistent differences in multivariate location based on our prescribed treatments, the ordination of 2018 root associated communities revealed differences in the within group dispersion in composition for certain combinations of inoculation and genotype. Beta-dispersion analysis, a multivariate analogue of Levene's test for homogeneity of variances, revealed that EFR plants supplementally inoculated with *R. solanacearum* had greater variance in community composition than their inoculated FL8000 counterparts (Figure 5, comparison of inoculated EFR to inoculated FL8000, p = 0.0061840; all other comparisons, p > 0.05). Dispersion of community composition within treatment groups did not differ between combinations of genotype and inoculation in root associated communities from 2017 or in xylem sap communities (p > 0.05 for all comparisons).

R. solanacearum influences community composition

For root samples collected in 2017, where the relative abundance of *R. solanacearum* was overall lower than 2018 (ANOVA, p = 2.00E-13, Table S2), we did not observe statistically significant effects of the relative abundance of *R. solanacearum* on alpha diversity metrics when included as a covariate in our linear models (Table 4A, Table 5A). However, the previously documented effects of supplemental inoculation on genera richness remained statistically significant even when controlling for variation in *R. solanacearum* relative abundance (p = 0.0125, Table 4A). Reanalysis of community composition (via perMANOVA) revealed potentially weak effects of both inoculation and *R. solanacearum* relative abundance on the structure of the non-Ralstonia community in 2017 (p < 0.10, Table 6A).

Root associated communities sampled in 2018 were influenced by the relative abundance of *R. solanacearum*. Both richness and Shannon-Weaver diversity index values were lower in communities associated with a high relative abundance of *R. solanacearum* (p = 0.0471 , p = 0.000131, respectively, Table 4B, 5B). Further, the overall composition of remaining community members was also influenced by the relative abundance of *R. solanacearum* (p = 0.001, Table 6B). Based on the sum of squares, the relative abundance of *R. solanacearum* explained 39.6% of the variation in the composition of the rest of the plant associated with the root community.

While root samples from 2018 were influenced by the relative abundance of *R. solanacearum*, effects of the pathogen on alpha diversity metrics were not observed in xylem sap samples from the same field season (p > 0.05, Table 4C, 5C). Importantly, the effect of EFR on increased genera richness in xylem remained significant even

when controlling for differences in *R. solanacearum* relative abundance ($p = 0.149$, Table 4C). Additionally, when controlling for variation in *R. solanacearum* relative abundance, supplemental inoculation no longer influenced the Shannon diversity value of the non-pathogenic community in the xylem ($p > 0.05$).

Discussion

In this study we used a metabarcoding approach to investigate how plants associate with a diverse microbial community that have the potential to trigger host defense responses. Specifically, we were interested in how the additional capacity to perceive a conserved and highly abundant MAMP interacted with endogenous tomato PTI and influenced the microbial communities that are associated with these plants. Supplemental inoculations in a field with a history of bacterial wilt allowed us to compare the impact of the *EFR* transgene on communities in circumstances where triggering of PTI was likely to impact plant health.

Given the ubiquity of the EF-Tu MAMP among prokaryotes, our initial hypothesis was that constitutive expression of an additional PRR would make plant associated niches more restrictive and decrease alpha diversity. This was based on the assumption that bacterial community assembly in the root endosphere and xylem sap would be influenced by biotic filtering as microbes migrate from soil and across the rhizoplane. Adding EFR to tomato plants would make this biotic filtering process more restrictive and decrease diversity, as the hypothesized greater intensity and/or consistency of plant PTI responses would act to prevent establishment of sensitive microbial taxa. Given this more stringent filtering process, we predicted that plants expressing

transgenic PRRs would harbor distinct and lower diversity communities of microbes from their isogenic counterparts.

While its insertion conferred resistance to bacterial wilt as expected, the constitutive expression of *EFR* by itself did not lead to differences in bacterial communities as measured by our methods. Expressing *EFR* in FL8000 tomatoes did not alter the richness of microbial communities associated with roots across two seasons of field data. Likewise, xylem communities from non-inoculated plants harbored similar numbers of genera irrespective of their genotype. *EFR* expression did not impact the Shannon-Weaver diversity or overall compositional variation of roots or xylem sap associated communities.

There could be several reasons for these unexpected results. First, our measurement of plant-associated bacterial communities may have simply missed the most important consequences of the transgene. PCR amplicon-based assessments of microbial communities lack information on total microbial biomass from environmental samples. It is possible that the *EFR* gene affected the total microbial load on experimental tomato plants without causing detectable changes in the relative abundance of microbial taxa. It is also possible that our measurements were not taken at the necessary time to capture ephemeral effects of EFR on bacterial communities. Root and xylem samples were collected near the end of the growing season, but the effects of PTI triggering may have been most evident immediately after tomato plants were planted in the field and exposed to the full soil microbial community. Specifically, ephemeral effects were likely to take place shortly after plants were introduced to *R.*

solanacearum through both supplemental inoculation and or natural disease pressure shortly following transplant.

Beyond these technical concerns, the unexpectedly weak response of bacterial community structure to the *EFR* gene may reflect important biological differences in how pathogenic and non-pathogenic microbes interact with the plant immune system. For instance, full triggering of PTI may require more than just the presence of MAMP ligands and PRR recognition. It has been suggested that PTI initiation requires simultaneous detection of both MAMPs and DAMPs (Zhou et al. 2020). If so, plants restrict their PTI response to only deploy if i) challenged by a pathogen or parasite that releases DAMPs during their invasion of plant cells or ii) mechanically wounded and subsequently colonized by microbes, pathogenic or otherwise. Moreover, PTI may only be initiated after a pathogen reaches a quantitative threshold involving timing, location, and/or population size. For instance, pathogens may trigger PTI only after achieving cell densities much higher than those typical of commensal plant endophytes.

Assessing the impacts of host-pathogen interactions on plant associated microbial communities in the field remains challenging. While supplemental inoculation may have synchronized the initial pathogen challenge with a known virulent strain, the level of disease pressure from native inoculum remains less predictable. In 2017, when *R. solanacearum* abundance was relatively low, supplemental inoculation increased microbial species richness in roots. Notably, both the relative abundance of *R. solanacearum* and richness were greater in 2018 root communities, but the years did not differ with respect to Shannon-Weaver indices. Taken together, these results suggest that *R. solanacearum* root colonization may aid other bacterial taxa in

colonizing roots at low levels, possibly because pathogenesis increases rhizodeposition of nutrients or because successful pathogen colonization suppresses general plant immunity. Conversely, supplemental inoculation of susceptible FL8000 plants resulted in xylem sap communities composed of fewer genera than their resistant EFR counterparts. This suggests that the interactions between host and pathogen may impact microbial communities in tissue-specific ways.

In addition to attempts to distinguish host and pathogen mediated effects on root and xylem microbiomes, we also observed interactions between EFR and supplemental inoculation. While we did not observe compositional differences with respect to plant genotype, the compositional variation among supplementally inoculated plants was greater than that of supplementally inoculated, susceptible FL8000 root associated communities. Additionally, the richness of bacterial communities in xylem tissue differed between supplementally inoculated EFR and FL8000 plants. Thus, plants possessing the capacity to initiate PTI in response to *R. solanacearum* infection may lead to more stochastic community assembly that increases compositional variation. *EFR* expression combined with sufficient pathogen challenge may have the direct but subtle effect of composition of associated microbial communities.

Our finding that the *EFR* gene only had detectable effects on bacterial community structure in the presence of experimental pathogen inoculation supports the hypothesis that PTI triggering requires more than just the presence of MAMPs. It may be that the experimental inoculation with a high dose of a strong pathogen combined with the high expression of the novel PRR gene led to a strong and consistent upregulation of PTI early in the growing season, with cascading effects on the assembly

of the resulting bacterial communities in roots and xylem. Since the native tomato PRRs do not recognize *R. solanacearum* in ways that prevent wilt disease development, experimental inoculation of the wildtype tomato genotype may not have resulted in the same plant defense response. Similarly, slow and heterogeneous colonization of the *EFR* genotype in non-inoculated plots by only the indigenous *R. solanacearum* population and other microbes may not have resulted in as consistent a PTI response compared to our experimental inoculation.

R. solanacearum pathogenesis has previously been associated with changes to tomato root microbiomes and reduced alpha diversity metrics (Wei et al. 2018). Thus, it can be difficult to disentangle plant mediated and pathogen mediated influences on the microbiome when comparing sick and healthy plants. To better understand the influence of pathogen mediated effects, we examined the relationship between variance in the relative abundance of *R. solanacearum* and the variation in the diversity of the remaining members of the bacterial community. In 2018, when higher levels of *R. solanacearum* were found throughout our experiment, pathogen relative abundance corresponded with depressed alpha diversity metrics. Further, 39.6% of the variation in composition of the other members of the community in 2018 was tied to the relative abundance of *R. solanacearum,* irrespective of plant genotype. These results suggest that pathogen mediated effects shape the associated microbiome under conditions conducive to pathogen success.

The aim of this study was to examine the microbiomes of isogenic tomato lines to assess if the transgenic expression of *EFR* alters the tomato microbiome. To do this, we characterized bacterial communities in whole roots and xylem sap samples from tomato

plants in field conditions with natural and supplemental *R. solanacearum* inoculum. Given the previously reported excellent bacterial wilt resistance conferred by EFR (Lacombe et al. 2010; Kunwar et al. 2018), we hypothesized that EFR tomato lines would harbor less diverse communities composed of fewer members and a lower relative abundance of *R. solanacearum*. Although we did not detect broad scale differences with respect to bacterial community composition, we did observe subtle host-pathogen interactions between EFR and *R. solanacearum* that influenced outcomes for plant associated microbial communities. While our data did not support our original hypothesis, they did raise interesting additional questions and suggested that a non-native PRR can be an environmentally non-disruptive disease resistance strategy. These results are encouraging in that they indicate that the deployment of transgenic, broad-spectrum resistance through PRR genes can occur without detrimental effects on plant microbiomes.

On a more basic level, our results indicate that interactions between pathogenic and non-pathogenic members of the plant microbiome and the plant innate immune system are more nuanced, complex and delicately regulated than previously appreciated.

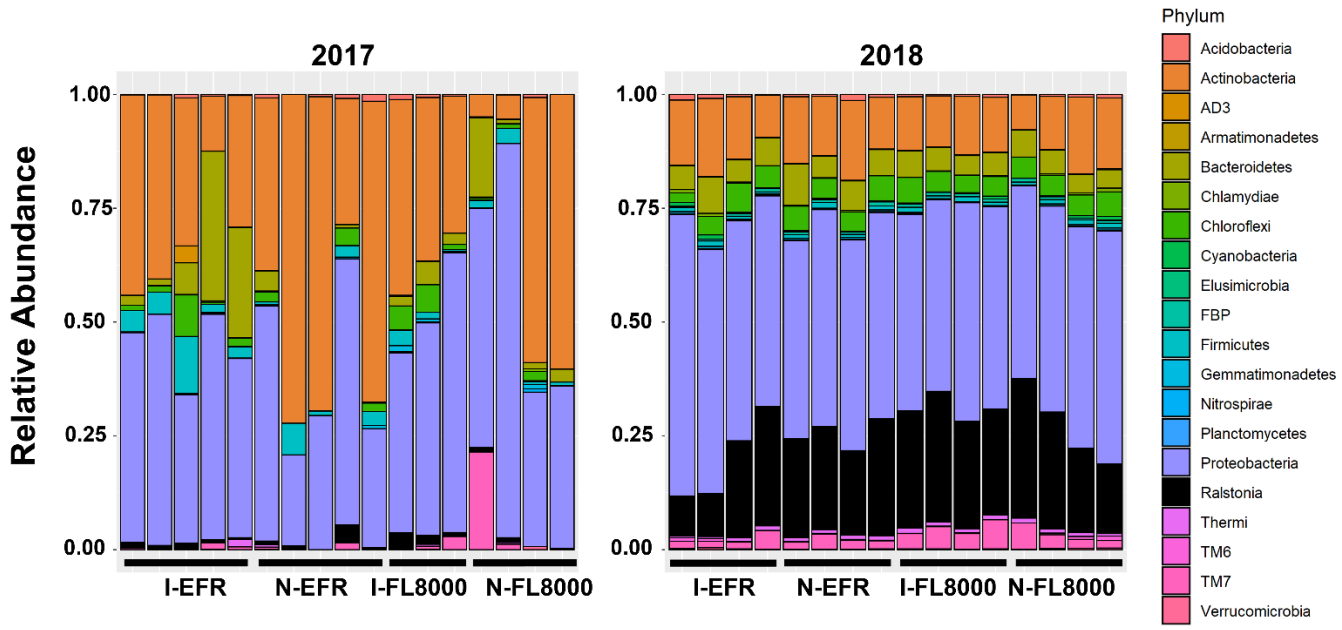

Figure 1: Root-associated communities are dominated by Proteobacteria, Actinobacteria. Stacked bar charts of root-associated taxa from 2017 (left) and 2018 (right) binned at the phylum level in FL8000 plants and FL8000-EFR plants and supplemental inoculation (In) and non-inoculated (non) treatments. Ralstonia (black) is displayed separately from other members of Proteobacteria.

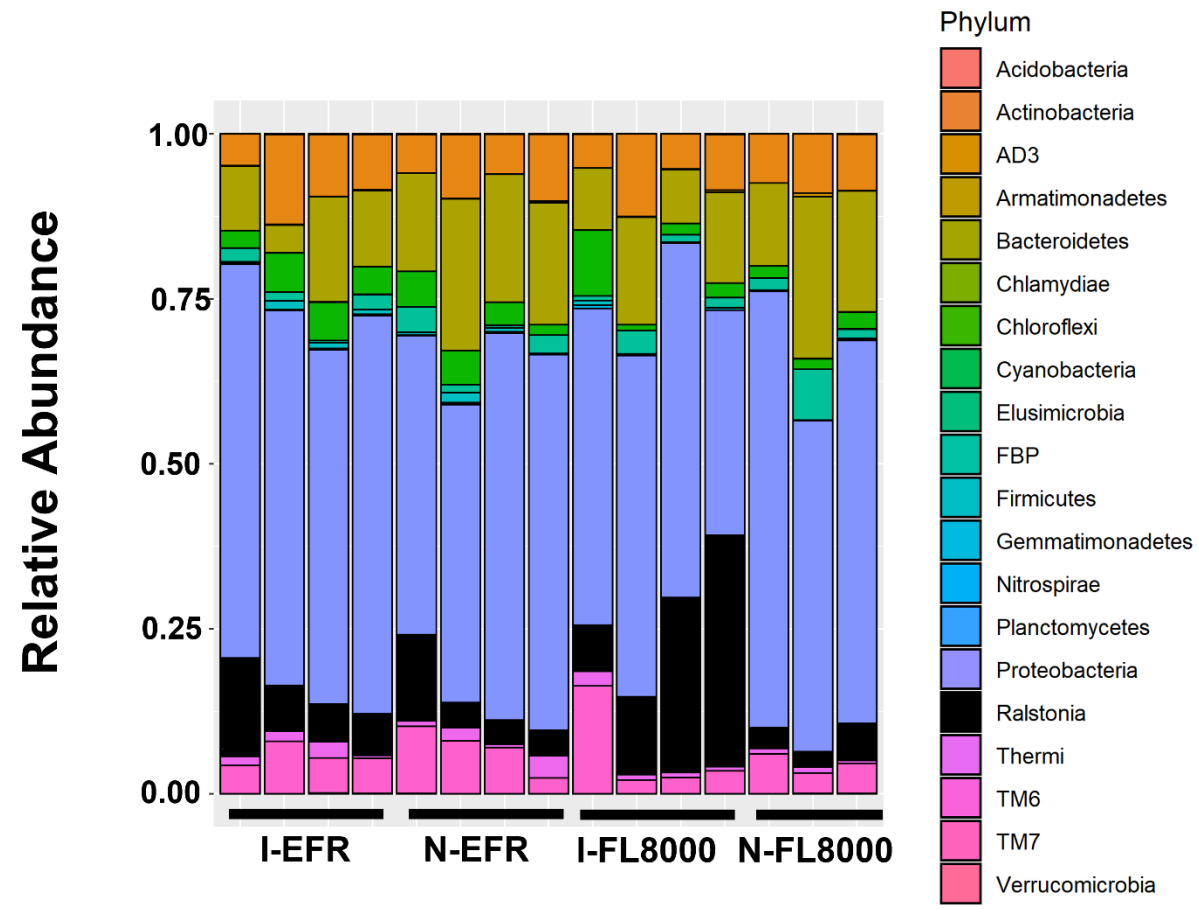

Figure 2: Xylem-associated communities are dominated by Proteobactera, Bacteriodetes. Stacked bar charts of root-associated taxa from 2018 binned at the phylum level in FL8000 plants and FL8000-EFR plants and supplemental inoculation (In) and non-inoculated (non) treatments. Ralstonia (black) is displayed separately from other members of Proteobacteria.

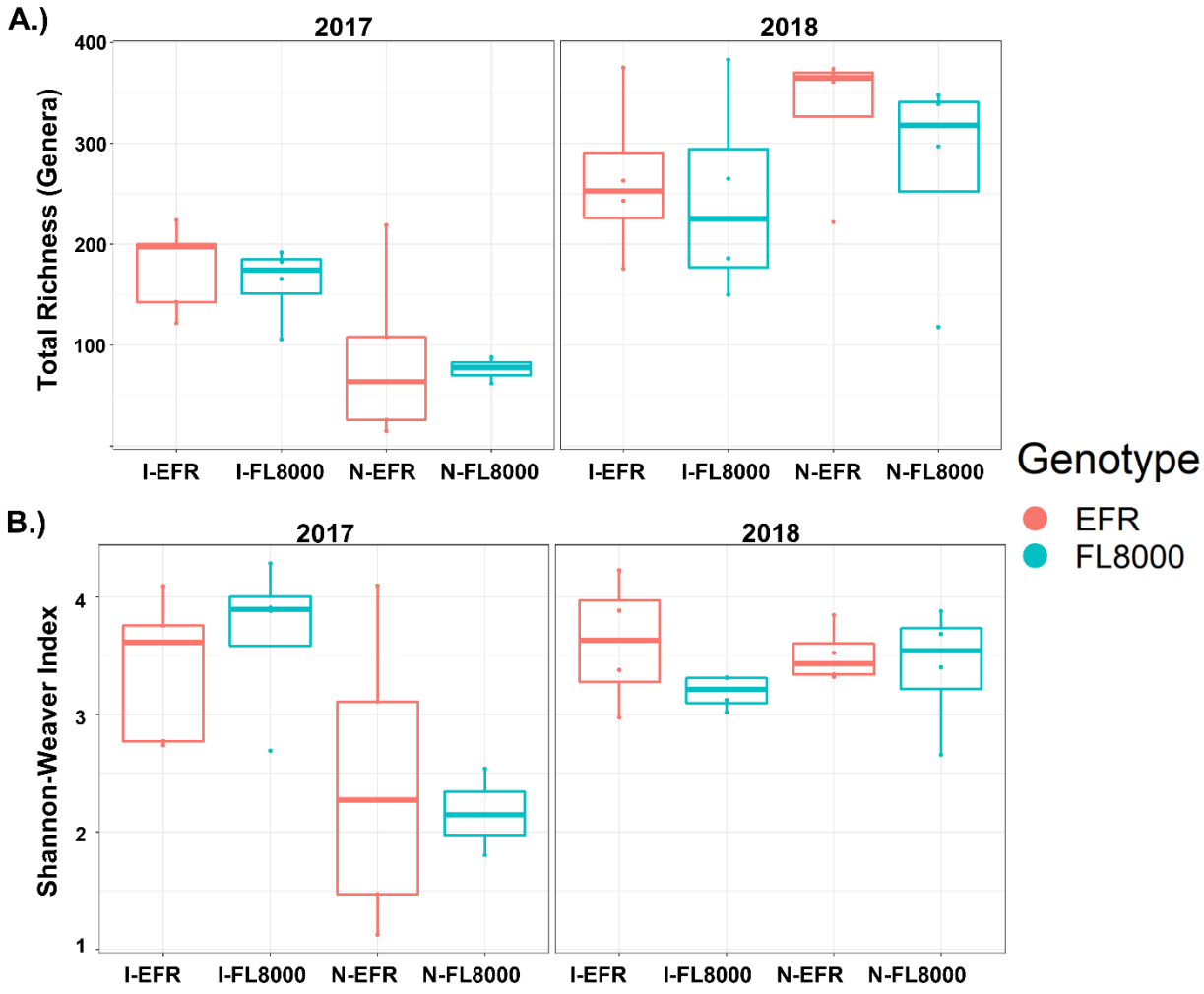

Figure 3. Transgenic expression of *EFR* affects richness, Shannon Index of the tomato root-associated bacterial community, but supplemental R. solanacearum inoculation increased Shannon diversity. (A) Total richness and (B) Shannon Index of bacterial genera on roots of wild-type cv. Florida8000 tomato (FL8000, in blue) and an isogenic *EFR*-expressing line (EFR, in red), based on 16S amplicons binned at the genus level. Plants were exposed to endemic bacterial wilt disease pressure from endemic soil population of *R. solanacearum* (N, not inoculated) or received supplemental inoculation with an endemic *R. solanacearum* strain (I, inoculated). Data shown were collected during two separate field seasons: 2017 and 2018. Tomato genotype did not affect bacterial species richness in either year ($p > 0.05$, ANOVA), but in 2017, supplemental inoculation increased total bacterial richness ($p < 0.05$). In 2017, supplemental inoculation increased Shannon entropy (ANOVA, $p < 0.05$).

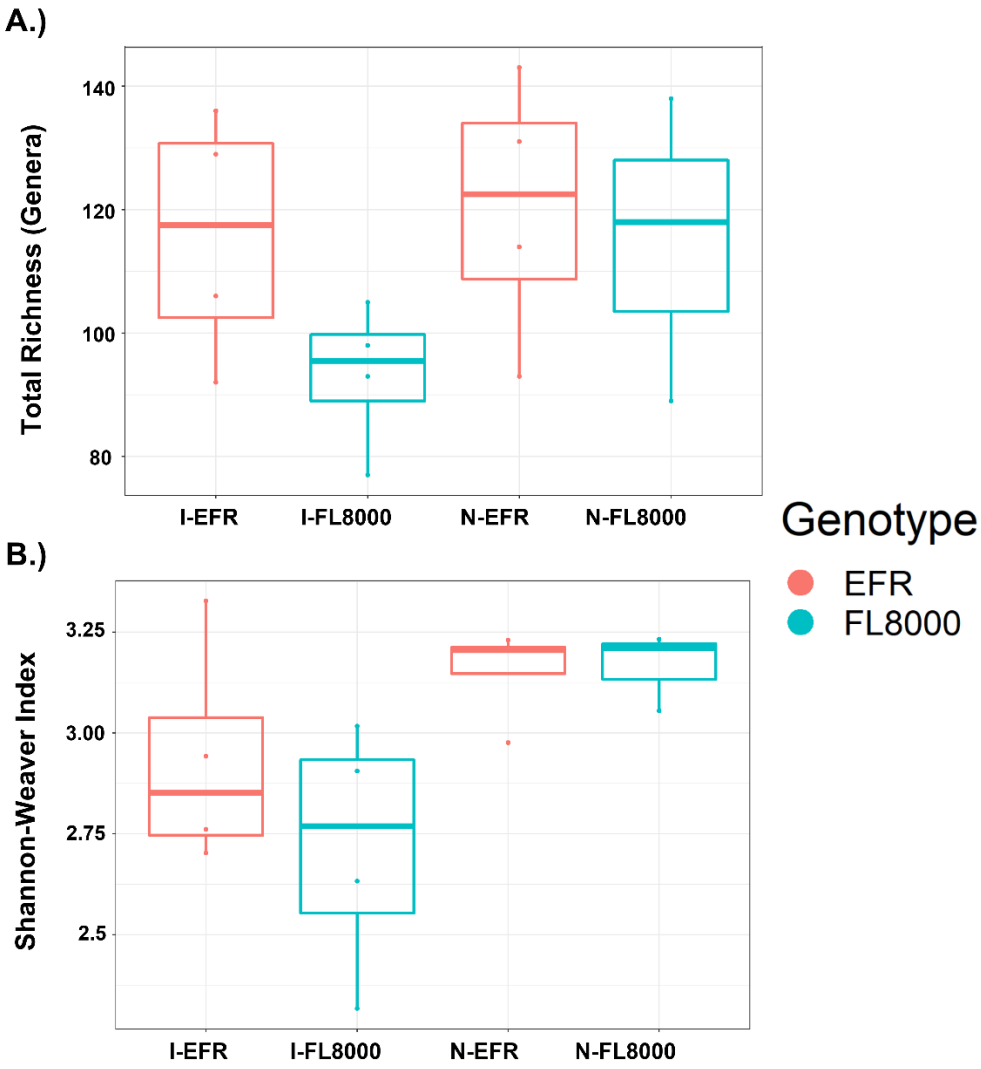

Figure 4. Transgenic expression of *EFR* increased xylem sap richness in supplementally inoculated plants, supplemental *R. solanacearum* inoculation decreased Shannon diversity in xylem-associated bacterial communities. (A) Total richness and (B) Shannon Index of bacterial genera on roots of wild-type cv. Florida8000 tomato (FL8000, in blue) and an isogenic *EFR*-expressing line (EFR, in red), based on 16S amplicons binned at the genus level. Plants were exposed to endemic bacterial wilt disease pressure from endemic soil population of *R. solanacearum* (N, not inoculated) or received supplemental inoculation with the endemic *R. solanacearum* strain (I, inoculated). EFR increased richness (ANOVA, $p < 0.05$). Further investigation of richness after adjusting for sequencing depth revealed that only the xylem sap from supplementally inoculated EFR plants contained a significantly larger number of genera than their FL8000 counterparts (Tukey's HSD, $p = 0.0233$). Supplemental decreased xylem sap Shannon entropy (ANOVA, $p < 0.05$).

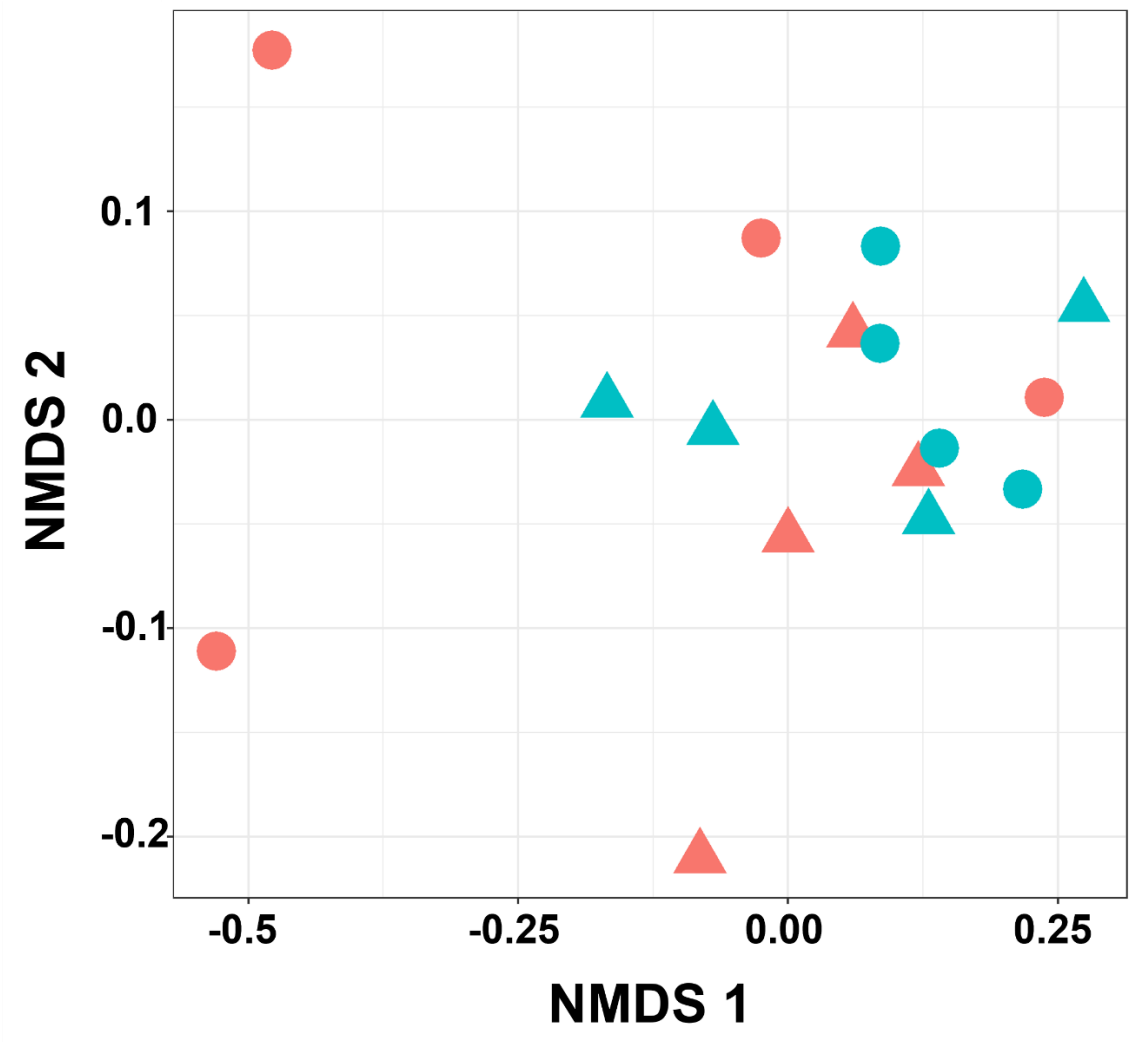

Figure 5. The composition of root-associated communities in 2018 was similar in transgenic *EFR* and isogenic FL8000 tomato plants. NMDS visualization of Bray-Curtis distance matrix from 2017 root associated communities from wild-type cv. Florida8000 tomato (FL8000, in blue) and an isogenic *EFR*-expressing line (EFR, in red), based on 16S amplicons binned at the genus level. Plants were exposed to endemic bacterial wilt disease pressure from endemic soil populations of *R. solanacearum* (N, not inoculated) or received supplemental inoculation with the an endemic *R. solanacearum* strain (I, inoculated). Neither expression of *EFR* or supplemental inoculation affected community composition. (permANOVA, $p > 0.05$).

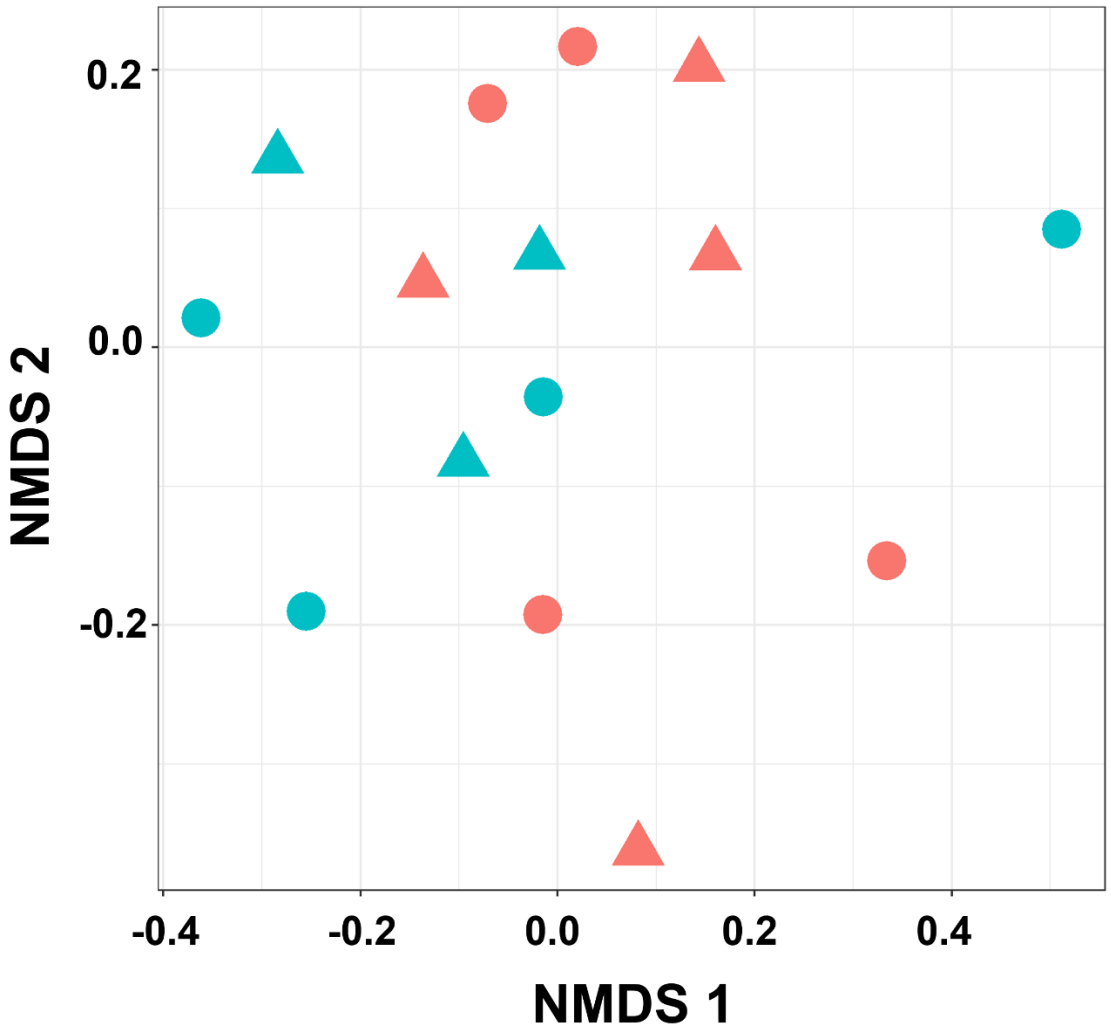

Figure 6. The composition of xylem associated communities in 2018 was similar in transgenic *EFR* and isogenic FL8000 tomato plants. NMDS visualization of Bray-Curtis distance matrix from 2018 xylem associated communities from wild-type cv. Florida8000 tomato (FL8000, in blue) and an isogenic *EFR*-expressing line (EFR, in red), based on 16S amplicons binned at the genus level. Plants were exposed to endemic bacterial wilt disease pressure from endemic soil populations of *R. solanacearum* (Circle, not inoculated) or received supplemental inoculation with the an endemic *R. solanacearum* strain (triangle, inoculated). The size of plotted points are proportional to their R. solanacearum relative abundance. Neither expression of *EFR* or supplemental inoculation affected community composition. (perMANOVA, $p > 0.05$).

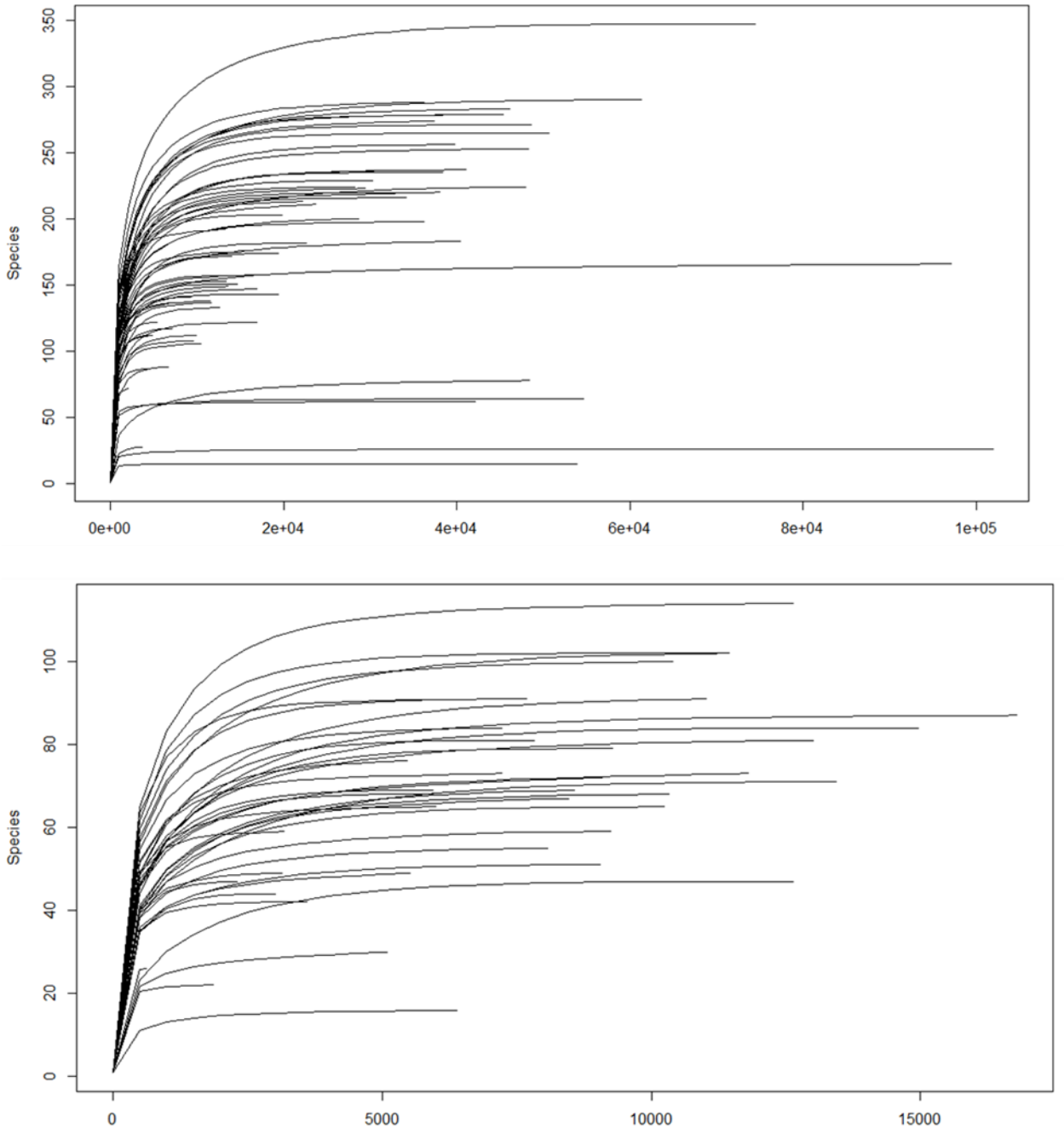

Figure S1 **Rarefaction curves of the number of genera per sample at increasing sampling depths in root and xylem communities.** Rarefaction curves for combined 2017 and 2018 roots (above) and xylem sap (below).

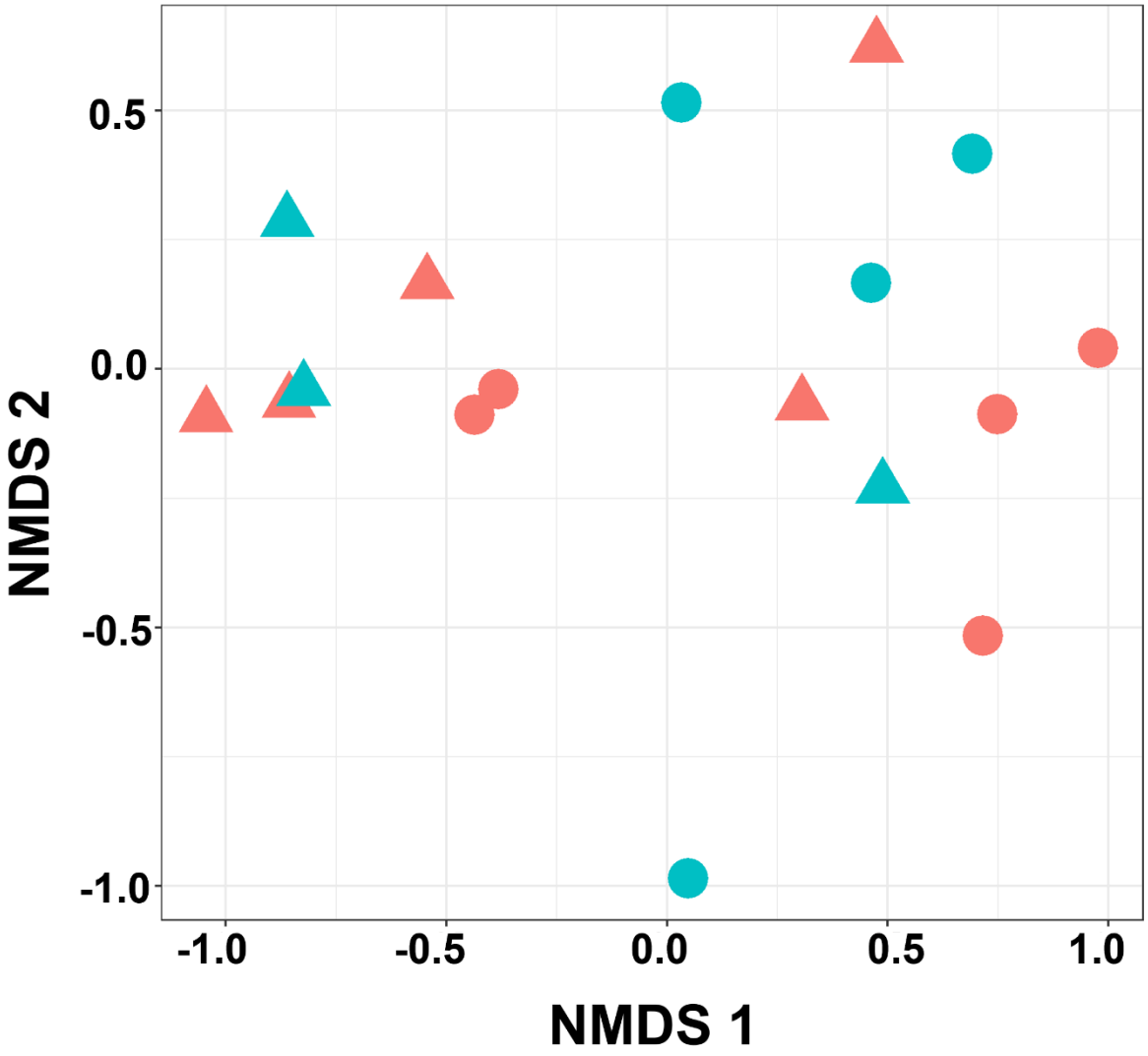

Figure S2. EFR root associated communities from 2017 did not compositionally differ from non-EFR communities. NMDS visualization of Bray-Curtis distance matrix from 2017 root-associated communities from wild-type cv. Florida8000 tomato (FL8000, in blue) and an isogenic *EFR*-expressing line (EFR, in red), based on 16S amplicons binned at the genus level. Plants were exposed to endemic bacterial wilt disease pressure from endemic soil populations of *R. solanacearum* (circle, not inoculated) or received supplemental inoculation with the an endemic *R. solanacearum* strain (triangle, inoculated). Neither expression of *EFR* or supplemental inoculation affected community composition. (permANOVA, $p > 0.05$).

Table 1. ANOVA results of richness in whole root and xylem sap communities.

Table 1 A: Anova of 2017 and 2018 Whole Root Richness			
	Degrees of Freedom	F value	Pr(>F)
Sequencing Depth	1	42.745	0.000000922
Year	1	25.704	**0.0000348**
EFR	1	0.17	0.6834
Inoculation	1	3.872	0.0608
Year x EFR	1	0.023	0.8801
Year x Inoculation	1	8.275	**0.0083**
EFR x Inoculation	1	0.368	0.5496
Year x EFR x Inoculation	1	0.105	0.7489
Residuals	24		
Table 1 B: Anova of 2017 Whole Root Richness			
	Degrees of Freedom	F value	Pr(>F)
Sequencing Depth	1	1.211	0.29272
EFR	1	0.092	0.76645
Inoculation	1	9.493	**0.00952**
Year x Inoculation	1	0.019	0.89193
Residuals	12		
Table 1 C: Anova of 2018 Whole Root Richness			
	Degrees of Freedom	F value	Pr(>F)
Sequencing Depth	1	114.947	**0.000000367**
EFR	1	0.054	0.82
Inoculation	1	0.121	0.735
Year x Inoculation	1	2.235	0.163
Residuals	11		
Table 1D: Anova of 2018 Xylem Sap Richness			
	Degrees of Freedom	F value	Pr(>F)
Sequencing Depth	1	24.24	**0.000602**
EFR	1	13.169	**0.004621**
Inoculation	1	0.617	0.450244
Year x Inoculation	1	1.556	0.240681
Residuals	10		

Table 2. ANOVA results of Shannon-Weaver indices in whole root and xylem sap communities.

Table 2A: Anova of 2017 and 2018 Whole Root Shannon-Weaver Index			
	Degrees of Freedom	F value	Pr(>F)
Sequencing Depth	1	1.384	0.251
Year	1	2.843	0.1047
EFR	1	0.04	0.8425
Inoculation	1	7.229	**0.0128**
Year x EFR	1	0.401	0.5324
Year x Inoculation	1	6.73	**0.0159**
EFR x Inoculation	1	0.01	0.9208
Year x EFR x Inoculation	1	0.897	0.3531
Residuals	24		
Table 2B: Anova of 2017 Whole Root Shannon-Weaver Index			
	Degrees of Freedom	F value	Pr(>F)
Sequencing Depth	1	0.76	0.401
EFR	1	1.79	0.206
Inoculation	1	0.019	0.893
Year x Inoculation	1	0.398	0.54
Residuals	12		
Table 2C: Anova of 2018 Whole Root Shannon-Weaver Index			
	Degrees of Freedom	F value	Pr(>F)
Sequencing Depth	1	2.237	0.1629
EFR	1	2.782	0.1235
Inoculation	1	0.761	0.4016
Year x Inoculation	1	3.981	0.0714
Residuals	11		
Table 2D: Anova of 2018 Xylem Sap Shannon-Weaver Index			
	Df	F value	Pr(>F)
Sequencing Depth	1	0.124	0.732
EFR	1	1.343	0.273
Inoculation	1	6.591	**0.028**
Year x Inoculation	1	0.853	0.378
Residuals	10		

Table 3. perMANOVA results of whole root and xylem sap bacterial community composition.

Table 3A: perMANOVA of 2017 and 2018 Whole Root Communities

	Degrees of Freedom	F Statistic	R^2	Pr(>F)
Sequencing Depth	1	3.0947	0.05618	**0.022**
EFR	1	1.5548	0.02823	0.172
Inoculation	1	1.9771	0.03589	0.111
Year	1	19.2886	0.35019	**0.001**
EFR x Inoculation	1	1.1781	0.02139	0.292
EFR x Year	1	0.6836	0.01241	0.624
Year x Inoculation	1	2.1688	0.03938	0.067
EFR x Inoculation x Year	1	1.1344	0.0206	0.273
Residuals	24	0.43573		
Total	32			

Table 3B: perMANOVA of 2017 Whole Root Communities

	Degrees of Freedom	F Statistic	R^2	Pr(>F)
Sequencing Depth	1	2.01318	0.11423	0.051
EFR	1	0.58512	0.0332	0.795
Inoculation	1	1.8332	0.10402	0.091
EFR x Inoculation	1	1.19166	0.06762	0.246
Residuals	12	0.68092		
Total	16			

Table 3C: perMANOVA of 2018 Whole Root Communities

	Degrees of Freedom	F Statistic	R^2	Pr(>F)
Sequencing Depth	1	2.22928	0.12697	0.095
EFR	1	1.46721	0.08357	0.215
Inoculation	1	0.60098	0.03423	0.624
EFR x Inoculation	1	2.25944	0.12869	0.085
Residuals	11	0.62653		
Total	15			

Table 3D: perMANOVA of 2018 Xylem Sap Communities

	Degrees of Freedom	F Statistic	R^2	Pr(>F)
Sequencing Depth	1	2.25991	0.14226	**0.014**
EFR	1	0.87206	0.0549	0.579
Inoculation	1	1.79514	0.11301	**0.042**
EFR x Inoculation	1	0.95818	0.06032	0.46
Residuals	10	0.62951		
Total	14			

Table 4. ANOVA results of richness in whole root and xylem sap communities with R. solanacearum removed from the dataset.

Table 4A: Anova of 2017 Whole Root Richness with Ralstonia Removed			
	Degrees of Freedom	F value	Pr(>F)
Sequencing Depth	1	1.103	0.316
Ralstonia	1	0.028	0.8699
EFR	1	0.14	0.7149
Inoculation	1	8.879	**0.0125**
EFR x Inoculation	1	0.003	0.956
Residuals	11		
Table 4B: Anova of 2018 Whole Root Richness with Ralstonia Removed			
	Degrees of Freedom	F value	Pr(>F)
Sequencing Depth	1	142.522	**0.000000307**
Ralstonia	1	5.124	**0.0471**
EFR	1	0.449	0.5178
Inoculation	1	0.857	0.3764
EFR x Inoculation	1	0.196	0.6671
Residuals	10		
Table 4C: Anova of 2018 Xylem Sap Richness with Ralstonia Removed			
	Degrees of Freedom	F value	Pr(>F)
Sequencing Depth	1	21.913	**0.00115**
Ralstonia	1	3.967	0.07757
EFR	1	9.015	**0.01489**
Inoculation	1	0.016	0.90086
EFR x Inoculation	1	0.91	0.36512
Residuals	9		

Table 5. ANOVA results of Shannon-Weaver indices in whole root and xylem sap communities with R. solanacearum removed from the dataset.

Table 5A: Anova of 2017 Whole Root Shannon-Weaver Index with Ralstonia Removed			
	Degrees of Freedom	F value	Pr(>F)
Sequencing Depth	1	3.368	0.0936
Ralstonia	1	0.94	0.3532
EFR	1	0.034	0.8566
Inoculation	1	4.585	0.0555
EFR x Inoculation	1	0.007	0.9349
Residuals	11		
Table 5B: Anova of 2018 Whole Root Shannon-Weaver Index with Ralstonia Removed			
	Degrees of Freedom	F value	Pr(>F)
Sequencing Depth	1	46.934	**0.0000445**
Ralstonia	1	36.085	**0.000131**
EFR	1	0.499	0.495901
Inoculation	1	1.071	0.325069
EFR x Inoculation	1	0.506	0.493046
Residuals	10		
Table 5C: Anova of 2018 Xylem Sap Shannon-Weaver Index with Ralstonia Removed			
	Degrees of Freedom	F value	Pr(>F)
Sequencing Depth	1	0	0.997
Ralstonia	1	2.31	0.163
EFR	1	0.008	0.93
Inoculation	1	2.82	0.127
EFR x Inoculation	1	0.005	0.946
Residuals	9		

Table 6. perMANOVAs results of whole root and xylem sap bacterial community composition with R. solanacearum removed from the dataset.

Table 6A: perMANOVA of 2017 Whole Root Communities with Rasltonia Removed				
	Degrees of Freedom	F Statistic	R^2	Pr(>F)
Sequencing Depth	1	2.17918	0.11525	0.058
Ralstonia	1	1.92695	0.10191	0.078
EFR	1	0.59887	0.03167	0.808
Inoculation	1	2.0335	0.10755	0.068
EFR x Inoculation	1	1.1696	0.06186	0.265
Residuals	11	0.58176		
Total	16			
Table 6B: perMANOVA of 2018 Whole Root Communities with Rasltonia Removed				
	Degrees of Freedom	F Statistic	R^2	Pr(>F)
Sequencing Depth	1	4.4042	0.14107	**0.005**
Ralstonia	1	2.2304	0.07144	0.094
EFR	1	0.9931	0.03181	0.342
Inoculation	1	12.3614	0.39594	**0.001**
EFR x Inoculation	1	1.2309	0.03943	0.268
Residuals	10	0.32031		
Total	15			
Table 6C: perMANOVA of 2018 Xylem Sap Communities with Rasltonia Removed				
	Degrees of Freedom	F Statistic	R^2	Pr(>F)
Sequencing Depth	1	2.09967	0.13693	**0.038**
Ralstonia	1	1.25369	0.08176	0.205
EFR	1	0.69113	0.04507	0.771
Inoculation	1	1.11199	0.07252	0.354
EFR x Inoculation	1	1.17733	0.07678	0.283
Residuals	9	0.58694		
Total	14			

Table S1. List of whole root samples used in 16S Metabarcoding experiment, their sequencing depth, rarefaction levels, and *R.solanacearum* relative abundance.

Tissue Type	Genotype	Inoculation	*R. solanacearum* abundance	Number of Reads	Year
Root	EFR	Inoculated	0.01129	19398	2017
Root	EFR	Inoculated	0.006806	16897	2017
Root	EFR	Inoculated	0.010165	36201	2017
Root	EFR	Inoculated	0.004861	47933	2017
Root	EFR	Inoculated	0.00331	28697	2017
Root	EFR	Non-Inoculated	0.008202	32919	2017
Root	EFR	Non-Inoculated	0.008504	53860	2017
Root	EFR	Non-Inoculated	0	101993	2017
Root	EFR	Non-Inoculated	0.025257	9621	2017
Root	EFR	Non-Inoculated	0.004848	54660	2017
Root	FL8000	Inoculated	0.036092	97141	2017
Root	FL8000	Inoculated	0.017775	13221	2017
Root	FL8000	Inoculated	0.008477	40464	2017
Root	FL8000	Inoculated	0.009032	10408	2017
Root	FL8000	Non-Inoculated	0.010733	6708	2017
Root	FL8000	Non-Inoculated	0	42171	2017
Root	FL8000	Non-Inoculated	0.002377	48380	2017
Root	EFR	Inoculated	0.098375	60550	2018
Root	EFR	Inoculated	0.066299	116341	2018
Root	EFR	Inoculated	0.194544	33866	2018
Root	EFR	Inoculated	0.225649	20363	2018
Root	EFR	Non-Inoculated	0.266302	115448	2018
Root	EFR	Non-Inoculated	0.21653	31481	2018
Root	EFR	Non-Inoculated	0.256639	133552	2018
Root	EFR	Non-Inoculated	0.208096	126164	2018
Root	FL8000	Inoculated	0.248482	147487	2018
Root	FL8000	Inoculated	0.308933	21924	2018
Root	FL8000	Inoculated	0.238258	13766	2018
Root	FL8000	Inoculated	0.301407	51547	2018
Root	FL8000	Non-Inoculated	0.262295	10723	2018
Root	FL8000	Non-Inoculated	0.199192	93630	2018
Root	FL8000	Non-Inoculated	0.21343	57223	2018
Root	FL8000	Non-Inoculated	0.185125	82142	2018

Table S2. List of xylem sap samples used in 16S Metabarcoding experiment, their sequencing depth, rarefaction levels, and *R.solanacearum* relative abundance.

Tissue Type	Genotype	Inoculation	*R. Solanacearum* abundance	Number of Reads	Year
Xylem	EFR	Inoculated	0.096979	12097	2018
Xylem	EFR	Inoculated	0.096802	16509	2018
Xylem	EFR	Inoculated	0.105222	22312	2018
Xylem	EFR	Inoculated	0.114201	18246	2018
Xylem	EFR	Non-Inoculated	0.22923	7768	2018
Xylem	EFR	Non-Inoculated	0.051702	22876	2018
Xylem	EFR	Non-Inoculated	0.046071	24021	2018
Xylem	EFR	Non-Inoculated	0.027591	33984	2018
Xylem	FL8000	Inoculated	0.08346	9088	2018
Xylem	FL8000	Inoculated	0.019996	24219	2018
Xylem	FL8000	Inoculated	0.06038	31431	2018
Xylem	FL8000	Inoculated	0.797841	15514	2018
Xylem	FL8000	Non-Inoculated	0.023057	17210	2018
Xylem	FL8000	Non-Inoculated	0.008847	31329	2018
Xylem	FL8000	Non-Inoculated	0.132765	30759	2018

Table S3 ANOVA results *of R. solanacearum* relative abundance in whole root and xylem sap communities.

Table 1 A: Anova of 2017 and 2018 Ralstonia Relative Abundance			
	Degrees of Freedom	F value	Pr(>F)
Sequencing Depth	1	19.002	**0.000212**
Year	1	212.664	**2.00E-13**
EFR	1	2.553	0.123152
Inoculation	1	0.512	0.48126
Year x EFR	1	1.933	0.177229
Year x Inoculation	1	0.674	0.419724
EFR x Inoculation	1	4.815	**0.038133**
Year x EFR x Inoculation	1	1.769	0.195999
Residuals	24		
Table 1 B: Anova of 2017 Whole Root Ralstonia Relative Abundance			
	Degrees of Freedom	F value	Pr(>F)
Sequencing Depth	1	0.76	0.401
EFR	1	1.79	0.206
Inoculation	1	0.019	0.893
Year x Inoculation	1	0.398	0.54
Residuals	12		
Table 1 C: Anova of 2018 Whole Root Ralstonia Relative Abundance			
	Degrees of Freedom	F value	Pr(>F)
Sequencing Depth	1	2.237	0.1629
EFR	1	2.782	0.1235
Inoculation	1	0.761	0.4016
Year x Inoculation	1	3.981	0.0714
Residuals	11		
Table 1D: Anova of 2018 Xylem Sap Ralstonia Relative Abundance			
	Degrees of Freedom	F value	Pr(>F)
Sequencing Depth	1	0.613	0.4518
EFR	1	2.507	0.1444
Inoculation	1	3.543	0.0892
Year x Inoculation	1	2.82	0.124
Residuals	10		

Literature Cited

Allen, C., Prior, P., and Hayward, A. C., 2005. Bacterial wilt disease and the *Ralstonia solanacearum* species complex.

Boller, T., and Felix, G. 2009. A renaissance of elicitors: perception of microbe-associated molecular patterns and danger signals by pattern-recognition receptors. *Annu. Rev. Plant Biol*. 60:379–406.

Bolyen, E., Rideout, J. R., Dillon, M. R., Bokulich, N. A., Abnet, C. C., Al-Ghalith, G. A., et al. 2019. Reproducible, interactive, scalable and extensible microbiome data science using QIIME 2. *Nat. Biotechnol*. 37:852–857.

Choi, K., Choi, J., Lee, P. A., Roy, N., Khan, R., Lee, H. J., et al. 2020. Alteration of bacterial wilt resistance in tomato plant by microbiota transplant. *Front. Plant Sci*. 11:1186.

Horvath, D. M., Stall, R. E., Jones, J. B., Pauly, M. H., Vallad, G. E., Dahlbeck, D., et al. 2012. Transgenic resistance confers effective field level control of bacterial spot disease in tomato. *PLoS One*. 7:e42036.

Hu, J., Wei, Z., Friman, V.-P., Gu, S.-H., Wang, X.-F., Eisenhauer, N., et al. 2016. Probiotic diversity enhances rhizosphere microbiome function and plant disease suppression. *MBio*. 7.

Hu, J., Yang, T., Friman, V.-P., Kowalchuk, G. A., Hautier, Y., Li, M., et al. 2021. Introduction of probiotic bacterial consortia promotes plant growth via impacts on the resident rhizosphere microbiome. *Proc. Biol. Sci*. 288:20211396.

Jones, J. D. G., and Dangl, J. L. 2006. The plant immune system. *Nature.* 444:323–329.

Jousset, A., and Lee, S.-W. 2023. Coming of age for the rhizosphere microbiome transplantation. *Soil Ecology Letters*. 5:4–5.

Kunwar, S., Iriarte, F., Fan, Q., Evaristo da Silva, E., Ritchie, L., Nguyen, N. S., et al. 2018. Transgenic expression of *EFR* and *Bs2* genes for field management of bacterial wilt and bacterial spot of tomato. *Phytopathology*. 108:1402–1411.

Kwak, M.-J., Kong, H. G., Choi, K., Kwon, S.-K., Song, J. Y., Lee, J., et al. 2018. Rhizosphere microbiome structure alters to enable wilt resistance in tomato. *Nat. Biotechnol*. 36:1100–1109.

Lacombe, S., Rougon-Cardoso, A., Sherwood, E., Peeters, N., Dahlbeck, D., van Esse, H. P., et al. 2010. Interfamily transfer of a plant pattern-recognition receptor confers broad-spectrum bacterial resistance. *Nat. Biotechnol*. 28:365–369.

Laforest-Lapointe, I., Paquette, A., Messier, C., and Kembel, S. W. 2017. Leaf bacterial diversity mediates plant diversity and ecosystem function relationships. *Nature*. 546:145–147.

Landry, D., González-Fuente, M., Deslandes, L., and Peeters, N. 2020. The large, diverse, and robust arsenal of *Ralstonia solanacearum* type III effectors and their *in planta* functions. *Mol. Plant Pathol*. 21:1377–1388.

Lopes, G. L., Lopes, C. A., Nomura, J. V., Nandi, G., and Piotto, F. A. 2022. Combining ability of tomato inbred lines to bacterial wilt resistance. *Bragantia.* 81:e3222.

Lowe-Power, T. M., Khokhani, D., and Allen, C. 2018. How *Ralstonia solanacearum* exploits and thrives in the flowing plant xylem environment. *Trends Microbiol*. 26:929–942.

Mansfield, J., Genin, S., Magori, S., Citovsky, V., Sriariyanum, M., Ronald, P., et al. 2012. Top 10 plant pathogenic bacteria in molecular plant pathology. *Mol. Plant Pathol.* 13:614–629.

McDonald, D., Price, M. N., Goodrich, J., Nawrocki, E. P., DeSantis, T. Z., Probst, A., et al. 2012. An improved Greengenes taxonomy with explicit ranks for ecological and evolutionary analyses of bacteria and archaea. *ISME J*. 6:610–618.

Mitre, L. K., Teixeira-Silva, N. S., Rybak, K., Magalhães, D. M., de Souza-Neto, R. R., Robatzek, S., et al. 2021. The *Arabidopsis* immune receptor EFR increases resistance to the bacterial pathogens *Xanthomonas* and *Xylella* in transgenic sweet orange. *Plant Biotechnol. J*. 19:1294–1296.

Nakano, M., and Mukaihara, T. 2019. Comprehensive identification of PTI suppressors in type III effector repertoire reveals that *Ralstonia solanacearum* activates jasmonate signaling at two different steps. *Int. J. Mol. Sci*. 2023, 5992.

Ngou, B. P. M., Ding, P., and Jones, J. D. G. 2022. Thirty years of resistance: Zig-zag through the plant immune system. *Plant Cell*. 34:1447–1478.

Planas-Marquès, M., Kressin, J. P., Kashyap, A., Panthee, D. R., Louws, F. J., Coll, N. S., et al. 2019. Four bottlenecks restrict colonization and invasion by the pathogen *Ralstonia solanacearum* in resistant tomato. J. Exp. Bot. 71:2157–2171.

Redford, A. J., Bowers, R. M., Knight, R., Linhart, Y., and Fierer, N. 2010. The ecology of the phyllosphere: geographic and phylogenetic variability in the distribution of bacteria on tree leaves. *Environ. Microbiol*. 12:2885–2893.

Schoonbeek, H.-J., Wang, H.-H., Stefanato, F. L., Craze, M., Bowden, S., Wallington, E., et al. 2015. *Arabidopsis* EF-Tu receptor enhances bacterial disease resistance in transgenic wheat. *New Phytol*. 206:606–613.

Schwessinger, B., Bahar, O., Thomas, N., Holton, N., Nekrasov, V., Ruan, D., et al. 2015. Transgenic expression of the dicotyledonous pattern recognition receptor EFR in rice leads to ligand-dependent activation of defense responses. *PLoS Pathog*. 11:e1004809.

Suchoff, D., Gunter, C., Schultheis, J., and Louws, F. J. 2015. On-farm grafted tomato trial to manage bacterial wilt. *Acta Hortic*. :119–127.

Wei, Z., Yang, T., Friman, V.-P., Xu, Y., Shen, Q., and Jousset, A. 2015. Trophic network architecture of root-associated bacterial communities determines pathogen invasion and plant health. *Nat. Commun*. 6:8413.

Wei, Z., Hu, J., Gu, Y. 'an, Yin, S., Xu, Y., Jousset, A., et al. 2018. *Ralstonia solanacearum* pathogen disrupts bacterial rhizosphere microbiome during an invasion. *Soil Biol. Biochem*. 118:8–17.

Wei, Z., Gu, Y., Friman, V.-P., Kowalchuk, G. A., Xu, Y., Shen, Q., et al. 2019. Initial soil microbiome composition and functioning predetermine future plant health. *Sci Adv*. 5:eaaw0759.

Xue, D., Christenson, R., Genger, R., Gevens, A., and Lankau, R. A. 2018. Soil microbial communities reflect both inherent soil properties and management practices in Wisconsin potato fields. *Am. J. Potato Res*. 95:696–708.

Zhou, F., Emonet, A., Dénervaud Tendon, V., Marhavy, P., Wu, D., Lahaye, T., et al. 2020. Co-incidence of damage and microbial patterns controls localized immune responses in roots. *Cell*. 180:440–453.e18.

Chapter 4: Conclusions to Microbiomes of Disease and Resistance: Deciphering the Role of a Plant Immune Receptor in Bacterial Community Assembly

Genetically modifying plants to express novel PRRs can generate crops with broad spectrum field resistance to diseases caused by phytopathogenic bacteria. However, plants naturally associate with a diverse consortia of commensal and beneficial microbes that synthesize the same MAMPs that trigger PTI in reductionist studies. Does the incorporation of an additional PRR and the resulting capacity to perceive an additional MAMP trigger increased basal defenses and thus alter the composition of plant associated microbial communities? Do microbial communities associated with plants expressing PTI-based resistance differ from those of non-transgenic but otherwise similar plants? How do changes in plant-pathogen interactions alter the microbial ecology of disease?

My doctoral research aimed to answer these questions by characterizing microbial communities associated with isogenic FL8000 and *EFR* tomato lines grown in commercial production conditions under high disease pressure. In Chapter 2, I contrasted PTI-based and ETI-based resistance to the phyllosphere pathogen *X. perforans*. While transgenic ETI-based resistance dramatically reshaped bacterial communities in the phyllosphere, plants expressing EFR harbored communities like those of their FL8000 counterparts despite significant differences in disease severity. In Chapter 3, I investigated how EFR-based resistance interacted with *R. solanacearum* by characterizing microbial communities associated with both whole roots and xylem sap. While I did observe subtle effects of EFR on communities in roots and xylem, this was only the case when pathogen populations were higher or plants were

supplementally inoculated. Together, these multi-year field studies demonstrate that deployment of transgenic, broad-spectrum resistance using PRRs does not appear to detectably disrupt plant microbiomes.

Metabarcoding is a powerful tool for characterizing the microbial communities associated with environmental samples. The broad-spectrum resistance that *EFR* confers when it is constitutively expressed under the powerful CaMV 35S promoter allowed me to study the effects of this PRR on two phytopathogenic bacteria that infect distinct plant compartments. This 16S metabarcoding approach assessed the influence of plant-pathogen interactions on plant-associated bacterial communities in commercial tomato production in a robust, culture-independent fashion. In order to ensure disease development, supplemental inoculation was used in both studies. However, ideal conditions for disease development created high disease pressure even in non-inoculated plots. These conditions meant that I was unable to confidently capture microbial communities in the absence of disease in either study.

Correlation between plant microbiomes and useful metadata such as disease ratings or yield data can identify desirable characteristics of plant-associated microbial communities. Further, sampling timing is a critically important element of experimental design. In both of these experiments, metabarcoding profiles represented snapshots of community composition associated with harvestable tomato plants. Collecting multiple timepoints, particularly very soon after seedlings are transplanted and while symptoms are developing, could provide additional insight about how plant defenses and bacterial pathogenesis alter the composition of plant associated microbial communities. The results and limitations of these studies can be used to improve future experiments

assessing resistance and disease-associated plant microbiomes using 16S metabarcoding.

If given the opportunity to further pursue metabarcoding approaches for this project, I would be particularly interested in investigating the impact of transgenic expression of the plant NLR Roq1 on plant associated microbial communities. While most NLRs confer ETI-based resistance in a gene-for-gene fashion, transgenic *Roq1* confers resistance to several plant pathogens in tomato, including *R*. *solanacearum*, *X*. *perforans*, and *Pseudomonas syringae* (Thomas et al. 2020). Results from Chapter 2 suggest that infection by two foliar pathogens can produce distinct microbial communities. I would gain further insight into pathogen-mediated vs plant-mediated effects on phyllosphere microbial communities by metabarcoding phyllosphere communities of transgenic *Roq1*-expressing tomatoes, which have resistance to *X*. *perforans* and *P. syringae* mediated by a single resistance gene. It would be interesting to compare communities of plants inoculated with one or both bacteria with those of uninoculated plants. Additionally, adding Roq1 resistance as an experimental condition would allow me to contrast the effects of ETI-pathogen interactions on microbial communities in multiple plant compartments, similar to my research characterizing EFR-pathogen interactions.

As mentioned above, healthy plants not challenged by the pathogen are a desirable control. Previous field studies of EFR-mediated bacterial wilt resistance in Florida found that this transgene did not reduce either marketable or total yield (Kunwar et al. 2018). This encouraging finding suggested that constitutively expressing this non-native PRR did not impose a growth-defense tradeoff on transgenic plants, possibly

because the plants did not continuously express innate immunity. However, the Florida field plots used in that study, like those in my Chapter 3 study, were infested with *R. solanacearum* and indeed all tested plants contained detectable levels of *R. solanacearum* as indicated by Agdia Rs immunostrips (Kunwar, unpublished results). This latent infection may have uniformly reduced yield across all plants. Further, bacterial wilt itself imposes a severe yield penalty. Thus it was not possible to know if transgenic plants actually suffered no yield reduction or if this result was a side effect of reduced disease. To disentangle these effects, Dr. Sanju Kunwar and I compared yields of FL8000 and isogenic *EFR* tomatoes growing in field plots at Arlington, Wisconsin in summer 2020. These plants grew in the absence of *R. solanacearum* or any other noticeable disease constraint. We found no differences in either marketable or total yield between these two tomato lines. This result, which is in preparation for publication, indicates that the *EFR* transgene does not impose a yield penalty and thus may not cause continuous high expression of PTI under field conditions. This inference would be consistent with my finding that the EFR transgene by itself did not alter composition of xylem or rhizosphere-associated microbial communities.

Additional experiments are required to better characterize how non-pathogenic bacteria and PRRs interact. Previous reciprocal grafting experiments revealed that plants expressing *EFR* limited *R. solanacearum* colonization in the upper stem above the grafting scar whether the *EFR* transgene was present only in rootstocks or only in scions (S. Kunwar, unpublished results). As a follow up, I would test the hypothesis that commensal strains of xylem-inhabiting bacteria induce a PTI response in EFR transgenic plants but not in the FL8000 parent. This would require inoculation of *EFR*

and WT FL8000 plants with a commensal bacterium and using qPCR to measure expression of PTI marker genes. Inoculations could be performed via soil soak to mimic the natural pathway of root infection and internal movement to xylem tissue or petiole inoculation. The latter can be used to inoculate plants at high cell densities in order to reach levels commensurate with those *R. solanacearum* reaches during infection.

However, failure to initiate a PTI response when inoculated at high cell density does not conclusively demonstrate that a given bacterial taxon is incapable of initiating PTI. Additional controls such as treating plants with exogenous DAMPs in tandem with inoculation can be used to infer if commensal bacteria fail to initiate PTI due to the absence of a co-requirement. The co-inoculation of commensals and a known PTI inducer such as *R. solanacearum* could serve as an additional control to assess if commensal bacteria suppress PTI in order to colonize plants.

Literature Cited

Kunwar, S., Iriarte, F., Fan, Q., Evaristo da Silva, E., Ritchie, L., Nguyen, N. S., et al. 2018. Transgenic expression of *EFR* and *Bs2* genes for field management of bacterial wilt and bacterial spot of tomato. *Phytopathology*. 108:1402–1411.

Thomas, N. C., Hendrich, C. G., Gill, U. S., Allen, C., Hutton, S. F., and Schultink, A. 2020. The immune receptor Roq1 confers resistance to the bacterial pathogens *Xanthomonas*, *Pseudomonas syringae*, and *Ralstonia* in tomato. Front. Plant Sci. 11:463.